

CRANFIELD UNIVERSITY

William Easdown

A Mission Architecture and Systems Level Design of Navigation,  
Robotics and Grappling Hardware for an On-Orbit Servicing  
Spacecraft

School of Aerospace, Transport and Manufacturing  
Astronautics and Space Engineering

MSc  
Academic Year: 2019 - 2020

Supervisor: Dr Leonard Felicetti  
August 2020

CRANFIELD UNIVERSITY

School of Aerospace, Transport and Manufacturing  
Astronautics and Space Engineering

MSc

Academic Year 2019 - 2020

William Easdown

A Mission Architecture and Systems Level Design of Navigation,  
Robotics and Grappling Hardware for an On-Orbit Servicing  
Spacecraft

Supervisor: Dr Leonard Felicetti  
August 2020

This thesis is submitted in partial fulfilment of the requirements for  
the degree of MSc Astronautics and Space Engineering

© Cranfield University 2020. All rights reserved. No part of this  
publication may be reproduced without the written permission of the  
copyright owner.



## **ABSTRACT**

On-orbit servicing (OOS) includes a range of servicing types that increase the lifetime of a satellite and its performance, as well as ensuring that it does not contribute to the growing issue of space debris. The avoidance of satellites becoming derelict is particularly important given the rise of ‘mega-constellations’. With the first cases in the 1970s, OOS has been achieved many times using crewed missions and robots controlled from the ground or by astronauts, for example during repairs and upgrades to the Hubble Space Telescope (HST) and on the International Space Station (ISS). This has allowed various space agencies and other organisations to mature processes and tools for several OOS mission types.

The Northrop Grumman Mission Extension Vehicle-1’s (MEV-1) success servicing Intelsat 901 in early 2020 demonstrated that OOS is now viable from a commercial as well as technical standpoint. However, due to low technology maturity, autonomous rendezvous and proximity operations (RPO) and servicing remain challenging, despite autonomous rendezvous and docking with space stations having been demonstrated many times.

This report will investigate the current state of the art in OOS and which technologies require further development to enable widespread adoption of OOS. A mission architecture to support OOS of satellites in the highest populated orbits will be described. Using this architecture, the report will focus on the selection of hardware required for guidance, navigation and control (GNC), for relative navigation towards and docking with the target satellite and of robotics to service the target. The report will use the design of the OneWeb satellites as a baseline for the target spacecraft but will also show how the servicing spacecraft’s services could be applied to a range of orbits and target spacecraft.

Keywords: technology readiness; mega-constellations; guidance, navigation and control; proximity operations

## **ACKNOWLEDGEMENTS**

I would like to thank the following people for their greatly appreciated help during this project:

**Dr Leonard Felicetti** – you have been a fantastic supervisor throughout my GDP and IRP and your support and enthusiasm have really helped me tackle challenges and keep moving forward.

**Zoë** – your support and keeping me motivated throughout this project have been amazing. Your notes and checklists have been a great help at keeping me on track and I really appreciate everything you've done to make sure I get the project finished completely and on time.

**Jonathan Goff and Eli Kopp-DeVol from Altius Space Machines** – thank you for your technical support on the DogTag and MagTag. The information has been extremely useful when writing this report and I've really appreciated the time you've spent to answer my questions.

**Kristen Facciol from the Canadian Space Agency** – thank you for taking the time out of your busy day to answer my questions on the Next Generation Canadarm and the Robotic Refuelling Mission.

# TABLE OF CONTENTS

ABSTRACT .....	iii
ACKNOWLEDGEMENTS.....	iv
LIST OF FIGURES.....	vii
LIST OF TABLES .....	x
LIST OF EQUATIONS.....	xi
LIST OF ABBREVIATIONS .....	xii
1 Executive Summary .....	1
2 Introduction .....	3
2.1 Background.....	3
2.2 Aim.....	6
2.3 Research questions .....	7
2.4 Report overview .....	8
3 Project Management .....	10
3.1 Work breakdown structure .....	10
3.2 Tools .....	10
3.2.1 Trello.....	10
3.2.2 OneDrive.....	12
3.3 Documentation.....	12
3.3.1 General Running Notes document.....	13
3.3.2 Main Central Control spreadsheet .....	13
3.3.3 Requirements document.....	14
3.3.4 Orbit selection document .....	14
3.3.5 CONOPS .....	15
3.3.6 Design Definition File .....	15
4 Literature Review .....	17
4.1 OOS types.....	17
4.2 OOS applications and benefits.....	19
4.3 Previous use of OOS .....	22
4.4 Current state of the art .....	25
4.4.1 Missions.....	25
4.4.2 Rendezvous, proximity operations & docking (RPOD) sensors ..	30
4.4.3 Robotics.....	34
4.4.4 Attachment methods.....	38
5 Mission Analysis and Design.....	45
5.1 Background.....	45
5.2 Orbit selection .....	49
5.3 Servicer sizing.....	54
5.3.1 Dry mass estimation .....	55
5.3.2 Fuel requirement estimation.....	57

6	Requirements Definition.....	63
6.1	Main requirements .....	64
6.2	Requirements verification and validation.....	64
7	Guidance, Navigation and Control (GNC) System .....	67
7.1	GNC architecture .....	67
7.2	GNC requirements .....	68
7.3	Control Loop.....	69
7.4	Sensors.....	70
7.4.1	Sensor requirements.....	70
7.4.2	Orbit determination methods and selection.....	71
7.4.3	Attitude determination methods and selection .....	73
7.5	Plant.....	76
7.6	Actuators.....	78
7.6.1	Actuator requirements.....	82
7.6.2	Orbit control methods and selection.....	83
7.6.3	Attitude control methods and selection .....	87
8	Relative Navigation System (RNS).....	90
8.1	RNS requirements.....	90
8.2	RNS concept and component selection .....	90
8.3	Safety .....	95
9	Grappling and Robotics.....	97
9.1	Grappling Fixture.....	97
9.2	Servicing arm .....	99
9.2.1	Servicing arm requirements .....	100
9.2.2	Servicing arm selection .....	100
9.3	Tooling and sensing .....	102
10	Areas for Future Development.....	104
10.1	Mission design and dynamics analysis .....	104
10.2	Systems engineering considerations.....	105
10.3	Other areas .....	107
11	Conclusion.....	108
	REFERENCES.....	109
	APPENDICES .....	142

## LIST OF FIGURES

Figure 3-1 - Project work breakdown structure .....	11
Figure 3-2 - The project page on Trello .....	12
Figure 3-3 - Screenshot of Propulsion page of Main Central Control spreadsheet [25].....	14
Figure 3-4 - Screenshot of the Design Definition File table of contents [31] .....	16
Figure 4-1 - Astronaut Dale Gardner capturing the Westar 6 satellite during STS-51-A in November 1984 [50].....	23
Figure 4-2 - Intelsat VI being captured by three crew of STS-49 [54].....	24
Figure 4-3 - Intelsat 901 as seen from Northrop Grumman's MEV-1 [69].....	27
Figure 4-4 - Astroscale ELSA-d spacecraft in a clean room [78] .....	29
Figure 4-5 - NASA's Raven relative navigation system installed on the International Space Station [104].....	32
Figure 4-6 - The FREND robot arm undergoing servicing rehearsals at the US NRL [117] .....	36
Figure 4-7 - Hubble Space Telescope grapple fixture [126] .....	38
Figure 4-8 - Screenshot of a slide showing NASA's grapple fixture family and, in the centre, Canadarm2's Latching End Effector (LEE). Top left: Flight-Releasable Grapple Fixture (FRGF), top right: Power and Data Grapple Fixture (PDGF), bottom left: Latchable Grapple Fixture (LGF), bottom right: Power and Video Grapple Fixture (PVGf) [132].....	39
Figure 4-9 - Altius Space Machines' DogTag grappling fixture [139].....	41
Figure 4-10 - Obruta Space Systems' Puck docking interface [141] .....	41
Figure 4-11 – Altius Space Machines MagTag active and passive half configurations [143] .....	42
Figure 4-12 - iBOSS iSSI [144].....	43
Figure 4-13 - The MDA grapple fixture used on DARPA's Orbital Express Mission [65].....	43
Figure 4-14 - Testing of the MEV's probe attachment mechanism [147].....	44
Figure 5-1 - OOS architecture [151] .....	46
Figure 5-2 - Render of a OneWeb satellite in its operational configuration [157] .....	48
Figure 5-3 - A stack of 60 Starlink satellites in their Falcon 9 launch vehicle's fairing prior to launch [158] .....	49

Figure 5-4 - Chart showing the distribution of satellites in the UCS database by apogee altitude [28] .....	50
Figure 5-5 - Chart showing the distribution of satellites in LEO according to the UCS database [28] .....	51
Figure 5-6 - Chart showing the distribution of satellites in the 400-700 km altitude band according to the UCS database [28] .....	51
Figure 5-7 - Chart showing the distribution of satellites in the UCS database by orbit eccentricity [28] .....	52
Figure 5-8 - Chart showing the distribution of satellites in the UCS database by apogee and inclination [28] .....	53
Figure 5-9 - Chart showing inclination versus frequency for the satellites in the UCS database [28] .....	53
Figure 5-10 – Chart of apogee versus inclination for satellites in the 500-700 km altitude and 97.2-97.8 ° inclination region, according to the UCS database [28] .....	54
Figure 5-11 - Geometry for the mission's noncoplanar rendezvous [166, p. 366] .....	57
Figure 5-12 - Noncoplanar phasing rendezvous manoeuvre algorithm [166, pp. 368-369] .....	58
Figure 7-1 - Basic servicer CAD model with labels showing thruster numbering and inset showing axes definitions .....	79
Figure 7-2 - Screenshot of the Main Central Control spreadsheet showing modelling of the servicer thrusters [25] .....	81
Figure 8-1 - Relative navigation sensor concept .....	95
Figure 9-1 - The Next Generation Small Canadarm [229] .....	101
Figure 9-2 - Tools for RRM. Clockwise from top left: Wire Cutter and Blanket Manipulation Tool, Multifunction Tool, Safety Cap Tool, Nozzle Tool [231] .....	102
Figure 9-3 – RRM Task Boards 3 (left) and 4 (right) [233] .....	103
Figure A-1 - Overview of satellite frequency by apogee .....	144
Figure A-2 - LEO satellite frequency by apogee .....	145
Figure A-3 - Satellite frequency by apogee between 400 and 700 km .....	145
Figure A-4 - The near Earth (up to 2000 km) altitude population [5, p. 6] .....	146
Figure A-5 - Satellite frequency by orbital eccentricity for apogees between 400 km and 700 km .....	147

Figure A-6 - Apogee vs inclination for 400 to 700 km apogees and 0° to 160° inclinations.....	148
Figure A-7 - Satellite frequency by inclination for apogees between 400 km and 700 km.....	149
Figure A-8 - Apogee vs inclination for 500 to 700 km apogees and 97.2° to 97.8° inclinations.....	149
Figure D-1 - ESA TRL definitions [240] .....	192
Figure D-2 - NASA TRL definitions [241, p. 23].....	193
Figure E-1 – CAD model showing the servicer body frame definition.....	194
Figure E-2 – CAD model showing the target body frame definition .....	195
Figure E-3 – CAD model showing the docked configuration .....	196

## LIST OF TABLES

Table 2-1 - Example launch vehicle usable fairing dimensions .....	6
Table 4-1 - Examples of existing LIDAR systems [98, p. 58].....	33
Table 5-1 - Servicer mass budget [25].....	56
Table 7-1 - Orbit determination method trade-off table.....	72
Table 7-2 – Attitude determination sensor trade-off table.....	76
Table 7-3 - Examples of available chemical thruster systems .....	85
Table 8-1 - Taxonomy of spaceborne relative navigation approaches and scenarios [98] .....	92
Table B-1 - Spacecraft operational modes .....	167
Table B-2 - Software flags .....	169
Table B-3 - GNC operational modes .....	171
Table B-4 - Robot arm operational modes.....	171
Table C-1 - Orbit determination accuracy per mission mode.....	181
Table C-2 - Attitude determination accuracy per mission mode .....	181
Table C-3 - Pointing accuracy per mission mode .....	182
Table C-4 - Maximum errors at moment of docking fixture contact .....	188

## LIST OF EQUATIONS

(5-1).....	60
(5-2).....	60
(7-1).....	80
(7-2).....	80
(7-3).....	88
(E-1) .....	196
(E-2) .....	197
(E-3) .....	198

## LIST OF ABBREVIATIONS

°	degrees
A	Ampere
ADR	Active Debris Removal
ADRAS-J	Active Debris Removal by Astroscale-Japan
AE	Approach Ellipsoid
ARTES	Advanced Research in Telecommunications Systems
ASM	Altius Space Machines
ATV	Automated Transfer Vehicle
BOL	Beginning of Life
CAD	Computer-Aided Design
CCR	Corner-Cube Reflector
CCR	Corner Cube Reflector
CDF	Concurrent Design Facility
CMG	Control Moment Gyroscope
CONFERS	Consortium for Execution of Rendezvous and Servicing Operations
CONOPS	Concept of Operations
COTS	Commercial Off The Shelf
CRD2	Commercial Removal of Debris Demonstration
CSA	Canadian Space Agency
DARPA	Defense Advanced Research Projects Agency
DCM	Direction Cosine Matrix
DLR	Deutsches Zentrum für Luft- und Raumfahrt
DOF	Degree of Freedom
DORIS	Doppler Orbitography and Radiopositioning Integrated by Satellite
EO	Electro-Optical
EOL	End of Life
EP	Electric Propulsion
EPM	Electropermanent Magnet
EROSS	European Robotic Orbital Support Services
ESA	European Space Agency

ETS-VII	Engineering Test Satellite No. 7
EVA	Extra-Vehicular Activity
FCC	Federal Communications Commission
FF	Formation Flight
FoV	Field of View
FRGF	Flight-Releasable Grapple Fixture
GEO	Geostationary Earth Orbit
GNC	Guidance, Navigation and Control
GNSS	Global Navigation Satellite System
GPS	Global Positioning System
GTO	Geostationary Transfer Orbit
HET	Hall Effect Thruster
HST	Hubble Space Telescope
HTV	H-II Transfer Vehicle
IADC	Inter-Agency Space Debris Coordination Committee
IDSS	International Docking System Standard
IMU	Inertial Measurement Unit
IR	Infrared
IRP	Individual Research Project
IRU	Inertial Reference Unit
IS-901	Intelsat 901
$I_{sp}$	Specific impulse
ISS	International Space Station
iSSI	Intelligent Space System Interface
ITT	Invitation To Tender
JAXA	Japanese Aerospace Exploration Agency
JWST	James Webb Space Telescope
km	Kilometres
KOS	Keep Out Sphere
L	Litre
LED	Light Emitting Diode
LEE	Latching End Effector
LEO	Low Earth Orbit

LGF	Latchable Grapple Fixture
LIDAR	Light Detection and Ranging
LV	Launch Vehicle
m	Metres
MCC	Main Central Control
MDA	MacDonald, Dettwiler and Associates
MEV	Mission Extension Vehicle
MIMO	Multiple-Input, Multiple-Output
MMH	Monomethylhydrazine
MMU	Manned Maneuvering Unit <sup>1</sup>
MON	Mixed Oxides of Nitrogen
N	Newtons
NASA	National Aeronautics and Space Administration
NExIS	NASA's Exploration and In-Space Services
NG	Northrop Grumman
OBC	On-Board Computer
OOA	On-Orbit Assembly
OOM	On-Orbit Manufacture
OOS	On-Orbit Servicing
ORU	Orbital Replacement Unit
OTV	Orbital Transfer Vehicle
PDGF	Power and Data Grapple Fixture
PID	Proportional-Integral-Derivative
POD	Payload Orbital Delivery
PPP	Public-Private Partnership
PVGF	Power and Video Grapple Fixture
RAAN	Right Ascension of the Ascending Node
RACE	Rendezvous Autonomous CubeSats Experiment
RAL	Rutherford Appleton Laboratory
RFI	Request for Information

---

<sup>1</sup> "Manned" in the context of human spaceflight is now outdated and has been replaced with "crewed" to improve space sector inclusivity. "Manned" is used here only because it is part of an initialism that was defined by NASA before the use of "crewed" became commonplace and before NASA's style guide was amended to encourage use of "crewed" over "manned".

RNS	Relative Navigation System
rpm	Revolutions per minute
RPO	Rendezvous and Proximity Operations
RPOD	Rendezvous, Proximity Operations and Docking
RQ	Research Question
RRM	Robotic Refuelling Mission
RSGS	Robotic Servicing of Geosynchronous Satellites
RSO	Resident Space Object
RW	Reaction Wheel
s	Seconds
SEU	Single-Event Upset
SISO	Single-Input, Single-Output
SL-OMV	Small Launch Orbital Maneuvering Vehicle
SLS	Space Launch System
SOW	Statement of Work
SPENVIS	Space Environment Information System
SPIDER	Space Infrastructure Dexterous Robot
SRMS	Shuttle Remote Manipulator System
SRP	Solar Radiation Pressure
SSCP	Space Servicing Capability Project
SSN	Space Surveillance Network
SSO	Sun Synchronous Orbit
T	Tesla
TALISMAN	Tension Actuated in Space MANipulator
TDRSS	Tracking and Data Relay Satellite System
TID	Total Ionising Dose
TMR	Triple Modular Redundancy
TOF	Time-of-Flight
TONS	TDRSS On-board Navigation System
TPAD	Trunnion Pin Acquisition Device
TRL	Technology Readiness Level
TVAC	Thermal Vacuum
UCS	Union of Concerned Scientists

VESPA	Vega Secondary Payload Adapter
Wb	Weber
$\Delta v$	Change of velocity

# 1 Executive Summary

On-Orbit Servicing (OOS) includes a variety of services that together could revolutionise access to and the capabilities of the space sector. For example, hardware replacement would give spacecraft longer lifetimes and allow their functionality to be upgraded post-launch, while on-orbit assembly (OOA) would allow large structures to be built in space to support new mission architectures. This report assesses the current state of the art in OOS to understand which technologies and mission types require further development.

'Mega-constellations' will be prime targets for OOS in future due to their large size and having satellites in similar orbits to each other. The OneWeb constellation is of particular interest because its satellites have a grapple fixture installed, enabling significantly easier capture for servicing. These satellites are therefore selected as the mission target. However, other orbits such as Sun-synchronous orbit (SSO) are more densely populated, so these will be used as the orbit baseline.

Guidance, navigation and control (GNC) and relative navigation systems (RNS) are particularly crucial for OOS missions, with autonomous operations being desirable to increase spacecraft efficiency and reduce the need for human intervention. Given careful consideration of a servicing spacecraft's requirements and operations though, current technologies can be used to implement fully autonomous GNC and RNS.

Robotics and grapple are two other critical areas, with these currently being less developed in terms of the availability of commercial off the shelf (COTS) components. This is however a rapidly growing market, with several grapple fixtures currently under development. A baseline is defined that uses mature robot arm technology for dexterous operations such as hardware replacement. A grapple fixture that can be attached to the fixture already in place on the OneWeb satellites will be used, although other available fixtures will also be investigated for use in future missions.



## **2 Introduction**

This report describes the work undertaken for the author's Individual Research Project (IRP), which studied mission architectures, and technologies for guidance, navigation and control (GNC), relative navigation and grappling and robotics within the context of on-orbit servicing (OOS).

### **2.1 Background**

The impact that OOS could have on addressing the issues described in this section is discussed in Sections 4.2 OOS applications and benefits and 5.1 Background, with the various forms of OOS that could be used being described in Section 4.1 OOS types.

With OOS not currently widely available, spacecraft designers must ensure that their spacecraft can complete its mission lifetime with only the hardware in place at launch. This means that spacecraft must use high reliability components and/or be designed as fault tolerant so the mission can continue in the event of component failures.

Fault tolerance can involve techniques such as protecting against single-event upsets (SEUs) through triple modular redundancy (TMR). With this technique, three identical copies of the same circuit are implemented in the spacecraft electronics, with a bitwise majority vote used to detect whether one of the circuits has failed due to an SEU [1]. Redundancy can also be used, with key components being duplicated or triplicated so that the failure of one does not cause the wider system to fail. Generally, spacecraft designers, particularly when designing for crewed spacecraft, build fault tolerance into systems wherever possible - for example SpaceX's Crew Dragon is "two-fault tolerant", meaning any two components can fail with the capsule still able to return the astronauts safely to Earth [2]. However, while these fault tolerance techniques improve the probability of mission success, they strongly impact upon the spacecraft mass and cost

budgets, meaning designers may be required to use more exotic lightweight materials to reduce mass, or implement less functionality to reduce cost.

A further impact of the inability to replace hardware post-launch is the need to validate and qualify its design for the space environment. This leads to expensive testing being carried out on hardware at the individual component, system and whole spacecraft levels. For example, thermal vacuum (TVAC) chambers and radiation total ionising dose (TID) test equipment may be used. This is in addition to shake testing that verifies the hardware's ability to survive launch, with the shake testing being carried out whether or not the hardware was expected to be replaced during the mission lifetime.

The qualification process is part of the larger process of demonstrating a component's technology readiness level (TRL, see Appendix D Technology Readiness Levels). As well as the testing previously described, this process may also feature the flying of technology demonstration missions. These demonstrate a wider mission concept or architecture and raise the TRL of the components and systems used to implement it. Therefore, when the mission is used in a commercial way, the customer can be assured of the components' and systems' ability to perform the mission given their high TRL. However, the qualification process takes a significant amount of time, often several years from first prototype to commercial part, leading to a delay in utilisation of components that the European Space Agency (ESA) terms the "time-to-market gap problem" [3]. The process also means that when parts do become available, they can often only be procured in small quantities with long lead times, meaning designers have to make component choices extremely early in the design process, thereby imposing limitations on other systems.

Another problem currently faced by spacecraft designers is that a spacecraft's hardware is fixed at launch, meaning that due to the heritage and environmental concerns hardware is often very outdated relative to ground-based components. For example, the processor in the National Aeronautics and Space Administration's (NASA's) Mars 2020 Perseverance rover, which was launched in July 2020 [4], uses a RAD750 processor running at up to 200 MHz [5]. The

RAD750 is based on the IBM PowerPC 750 [6] that was introduced to the consumer market in 1997 and widely used in Apple consumer desktop computers [7]. Comparing this against a modern processor, the AMD Ryzen 5 3600 is a consumer mid-range desktop Central Processing Unit (CPU) released in 2019 [8] with six cores running at a base speed of 3.6 GHz [9]. This means the AMD processor has a single-core clock speed 18 times faster than the RAD750, with significantly more performance available through utilisation of all six cores.

Despite the precautions in selecting high TRL components and using redundancy and fault tolerance techniques, failures that threaten a mission still sometimes occur. Effects of failures could include a spacecraft that begins tumbling, loss of contact with ground controllers or loss of important payload data. With no method of replacing failed hardware once in orbit, except in the case of crewed missions where an extra-vehicular activity (EVA) can be performed, the spacecraft is left with permanently degraded performance unless ground controllers can find a workaround using hardware in a different way to how it was originally designed.

Even without component failure, a spacecraft's propellant will eventually become depleted. In this scenario, components may have several years of lifetime remaining, but the mission is forced to end as the spacecraft is left unable to manoeuvre to new orbits or to change its attitude if using thrusters for attitude control. An example of servicing the spacecraft to handle this scenario, Northrop Grumman's Mission Extension Vehicle 1 (MEV-1), is given in Section 4.4.1 Missions.

The disposal of a satellite once it has reached end of life (EOL) also needs to be considered. An international guideline has been established by the Inter-Agency Space Debris Coordination Committee (IADC) stating that within 25 years of EOL a satellite should re-enter the Earth's atmosphere or be retrieved if its orbit is in or passes through the low Earth orbit (LEO) region, defined as being below 2000 km altitude [10]. However, this may not be possible if the satellite's orbit is not significantly affected by atmospheric drag and/or its de-orbit system fails. In this event, the satellite would become space debris, putting it at risk of collision with

other resident space objects (RSOs) and risking the triggering of Kessler syndrome that could ultimately block access to large regions of space [11] [12].

A final issue surrounds the construction of large structures such as communications reflectors or observatories. Currently, the size of these structures is constrained by the dimensions of the launch vehicle (LV) fairing, in particular its diameter and height. Examples of these are shown for several launch vehicles in Table 2-1. Current technology is now approaching the limits of these fairings with, for example, the James Webb Space Telescope (JWST) having to use a complex series of mechanisms to deploy its sunshield, reflector and other components [13]. Even with redundancy, the greater number of mechanisms increases the likelihood that a critical failure will occur that will bring a premature end to the mission.

**Table 2-1 - Example launch vehicle usable fairing dimensions**

<b>Launch Vehicle</b>	<b>Fairing diameter (m)</b>	<b>Fairing height (m)</b>	<b>Reference</b>
Falcon 9/Heavy	4.6	11	[14, p. 37]
Ariane 5	4.57	15.589	[15, pp. A5-2]
Ariane 6	5.4	18	[16, pp. 5-5]
Space Launch System (SLS)	9.1	Approx. 24.53	[17, p. 68]

## **2.2 Aim**

This report will investigate how OOS can be used to tackle the issues described in the previous section. It aims to use literature to build understanding of the limitations of previous implementations of OOS and how these can be overcome using current technology to enable wider adoption of OOS.

A systems engineering approach will be used throughout to examine what technologies are required to enable OOS and whether those technologies are currently available. By examining OOS on a systems level, the report aims to highlight the considerations that will need to be made by future spacecraft designers when designing their spacecraft to support OOS, primarily as a servicer but also as a client.

In particular, the report will focus on technologies for guidance, navigation and control (GNC), rendezvous and proximity operations (RPO), grappling and robotics. These technologies are critical for a servicer spacecraft [18], with the ESA Technology Strategy calling for advancements in “technology fields such as advance capturing, image processing and proximity guidance, navigation and control” [19, p. 23] to support OOS.

Finally, the report will give examples of future work across various disciplines that would be needed to further develop the presented design, such as radiation analysis and detailed control loop simulation.

## **2.3 Research questions**

To ensure this report’s focus remains targeted at the aims described previously, the following research questions (RQs) will be answered, either by the literature review or later systems analysis and design.

- RQ 1      What are the different types of on-orbit servicing?
- RQ 2      What OOS has been achieved previously?
- RQ 3      What is the current state of the art in OOS?
- RQ 4      Which technologies will need to be developed to enable greater use of OOS and which are currently available?
- RQ 5      How could a servicing spacecraft’s GNC and robotics be designed to support fully autonomous OOS?

These questions seek to provide a solid foundation of knowledge on OOS that can then be developed to discover which current technologies can be used for OOS and which will require further development.

## **2.4 Report overview**

Overall, this report seeks to use an evidence-based approach combined with systems engineering to answer the RQs outlined in the previous section. Firstly, the report will describe aspects of the project's management including a work breakdown structure, tools used and important documentation.

Section 4 Literature Review will assess past uses of OOS and the current state of the art in terms of missions and various types of hardware. This will provide an academic foundation that will then be built upon with systems engineering processes throughout the document.

A systems engineering approach will be followed for the remainder of the report while defining an example OOS mission and the technologies to be used by the mission's servicer spacecraft. In Section 5 Mission Analysis and Design an example OOS mission with a servicer spacecraft and a target will be defined. This will include why servicing of targets similar to the satellites of the OneWeb 'mega-constellation' was chosen as the mission's focus. It will also outline the orbit selection process for the mission, which is shown in greater detail in Appendix A Satellite Distribution Research and Orbit Selection. Initial sizing of the tug spacecraft that will complete the servicing will be described, with these estimates being used in later sections when designing the tug's systems.

Section 6 Requirements Definition will focus on how the mission, tug and system requirements were derived from the mission architecture and how they were verified. System verification against these requirements will then be discussed in the systems' relevant sections throughout the report. The requirements list will be shown in full in Appendix C Space Servicer Requirements Specification.

The three sections following requirements definition are dedicated to selection of components for the guidance, navigation and control (GNC) system, the relative navigation system and the robotics and grappling systems. When discussing GNC and relative navigation the systems' requirements will be addressed, and suggestions will be made for components that could fulfil them. However, in a real industrial design scenario more detailed analysis would be required by the mission's dedicated GNC and relative navigation engineers, which is out of this report's scope due to its systems-level focus.

The GNC will be broken down into sensors and actuators in Section 7 Guidance, Navigation and Control (GNC) System, both for attitude and orbit determination and control. This section will also give an overview of the GNC control loop and plant as well as various calculations that feed into them.

In Section 8 Relative Navigation System (RNS), the report's focus will turn to the sensors used by the servicer to perform relative navigation towards its target. This will discuss the architecture for the sensor suite and how specific types were selected. Examples of viable components will be given, but detailed trade-off of these is again left to a dedicated RNS engineer.

Section 9 Grappling and Robotics will focus on the mechanism used to attach the servicer to the target and on the servicer's robotic arm used for servicing operations once docked. This will describe how the grappling fixture selection is directly related to the mission background described in Section 5.1 Background and will then discuss the selection of an appropriate robot arm.

Finally, the report will outline in Section 10 Areas for Future Development a selection of items that would need to be carried out for the project to be developed further. The report's conclusions will then be discussed in Section 11 Conclusion.

Several documents that were produced during the course of the project, as well as detailed calculations used to find centres of mass and inertia matrices, are provided in full in the report's appendices.

## **3 Project Management**

This section is written in the same style as the author's Group Design Project (GDP) report [20].

### **3.1 Work breakdown structure**

The work breakdown structure (WBS) shown in Figure 3-1 was used to compartmentalise the various aspects of the project into work packages (WPs). The author worked across all of these WPs during the course of the project. While the structure was useful for categorising various tasks, it was not used extensively. This was because the individual nature of the project meant WPs could not be shared between team members in the same way that they were successfully during the author's GDP.

### **3.2 Tools**

#### **3.2.1 Trello**

Figure 3-2 shows a page that was created on Trello [21] at the start of the project to aid in task management. This was done to enable easy compartmentalisation and tracking of tasks to ensure none were missed. Each task was shown in a 'card', with cards grouped together in 'lists'. A key anticipated advantage of the Trello page over a more manual approach was its Gantt chart functionality, enabled through use of the Elegantt plugin for Google Chrome [22]. However, shortly after creating the project Gantt chart in Elegantt, it was realised that the software only allowed tasks with a start date in the past to be viewed if using a paid version of Elegantt. This lack of functionality, combined with the author's experience managing projects without using Trello, led to tasks being managed using a more traditional systems engineering approach.

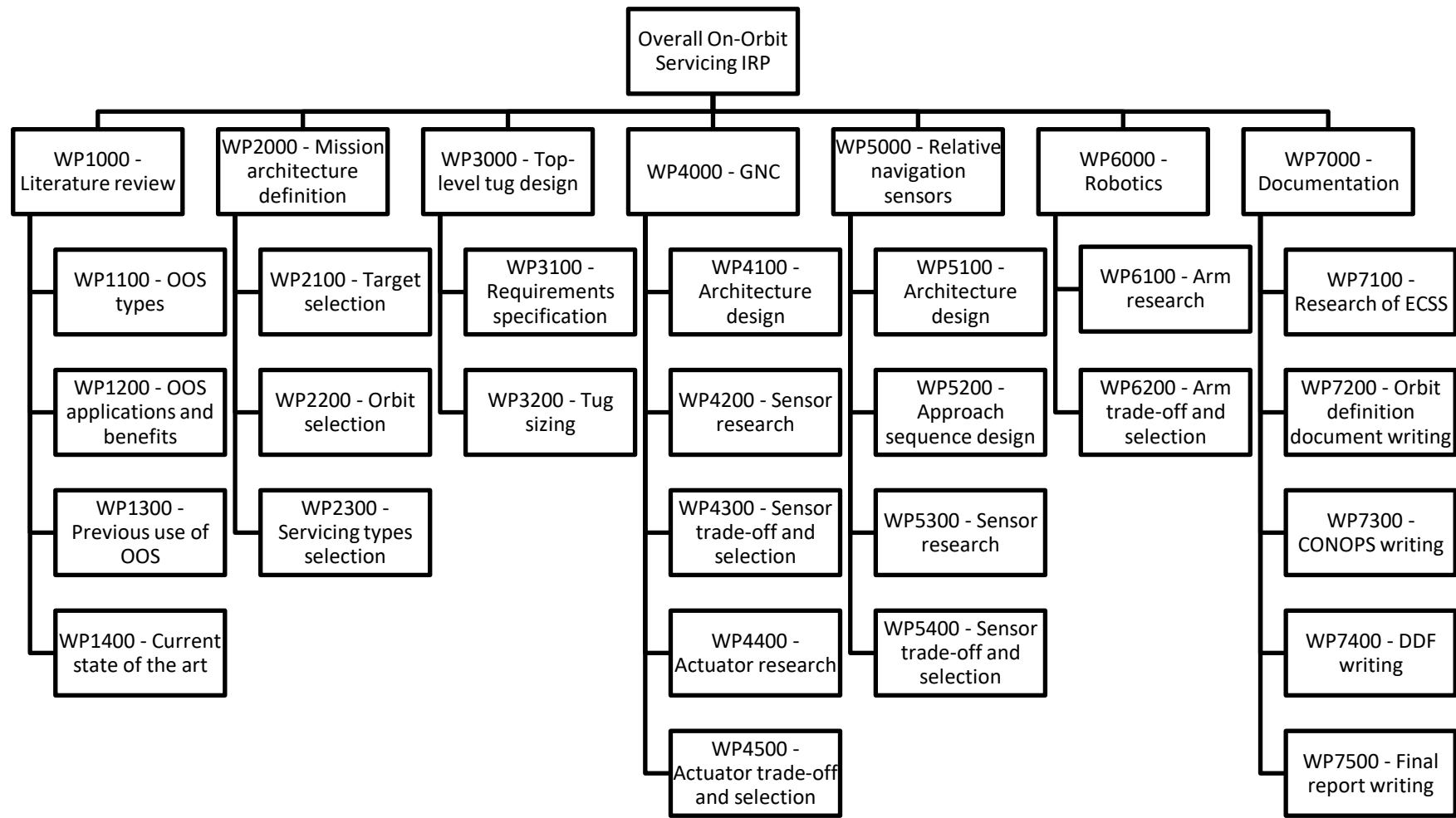


**Figure 3-1 - Project work breakdown structure**



**Figure 3-2 - The project page on Trello**

### **3.2.2 OneDrive**

Throughout the project, working documents such as this report were stored locally on the author's personal computer to allow quick opening times and independence from an internet connection. However, Microsoft OneDrive [23] was also used extensively. This was primarily done to give a common storage area with project supervisor Dr Leonard Felicetti. By using OneDrive in this way, useful papers and other resources could be shared and Dr Felicetti could easily track the project's progress. Documents were separated into folders by type with, for example, folders for meeting minutes and for papers.

As well as shared storage, OneDrive was used as an online backup location, with periodical uploads of all locally stored files to OneDrive. This ensured that in the event of a catastrophic event such as a fire that destroyed the local main files and backup (which was automatically taken hourly), the author could still access a version of the files that were stored in a different geographical location to continue the project.

### **3.3 Documentation**

Throughout the project, several pieces of documentation were produced to aid information tracking, to describe selection processes for mission elements and to

formalise the design of the tug and wider mission architecture. Several of these are shown in the appendices.

### **3.3.1 General Running Notes document**

The first of these was a General Running Notes document [24]. This was an informal document used to contain project notes in a single location and grouped by date, enabling easy reference to them throughout the project. For example, notes included important equations, examples of parts to be traded off and links to reliable sources of information useful to the project.

### **3.3.2 Main Central Control spreadsheet**

For tracking of system values and to enable system engineering processes to be followed, a spreadsheet called Main Central Control (MCC) was created [25]. This contained a range of pages to cover aspects such as mass budgets, orbital manoeuvres and thruster design. A screenshot of the Propulsion page of the spreadsheet is shown in Figure 3-3 as an example. By linking between cells across the various pages, relationships were established between mission architecture aspects and tug systems.

For example, the Space Tug page included a mass budget. The dry mass value from this was combined with a total  $\Delta v$  requirement calculated on the Propulsion page to feed into a total tug wet mass, with the wet mass then used on the Thruster page to work out the maximum acceleration that the spacecraft thrusters (described in more detail in Section 7.6.2 Orbit control methods and selection) could provide. By linking cells' values and equations in this way, impacts of changes to the tug design on various spacecraft systems could be seen instantly and easily. This allowed the author to follow a model-based system engineering (MBSE) approach, which was adopted by ESA in 2013 for its e.Deorbit mission (see Section 4.4.1 Missions) over their existing approach using written documentation [26].

Non-coplanar phasing manoeuvre (Vallado)		Process		Output	
Input					
$h_{station}$ (start of transfer)	600 km	$\omega_{interceptor}$	0.00108 rad.s <sup>-1</sup>	$T_{trans}$	47.927 min
$h_{target}$ (end of transfer)	520 km	$\omega_{target}$	0.00110 rad.s <sup>-1</sup>	$T_{phase}$	93.59 min
$\theta_{interceptor}$	6,978 km	$\theta_{transfer}$	6,938.000 km	$h_p$ phase	301.04 km
$\theta_{target}$	6,898 km	$\alpha_c$	181.6 °	$\Delta V_{phase}$	0.083 km.s <sup>-1</sup>
$\kappa_{target}$	25 -	$\Delta V_{int}$ to node	176.0 °	$\Delta V_{trans1}$	0.061 km.s <sup>-1</sup>
$\kappa_{interceptor}$	25 -	$\Delta t_{node}$	47.268 min	$\Delta V_{trans2}$	0.045 km.s <sup>-1</sup>
$\omega_{interceptor}$	4 °	$\omega_{tgt}$ to node	179.1 °	$T_{total}$	188.789 min
$\Omega_{interceptor}$	45 °	$\lambda_{true}(tgt1)$	359.1 °	$\Delta V_{total, rendezvous}$	0.1900 km.s <sup>-1</sup>
$\lambda_{true}(target)$	180 °	$\lambda_{true}(int1)$	225.0 °	$\Delta V_{docking}$	0.0250 km.s <sup>-1</sup>
$\Delta i$	0.3 °	$V_{new}$	-134.1 °	$\Delta V_{total}$	0.2150 km.s <sup>-1</sup>
		$\alpha_{new}$	45.9 °	$\Delta V_{total}$ w/ margin	0.2258 km.s <sup>-1</sup>
		$P_{phase}$	2339.9 min		<a href="#">Margin per MAR-DV-010</a>
		$\theta_{phase}$	6828.518 km		
		$V_{int}$	7.558 km.s <sup>-1</sup>		
		$V_{tgt}$	7.602 km.s <sup>-1</sup>		
		$V_{phase}$	7.475 km.s <sup>-1</sup>		
		$V_{trans1}$	7.536 km.s <sup>-1</sup>		
		$V_{trans2}$	7.624 km.s <sup>-1</sup>		
		$\Delta V_{trans2}$	0.002 km.s <sup>-1</sup>		

Thruster Properties		Process		Output	
Input					
Max % of period for impulsive	5%	$T_{max}$ $T_{phase}$ impulse	4.680 min	$\mu_{min, dv, phase}$	0.296 m.s <sup>-2</sup>
$m_{total, docked}$	455.9 kg	$T_{max}$ $T_{trans}$ impulse	4.793 min	$\mu_{min, dv, trans1}$	0.213 m.s <sup>-2</sup>
				$\mu_{min, dv, trans2}$	0.158 m.s <sup>-2</sup>
				$\mu_{min, overall}$	0.296 m.s <sup>-2</sup>
				$\mu_{min, w/ margin}$	0.356 m.s <sup>-2</sup>
				$F_{min, total}$	135.07 N
				$F_{min, total}$ w/ margin	162.08 N

Propellant Properties	
Input	Output
Fuel/Oxi	Hydrazine/N <sub>2</sub> O <sub>4</sub>
Fuel/Oxi density	1.22 kg/L
$t_{sp}$	215 s

Propulsion system sizing	
Input	Output
Return 2	

Figure 3-3 - Screenshot of Propulsion page of Main Central Control spreadsheet [25]

### 3.3.3 Requirements document

The document Space Servicer Requirements Specification [27] was written to encapsulate the requirements for the overall spacecraft and its systems. The requirements contained in this document are discussed in Section 6 Requirements Definition and in the subsequent system sections.

### 3.3.4 Orbit selection document

A key task early in the project that had wide-ranging implications later on was the selection of the orbits that the tug would use as its starting point and where its

customers would be. The orbit selection process is described in more detail in Section 5.2 Orbit selection. To facilitate the selection and to document the research that led to it, a document called Satellite Distribution Research and Orbit Selection [28] was created, which is shown in full in Appendix A Satellite Distribution Research and Orbit Selection.

This document used the April 1<sup>st</sup>, 2020 version of a dataset of over 2,600 satellites compiled by the Union of Concerned Scientists (UCS) [29]. The data were analysed to determine which orbits were most densely populated, with these orbits becoming the targets for the project's OOS tug. This document therefore had a large impact on the rest of the project. More detail of the research carried out in the document and the results obtained from it can be found in Section 5.2 Orbit selection.

### **3.3.5 CONOPS**

A Concept of Operations (CONOPS) document [30] was written to formalise the project's mission architecture and operations matters such as operational modes and contingency operations. The CONOPS, particularly the operational modes, were referred to throughout the design process to ensure components were traded off and selected with the same mission parameters in mind. The CONOPS is shown in full in Appendix B CONOPS.

### **3.3.6 Design Definition File**

A Design Definition File (DDF) [31] was constructed to formally describe the design of the tug's GNC, relative navigation and robotic systems. ECSS-E-ST-10C [32], which details general system engineering requirements for space missions, was referred to while structuring this. In particular, its Annex G describes the requirements for a DDF, which ensured that the DDF would contain the information needed for later design work and would describe the tug's systems in sufficient depth. DDFs for other missions were also referred to. These

included the Sentinel-2 Agriculture software processing system [33], GMV’s BIBLOS software suite [34] and the Finnish Meteorological Institute’s GlobSnow project [35], with these providing useful insight into the structure required for the tug DDF. The DDF table of contents is shown in Figure 3-4. However, due to the time constraints of the project, development of the document beyond initial structuring did not progress significantly.

**TABLE OF CONTENTS**

LIST OF FIGURES .....	iii
LIST OF TABLES .....	iv
LIST OF EQUATIONS .....	v
LIST OF ABBREVIATIONS .....	1
1 Introduction .....	3
2 References .....	4
2.1 Applicable Documents .....	4
2.2 Reference Documents .....	4
2.3 Definitions .....	4
3 Docking Interface .....	5
3.1 Detailed Description .....	5
3.2 Flow Diagram .....	5
3.3 Interfaces .....	5
3.4 Scope and Limitations .....	5
3.5 External Libraries .....	5
3.6 Errors and Warnings .....	5
4 GNC .....	5
4.1 Detailed Description .....	5
4.2 Flow Diagram .....	5
4.3 Interfaces .....	6
4.4 Scope and Limitations .....	6
4.5 External Libraries .....	6
4.6 Errors and Warnings .....	6
5 Robotics .....	6
5.1 Detailed Description .....	6
5.2 Flow Diagram .....	6
5.3 Interfaces .....	6
5.4 Scope and Limitations .....	6
5.5 External Libraries .....	6
5.6 Errors and Warnings .....	7
Annexes .....	9
Annex A Reference Frames .....	9

**Figure 3-4 - Screenshot of the Design Definition File table of contents [31]**

## 4 Literature Review

This literature review seeks to understand what examples of OOS have previously been demonstrated, what the current state of the art is, and which technologies will require further development to enable autonomous OOS. This enables a literature-supported baseline to be set for the technology to be used in this report's mission.

Section 4.1 OOS types will address RQ 1, while Sections 4.3 Previous use of OOS will answer RQ 2. Section 4.4 Current state of the art will partially cover RQ 4, with this being discussed further and RQ 5 being addressed by later sections of this report.

### 4.1 OOS types

On-orbit servicing as a whole can be split into five distinct operation types:

- 1) **Active Debris Removal (ADR)** –derelict satellites or other dangerous resident space objects (RSOs) are removed from orbit to avoid collisions with active satellites or triggering of Kessler Syndrome [11] [12] (e.g. Astroscale ELSA-d – see Section 4.4.1 Missions)
- 2) **Orbit maintenance** – if a client spacecraft has run out of fuel, a servicer can be used to maintain its orbit to extend mission lifetime (e.g. Northrop Grumman Mission Extension Vehicle 1 – see Section 4.4.1 Missions). The servicer could also move the client to new orbits as client mission needs dictate. Note that this definition does not include vehicles such as the Moog Small Launch Orbital Maneuvering Vehicle (SL-OMV) [36], Firefly Aerospace Orbital Transfer Vehicle (OTV) [37] or similar vehicles from Momentus Space [38], as these transfer vehicles are attached to the client spacecraft during launch rather than rendezvousing and docking with it later in the mission

- 3) **Hardware replacement/refuelling** – hardware replacement enables the mission to be extended beyond its original lifetime by replacing broken components. Spacecraft could also have functional components replaced to upgrade to new technology that was not available at the time of launch. Refuelling extends mission lifetime and enables missions to more distant destinations that have a higher  $\Delta v$  requirement
  
- 4) **On-orbit assembly (OOA) of large structures** – spacecraft can be assembled that have greater capability than could be launched in a single launch vehicle. Example applications include communication arrays (previously investigated by Airbus Defence & Space under the Vast Satcom ANTenna (VASANT) project) and observatories (e.g. eventual replacement for James Webb Space Telescope). Robotic OOA “is a long-term NASA goal to reduce launch costs and enable larger scale missions” [39, p. 1]
  
- 5) **On-orbit manufacture (OOM) of high value components** - uses the microgravity, high vacuum and extreme temperature properties of the space environment to produce components that would be impossible to manufacture on Earth or to produce them to higher quality levels (e.g. SpaceForge fibre optic cable – see Section 4.2 OOS applications and benefits)

In 2019, ESA published a Statement of Work (SOW) for the preliminary design of an “on-orbit servicing station for satellite manufacture, refurbish and recycle” [40]. The SOW considers the following applications for the servicing station: on-orbit assembly/disassembly of client spacecraft, re-use of components from one spacecraft in another, refurbishment of spacecraft by replacing parts, on-orbit manufacture of spacecraft parts from raw materials or basic components,

recycling of old spacecraft parts or debris into raw material that can be used for OOM. While the ability to support these applications would clearly be advantageous for the future space economy, this report will focus on OOS where only a servicer or tug spacecraft and the client spacecraft are involved. This is significantly simpler than using a servicing station and therefore can be implemented sooner, with complex steps such as creation of a servicing station coming once more basic forms of OOS have been matured. All of the aforementioned servicing types could be achieved without a dedicated servicing station, albeit with potentially more complex mission architectures.

ESA's Concurrent Design team is studying on-orbit servicing under its On-orbit Manufacturing Assembly and Recycling (OMAR) activity. Under this activity, invitations to tender (ITTs) have been published to address on-orbit manufactured spacecraft, the aforementioned on-orbit servicing station, and design of spacecraft for recycling [3].

## **4.2 OOS applications and benefits**

This section will describe how OOS can be used to address the issues discussed in Section 2.1 Background.

The problem of needing to design hardware for the challenging launch and on-orbit environments can be addressed by replacing hardware on orbit. As the hardware will not have to be in its final location within the target satellite at launch, it could be launched in an enclosure that gives it more protection from the launch vibration and acoustic environment. This would reduce the stress on the component during launch, meaning lower rated components could be used.

Hardware replacement would also mean the hardware could be designed for a significantly shorter lifetime. This would lower the radiation TID experienced, meaning parts with decreased radiation tolerance such as rad tolerant or even COTS parts could be used in place of expensive rad hard components. These parts would have reduced cost relative to traditional space-rated components.

Because a reduced level of testing is required, expensive test chambers would not have to be hired for as long a duration, reducing cost significantly.

These components would likely have shorter lead times than fully rad hard components, speeding up hardware development and allowing newer parts to be selected. This would mean that replacement hardware modules could bring upgraded or new capability to the satellite, enhancing its performance part way through the mission lifetime. This upgrade process was used on the Hubble Space Telescope (HST) – see Section 4.3 Previous use of OOS.

Hardware replacement not only allows improvement of spacecraft capability over time but also the replacement of broken components that would otherwise cause a degradation of the satellite's functionality. For example, a broken solar panel could be replaced with a new unit, as is planned to be demonstrated by DARPA's Robotic Servicing of Geosynchronous Satellites (RSGS) program (see Section 4.4.1 Missions). Similarly, OOS could be used to repair malfunctioning hardware, such as a solar panel that has failed to deploy. Due to the above reasons, hardware replacement offers to create a new paradigm for space engineering and could enable cheaper, faster access to space, making space services available to a much wider selection of users.

ADR is another important area of OOS and seeks to remove inactive resident space objects (RSOs) before they can pose a threat of collision to active satellites or collide with other objects to create a larger debris field. For example, the destruction of the Fengyun 1C weather satellite by a Chinese anti-satellite weapon test in 2007 and the collision between Cosmos 2251 and Iridium 33 in 2009 together account for "over 30% of all catalogued resident RSOs" [41, p. 1]. ADR and OOS more widely are key elements of ESA's Technology Strategy, which is aiming to "invert Europe's contribution to space debris by 2030" [19, p. 26]. However, due to the ADR's added challenge of grappling targets that are likely to be tumbling, ADR is out of scope for this research.

The orbit maintenance OOS type enables a spacecraft to have its lifetime extended by a servicer docking and acting as its propulsion system. Northrop Grumman's MEV-1 discussed in Section 4.4.1 Missions is an example of an

implementation of this. This can be used when a spacecraft's lifetime is limited by its fuel reserves rather than the lifetime of its components, as is often the case for geostationary Earth orbit (GEO) satellites like those serviced by the MEV. Approximately 20 satellites are retired annually due to propellant depletion [42, p. 41], with many of these likely being potential servicing customers. In an orbit maintenance scenario, the servicer docks with the cooperative target but no transfer of fuel or materials take place, making this easier to implement than ADR or refuelling.

Spacecraft refuelling is an area of OOS that would be of great benefit to satellite operators. This can extend the lifetime of a satellite as with orbit maintenance, but specialist refuelling hardware is required on the servicer to transfer propellant between the two vehicles. Significant research is being undertaken into refuelling on-orbit (see Section 9.3 Tooling and sensing) but it is not yet used commercially.

A key advantage of the fourth servicing type, on-orbit assembly (OOA), is it allows structures to be built in space that could not be launched in a single launch. These structures include, for example, reflectors for future space-based observatories [43]. This means that significantly greater capability can be built into mission architectures than could be delivered using a single-launch satellite. The assembly of space stations and large transit vehicles for interplanetary spaceflight can also be considered applications of OOA. In this way, OOA can enable entire new mission architectures. While this report will not explicitly examine OOA, many of the technologies and techniques described will be applicable to OOA.

On-orbit manufacture (OOM) is an area of OOS that is currently in the early phases of development by companies such as SpaceForge [44] and Made In Space [45], with the former designing a system to manufacture high quality fibre optic cable on orbit. While the created materials have to be of high value to compensate for the high launch cost of the raw materials, space's microgravity environment enables more exotic materials (such as fibre optic cable) than can be produce on Earth. However, OOM is also out of scope of this report as its use of a single spacecraft means it is not reliant on new GNC technology for

rendezvous and proximity operations (RPO) but rather on materials science and engineering to create products.

### **4.3 Previous use of OOS**

Before beginning development of a new OOS mission, it is important to understand previous implementations and the current state of the art, so these can be built upon moving forward. This section discusses previous missions that have demonstrated or made use of OOS, with the current state of the art discussed in the following section.

NASA have extensive experience of OOS, with the replacement of Skylab's heat shield in 1973 being the first example [46]. The crew of the SL-2 mission deployed a sun shade to reduce the temperature inside the station and freed a jammed solar array, giving Skylab sufficient power to continue its mission [47].

The first uncrewed satellite to be repaired in orbit was the Solar Maximum Mission, or SolarMax [48, p. 116]. After failures in its attitude control system, an attempt was made during the STS-41C Space Shuttle Challenger mission in April 1984 to capture the satellite so it could be returned to Earth. The mission plan called for astronaut George Nelson to use a tool called the Trunnion Pin Acquisition Device (TPAD) to try to capture docking pins on SolarMax's service module. Nelson would then tow SolarMax back to Challenger's payload bay using his Manned Maneuvering Unit's (MMU) thrusters [48]. The mission failed after the TPAD bounced off during attempts to mate with SolarMax. An investigation revealed the cause to be a grommet that had not been accounted for during design of the TPAD [49]. Subsequent use of Challenger's "Canadarm" Remote Manipulator System allowed the crew to grapple SolarMax and berth it to the Shuttle, despite this procedure having been judged by flight controllers pre-flight to be too risky [48, p. 116]. During a second EVA, crew members were then able to repair the satellite.



**Figure 4-1 - Astronaut Dale Gardner capturing the Westar 6 satellite during STS-51-A in November 1984 [50].**

In November 1984, the STS-51-A mission with the Space Shuttle Discovery recovered the satellites Palapa B2 and Westar 6, marking the first time that a satellite had been brought back intact from orbit [51]. Both had experienced failures of their perigee kick motors after both being deployed from the Space Shuttle Challenger during STS-41-B in February 1984. To enable the Shuttle's recovery of the satellites, their apogees were lowered from around 970 km to around 350 km and their spin rates reduced to around 1 revolution per minute (rpm) [49, p. 297]. For the capture itself (see Figure 4-1), astronauts Joseph Allen and Dale Gardner performed an EVA, again using the MMU. Each astronaut had a 'stinger' device attached to their MMU with a probe that was inserted into the apogee kick motor of the respective satellite [48, p. 116]. With the two satellites having extremely similar designs, the same method could be used on both [52]. The original plan then called for a grapple fixture to be fixed in place of each satellite's omnidirectional antenna, which would then be grappled by the Shuttle's Canadarm. However, a previously unknown clearance issue on Palapa B2 meant the fixture could not be attached. Instead, Gardner was able to attach an adapter

to the bottom of the satellite so it could be stowed in the Shuttle's payload bay. This procedure was repeated for Westar 6 [52].

The STS-41C and STS-51-A missions proved that on-orbit servicing of satellites was possible, despite unexpected challenges being faced on both missions. They also showed the value in having crew in-situ to provide feedback on progress and improvise when necessary.

During 1992's STS-49, three crew members captured the Intelsat VI satellite by hand as shown in Figure 4-2 after earlier attempts to attach a capture bar had failed. The EVA was the longest of the Shuttle era and the only one to use three crew members [48, p. 118] [53].



**Figure 4-2 - Intelsat VI being captured by three crew of STS-49 [54]**

The Hubble Space Telescope is a particularly notable examples of early OOS, with five servicing Shuttle missions taking place to repair and upgrade the telescope between 1993 and 2009 [48, p. 25]. These included fixing the primary mirror and replacing or upgrading Hubble's equipment such as gyroscopes and

cameras to extend its mission lifetime [48, p. 325]. Hubble also made extensive use of orbital replacement units (ORUs) for hardware such as cameras, batteries and communications equipment, with 70 ORUs in total that could be swapped out on orbit [55]. This made Hubble one of the first uncrewed satellites, after SolarMax, to be designed for hardware replacement.

Japan's Engineering Test Satellite No. 7 (ETS-VII) launched in 1997. It was the first satellite to use a robot arm [56, p. 417] and the first spacecraft to perform autonomous rendezvous and docking [57]. The satellite included a 2,500 kg chaser satellite and a 400 kg target. The robot arm was 2 m long and had a camera suite mounted to its end effector. The rendezvous and docking system featured a proximity camera for pose measurements within 2 m range and a LDIAR for range measurements between 2 m and 500 m. Beyond 500 m, the distance between the satellites and their relative velocity was found using GPS receivers mounted on both satellites [56, p. 417].

## **4.4 Current state of the art**

### **4.4.1 Missions**

ESA's e.Deorbit ADR programme began work in 2013, initially studying the removal of the Envisat Earth observation satellite. Five years of work enabled funding to be found for technology development, but not for the e.Deorbit mission specifically. As a result, in 2018 the mission pivoted from ADR to OOS more widely and ESA "asked industry to make proposals to remove a defunct ESA satellite while demonstrating in-orbit servicing" [26]. This was formalised in a request for information (RFI) published by ESA [58]. According to e.Deorbit's study manager, Robin Biesbroek, "the main challenge is not technical – it is to get the money" [26].

However, during the mission development, the team did also discover that the net-based system that had been designed would lead to challenges, such as controlling Envisat after capture [59]. These issues are described in detail in Section 4.4.4 Attachment methods. e.Deorbit's final presentation took place in

November 2018 [26], meaning the mission development in its original form has now concluded.

The University of Surrey's RemoveDEBRIS was an ADR technology demonstration mission that commenced operations in June 2018 [60]. Its main goal, which it completed successfully, was to demonstrate net and harpoon technologies to capture a tumbling target. These are discussed further in Section 4.4.4 Attachment methods.

Orbital Express was a 2007 mission by the US' Defense Advanced Research Projects Agency (DARPA). It was comprised of a prototype servicing satellite called ASTRO and a serviceable satellite called NextSat [61]. Its purpose was to "demonstrate the operational utility, cost effectiveness, and technical feasibility of autonomous techniques for on-orbit satellite servicing" [62, p. 8]. Orbital Express successfully demonstrated autonomous rendezvous and proximity operations as well as transfer of hydrazine propellant and replacement of battery and computer hardware [62]. During operations, the ASTRO vehicle experienced a sensor computer failure that almost halted the mission, but ground controllers were able to re-mate it with NextSat [62].

DARPA's Robotic Servicing of Geosynchronous Satellites (RSGS) [63] is a mission currently under development that is scheduled to launch in 2023 [64]. It seeks to develop and demonstrate "technologies that would enable cooperative inspection and servicing in GEO" [63]. This has involved development of technologies such as the Front-end Robotics Enabling Near-term Demonstration robot arm that is discussed further in Section 4.4.3 Robotics and a grappling fixture discussed in Section 4.4.4 Attachment methods. The mission will include the use of Payload Orbital Delivery (POD) systems [65] that would be used to transport payloads to GEO and "could deliver robotic servicing and replacement or augmentation components to the [DARPA RSGS] Servicer/Tender on an as-needed basis" [65, p. 1]. In March 2020, Space Logistics LLC was announced as a commercial partner on the RSGS program. Space Logistics is the wholly-owned subsidiary of Northrop Grumman that produces the Mission Extension Vehicle

(see below) [64] [66], meaning RSGS will allow Northrop Grumman to further develop their GEO servicing technology.

Airbus O.CUBED Services is a programme being developed by Airbus Defence & Space that will use a new vehicle known as SpaceTug to perform servicing in GEO and LEO as well as ADR [67] [68]. It will provide services similar to Northrop Grumman's Mission Extension Vehicle (MEV, see below) as well as offering hardware replacement and inspection services, while a 'Carrier' version of the SpaceTug will tow satellites from LEO to GEO or aid deployment of constellations [67]. The 'Cleaner' version of the spacecraft, for ADR, will use technologies and techniques developed for and demonstrated by the RemoveDEBRIS mission to de-orbit space debris [67].

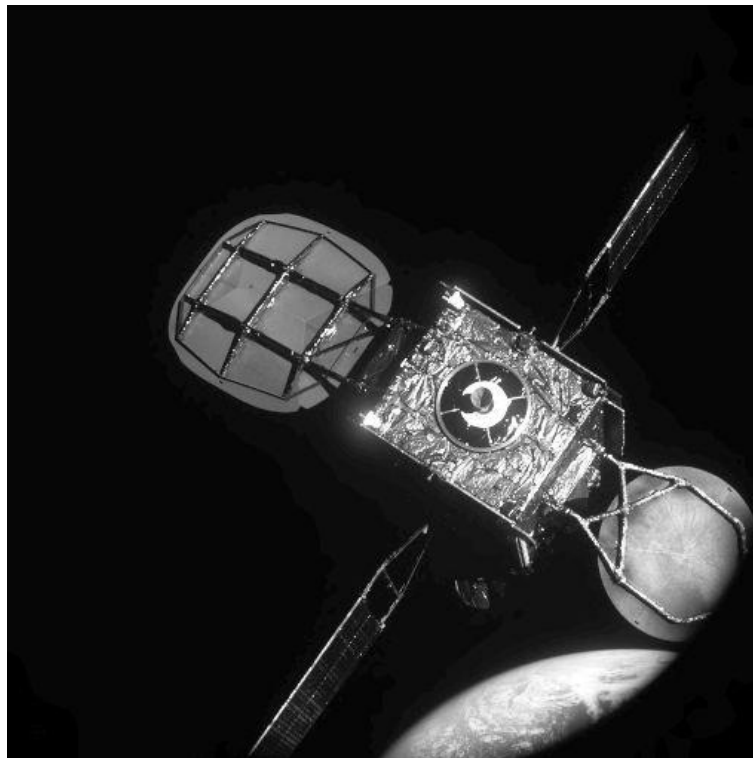


**Figure 4-3 - Intelsat 901 as seen from Northrop Grumman's MEV-1 [69]**

In 2019, the Intelsat 901 (IS-901) GEO satellite was approaching fuel depletion, which would have necessitated its end of life (EOL). The satellite was taken out of service and moved to a graveyard orbit to meet Northrop Grumman's (NG) Mission Extension Vehicle 1 (MEV-1). The two spacecraft docked in February 2020, marking the first docking of two commercial satellites [69]. MEV-1's

approach to IS-901 is shown in Figure 4-3. MEV-1 acted as an add-on propulsion system and manoeuvred IS-901 back into an operational orbit, enabling it to re-enter commercial service in April 2020 with five further years of life expected from the Intelsat satellite [70]. Once MEV-1 has completed its mission with IS-901, it will move on to a second client [69].

MEV-2 successfully launched on August 14<sup>th</sup>, 2020 and will service the IS-1002 satellite [71] in the same way as IS-901. Due to the success of MEV-1, IS-1002 will not be moved out of its operational orbit. This manoeuvre with IS-901 had been done to reduce the risk of any debris from a failed docking affecting other operational satellites in GEO [72]. Instead, MEV-2 will dock with IS-1002 in GEO while IS-1002 is still in service [73]. Docking is expected to occur in early 2021 [74], with the disruption to IS-1002's services to last only 20-30 minutes [72].

In 2018, British company Effective Space Solutions (ESS) partnered with Israeli Aerospace Industries on a development of a spacecraft called Space Drone that would provide similar services to the MEV [75]. ESS was then bought by Astroscale US in June 2020, with a new Astroscale Israel arm being established. As part of this, the Space Drone programme "will evolve into an Astroscale US life-extension platform" for GEO satellites [76]. According to Astroscale, independent valuations estimate that "life extension and other on-orbit satellite services will generate more than \$4 billion in revenues by 2028" [77].

Astroscale's new venture in GEO life extension services complements their existing work on disposal of satellites that have reached EOL. Their End-of-Life Services by Astroscale (ELSA) programme is developing technologies to de-orbit failed spacecraft, with a demonstration mission, ELSA-d (shown in Figure 4-4), scheduled to launch in late 2020 [78]. ELSA-d will include a 175 kg servicer and a 17 kg client spacecraft that will demonstrate absolute and relative navigation, safety procedures and capturing of tumbling and non-tumbling clients. As well as required technology, the mission will demonstrate Astroscale's CONOPS for a full servicing mission [79].

The ELSA architecture is being particularly aimed at large constellations in LEO [78]. Astroscale is developing a version of the ELSA mission to specifically target

OneWeb's satellite constellation. Called ELSA-OW, it has been funded under ESA's Project Sunrise public-private partnership (PPP) and will use technology demonstrated on ELSA-d. The mission will make use of the grapple fixture attached to each OneWeb satellite (see Section 5.1 Background) to allow the servicer to dock. Multiple OneWeb satellites would be de-orbited by the ELSA-OW servicer, with it using electric propulsion to move between orbits [80].



**Figure 4-4 - Astroscale ELSA-d spacecraft in a clean room [78]**

Italian company D-Orbit also has an agreement with OneWeb under the Project Sunrise PPP to “develop the Phase A feasibility study for an ADR solution based on proprietary technology and heritage” [81]. The PPP has OneWeb on the private side, with ESA's Advanced Research in Telecommunications Systems (ARTES) programme on the public side. ARTES allows other private organisations to be involved in the project [81].

Astroscale is also developing a mission architecture for ADR and have been selected by the Japanese Aerospace Exploration Agency (JAXA) as a partner in JAXA's Commercial Removal of Debris Demonstration (CRD2) project [82]. This will involve Astroscale's Active Debris Removal by Astroscale-Japan (ADRAS-J)

mission observing, characterising and removing a Japanese H2-A rocket upper stage [83] [84]. Astroscale is aiming to launch Phase I of the project by April 2023 [83], but the Phase I CONOPS does not include de-orbit of the target [84].

Swiss company ClearSpace has been awarded a contract from ESA for their ClearSpace-1 ADR mission, with launch planned for 2025 [85]. The mission aims to de-orbit a 100 kg Vega Secondary Payload Adapter (VESPA) but later missions may target larger objects or multiple satellites [85].

ESA's Rendezvous Autonomous CubeSats Experiment (RACE) will use two 6-unit CubeSats to demonstrate proximity operations by flying around each other, followed by an automated docking. The mission will also "as an in-orbit testbed for advanced guidance, navigation and control software and autonomous system behaviour" [86].

NASA's On-orbit Servicing Assembly and Manufacture 1 (OSAM-1) mission, formerly known as Restore-L is aiming to launch in 2023, having passed its key decision point C in May 2020 [87] [88]. It will autonomously navigate and capture the Landsat 7 spacecraft, tow it to a new orbit, inspect it closely and then transfer propellant to it" [89], as well as acting a demonstration mission for relevant technologies [90]. However, the mission was originally meant to launch in 2020 and "is no longer working to preliminary cost and schedule estimates" [87, p. 43]. The project cost is expected to increase from the \$1.043 bn estimated in June 2018 due to the delay, which was caused by the addition of the SPIDER robot arm (discussed in Section 4.4.3 Robotics) and subsystem delays. The mission is also facing financial troubles as its "current level of funding does not include sufficient cost reserves for fiscal year 2020" [87, p. 44].

#### **4.4.2 Rendezvous, proximity operations & docking (RPOD) sensors**

One of the earliest developed RPOD technologies was the Kurs system used to dock Progress and Soyuz spacecraft to the Mir space station and now to the Russian segment of the ISS. This uses a two-way radio link between the visiting vehicle and the station, meaning the target can be considered actively

cooperative [91]. It was this level of cooperation that enabled the first automated Kurs docking to take place in 1986 [92].

In 2010, NASA's Space Servicing Capability Project (SSCP), now NASA's Exploration and In-Space Services (NExIS) division, published a report on OOS that included the level of technology available at the time. The report's technology gap assessment states that "all of the technologies required for satellite servicing exist at a fairly high level of maturity, with the exception of those associated with autonomous operations." [93, p. 67]. It also describes how rendezvous and docking technology at the time was mature for cooperative, non-spinning targets and for teleoperation or semi-autonomous control [93, p. 68]. This is thanks to the development of the technologies for use on the ISS and its visiting vehicles. Regarding RPO sensors specifically, the report states that 3D LIDAR tracking had been demonstrated in a laboratory environment, with 2D optical tracking having been performed on Orbital Express (see Section 4.4.1 Missions).

In recent years, various light detection and ranging (LIDAR) sensors have been developed in a range of sizes and a variety of types, such as flash or continuous wave [94, p. 2]. SpaceX's Dragon capsule uses a combination of LIDAR and thermal imagers for close-range guidance when less than 250 m from the ISS [95, p. 5]. LIDAR units have been used on ESA's Automated Transfer Vehicle (ATV) and Japan's H-II Transfer Vehicle (HTV), with both making use of retroreflective markers mounted on the ISS to aid tracking [94, p. 5]. Neptec's TriDAR system does not require these markers as it uses a mixture of time-of-flight and triangulation techniques to provide pose information using only its own sensors [96, p. 1]. This is used as the primary rendezvous and docking sensor for the Cygnus ISS cargo resupply vehicle [97]. Other examples of specific LIDAR sensors are shown in Table 4-1 [98, p. 58]. The Orion capsule under development for NASA will also use a flash LIDAR for RPOD with the Lunar Gateway, with this sensor having been tested on the Space Shuttle in 2011 [99, p. 1] [100, p. 1].

On a smaller scale, the RemoveDEBRIS mission used a combination of a flash LIDAR and a colour camera to provide data on range and range rate when imaging its target [101]. ADRAS-J will use three layers of sensors in its relative

navigation system (RNS): a visible camera from 80 km to 1 km range, an infrared (IR) camera from 1 km to 250 m and a LIDAR within 250 m [84].

Other camera systems for RPOD have also been developed. For example, in the run up to the fourth Hubble Space Telescope servicing mission, an experimental RNS unit was used that contained three cameras to track the relative pose of a mock-up of the telescope [102, p. 1]. The Raven sensor suite shown in Figure 4-5 uses “a visible camera with a variable field of view lens, a long-wave infrared camera, and a short-wave flash LIDAR” [103]. Raven was launched to the ISS in 2017 and has been used for testing the sensors that will be used on OSAM-1 [104].

Neptec, now owned by Maxar, have developed their Long Range Infrared Camera (LWIR) and VisCam units. LWIR further develops technology previously tested on the ISS and has “a mass of less than 2.5 kg and power consumption less than 10 W” [105]. Both LWIR and VisCam will be used on OSAM-1 [106] [97], with VisCam having wide and narrow field of view variants [105]. While it is likely that these are iterations of the sensors used on Raven, the author was not able to confirm this.

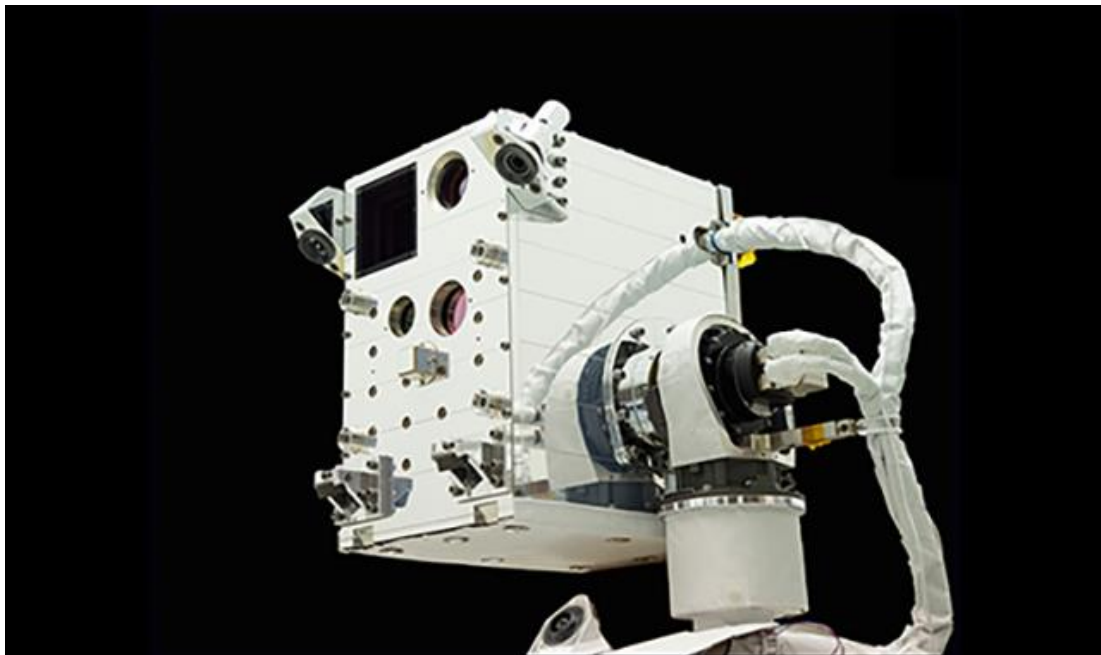


**Figure 4-5 - NASA's Raven relative navigation system installed on the International Space Station [104]**

**Table 4-1 - Examples of existing LIDAR systems [98, p. 58]**

<b>System (developer)</b>	<b>Operational mode</b>	<b>Technology &amp; measurement principle</b>	<b>Operational range (m)</b>	<b>Documented range accuracy</b>
LARS (CSA)	Cooperative	Scanning CW Triangulation Pulsed TOF	0.5-10 10-10,000	Sub-mm 3 cm
LCS (Neptec)	Cooperative Non-cooperative	Scanning CW Triangulation	1-10	0.1 mm – 5mm (1 $\sigma$ )
LAMP (JPL)	Cooperative Non-cooperative	Scanning Pulsed TOF	<5,000	10 cm (bias) 2.6 cm (3 $\sigma$ )
RVS (Jena-Optronik)	Cooperative	Scanning Pulsed TOF	<2500	0.01 m – 0.5 m (bias) 0.01 m - 0.1 m (3 $\sigma$ )
RVS-3000 (Jena-Optronik)	Cooperative Non-cooperative	Scanning Pulsed TOF	1-500 1-100	N/F
TRIDAR (Neptec)	Non-cooperative	Scanning CW Triangulation Pulsed TOF	0.5-2,000	N/F
LDRI (SNL)	Non-cooperative	Scannerless CW AM	<45	0.25 cm

DragonEye (ASC Inc.)	Non-cooperative	Scannerless Pulsed TOF	<1,500	10 cm (bias) 15 cm (3 $\sigma$ )
GoldenEye (ASC Inc.)	Non-cooperative	Scannerless Pulsed TOF	<3,000	10 cm (bias) 15 cm (3 $\sigma$ )
VNS (Ball Aerospace)	Cooperative (potentially non-cooperative)	Scannerless Pulsed TOF	<5,000	10 – 20 cm (3 $\sigma$ at 10 m)

### 4.4.3 Robotics

Early OOS missions involving the use of Extra-Vehicular Activity (EVA) demonstrated the use of crew for OOS (see 4.4.1 Missions). However, EVAs have limitations, with astronauts experiencing significant fatigue, the bulky space suit and life support system limiting dexterity, and the complex EVA operations impacting mission planning [48, p. 119]. These factors have led to the study of ground-operated and autonomous robotics for OOS. This section will discuss a variety of arms and other robotics elements currently under development. If a particular mission is discussed as being associated with the robotics in this section, more details of it can be found in Section 4.4.1 Missions.

Probably the best-known robotic arm series, the Canadarms began with the Shuttle Remote Manipulator System (SRMS), also known simply as the Canadarm. The arm first flew in 1981 [107] and was used extensively throughout the Space Shuttle programme, including on several missions discussed in Section 4.3 Previous use of OOS.

The original Canadarm was followed by the Space Station Remote Manipulator System (SSRMS), also known as Canadarm2, which has been used on the International Space Station (ISS) for assembly of the station, moving of payloads and berthing of visiting vehicles [108]. A series of grapple fixtures, discussed in

greater detailed in Section 9.1 Grappling Fixture, allow Canadarm2 to move along the ISS to reach different targets [108].

Canadarm3 is the latest addition to the Canadarm family and is currently under development for use on the NASA-led Lunar Gateway space station [109]. The arm is significantly smaller than Canadarm2 and the original Canadarm, at 8.5 m long versus 15 m and 17 m respectively [110]. All three arms were or are being built by Canadian company MacDonald, Dettwiler and Associates (MDA) for the Canadian Space Agency (CSA), with MDA now owned by Maxar Technologies [111].

MDA have also previously developed the Next Generation Canadarm (NGC) family for the CSA, not to be confused with the Canadarm3. The arm was designed in Small and Large versions specifically for OOS, with the Large version being designed for grappling spacecraft and the Small arm for satellite repair [112]. The NGC Large arm is 15 m long, while the Small variant is 2.5 m long. As part of the contract, MDA also developed a proximity operations system testbed to simulate satellite docking and a semi-autonomous docking system for simulation of docking scenarios [112].

For NASA's OSAM-1 mission, Maxar is developing the 5 metre Space Infrastructure Dexterous Robot (SPIDER) arm in partnership with NASA and the West Virginia Robotics Technology Center [113]. SPIDER will be used on OSAM-1 to "assemble multiple antenna reflector elements into one large antenna reflector" [114]. The arm was formerly known as the Robotic Servicing Arm and is heavily based on DARPA's Front-end Robotics Enabling Near-term Demonstration (FRIEND) arm that is discussed in greater detail below [115]. Maxar is also building the 1300-class bus for OSAM-1 [114] and Maxar is the parent company of Neptec that is providing a VISCAM camera unit for the mission [106]. In addition, Maxar is developing two robot arms for the mission that will be used for refuelling of the Landsat-7 target satellite [116].

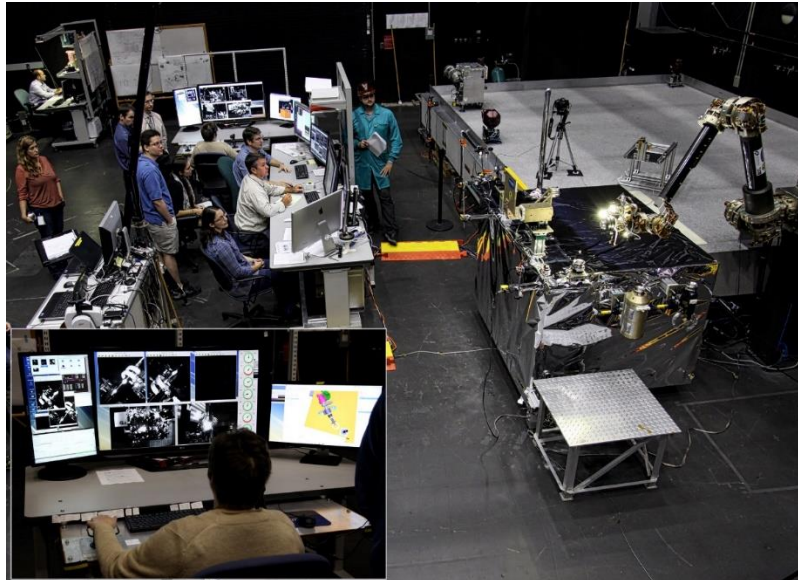


**Figure 4-6 - The FRENDA robot arm undergoing servicing rehearsals at the US NRL [117]**

The FRENDA arm has been developed by Alliance Spacesystems for DARPA's RSGS programme [118], with two FRENDA units planned to be used on the RSGS demonstration spacecraft [119]. The arm has  $\pm 2\text{mm}$  linear and  $\pm 0.4^\circ$  angular tool tip positioning requirements, with the arm in the "two-meter class" [118, p. 2]. Its mass is "77 kg including cabling and launch locks and excluding the 5 kg end-effector payload and the drive electronics" [118, p. 6]. FRENDA was tested in the US Naval Research Laboratory's (NRL) Proximity Operations Test Facility (example shown in Figure 4-6) along with "its associated avionics, end-effector, and algorithms" [118, p. 2]. The arm has also been tested in a TVAC chamber [118] [119], further increasing its TRL to around 6 or 7 per the NASA scale shown in Appendix D Technology Readiness Levels.

NASA has worked on a robotic arm called the Tension Actuated in Space MANipulator, or TALISMAN). This is a long reach arm that uses "tension members for stiffening" and a series of cables [120], rather than a more traditional layout with links attached together with joints containing servos. This means the arm has limited degrees of freedom but has an order of magnitude reduction in mass, packaging volume and power requirements compared to a normal arm [120]. The arm has not specifically been designed for OOS, but suggested

applications include nuclear fuel manipulation and confined space applications [120], both of which would have parallels to OOS.

In Europe, both the German Aerospace Center (DLR) and ESA have investigated OOS robotics. DLR's ROKVISS experiment is a two-joint manipulator that was installed on the ISS in January 2005. It qualified the robot's lightweight components in the space environment, as part of ROKVISS's goal of developing robotics hardware and tele-robotic control methods for OOS. These included modular light-weight robotic joints that could be applied to future space robots [121].

ESA's Clean Space initiative includes the Robotic Elements for Servicing and Debris Removal (RENEGaDE) activity. This will focus on "advancing key elements of robotic manipulator technologies" [122] for a range of OOS and ADR scenarios. In May 2018, ESA issued a €6m invitation to tender (ITT) for a one to two-year project to develop elements for OOS robotics. These included robotic joints, arm control, mechanisms to attach to a servicer, end effectors, tools and tool exchange systems [122]. However, the author could not find any evidence of organisations being awarded contracts as a result of the ITT.

ESA has also made OOS robotics an area of its Technology Strategy and is aiming to develop "a set of standard and sufficiently generic robotic elements (physical or software) that can be used across space robotics missions and applications" [19, p. 64]. RENEGaDE is likely part of the implementation of this.

Separate from ESA, a group of companies called the European Robotic Orbital Support Services (EROSS), led by Thales Alenia Space and part funded by a European Union (EU) Horizon 2020 grant [123] have been investigating enabling technologies for OOS. The group's objective is to "develop a whole engineering solution to enable the autonomous realization of servicing tasks in orbit", with the main goal of demonstrating a servicer satellite performing operations such as capture and manipulation of a target satellite including services such as refuelling and payload transfer [124].

#### 4.4.4 Attachment methods

A range of attachment methods have been designed for servicing spacecraft to gain control of their targets. These can generally be broken down into four categories: grapple fixtures, probe systems, nets and harpoons. These types are discussed in turn below, with selection of a fixture for this report's mission shown in Section 9.1 Grapple Fixture. More details of the missions discussed in this section can be found in Section 4.3 Previous use of OOS and Section 4.4.1 Missions.

During the Hubble Space Telescope (HST) servicing missions a grapple fixture, shown in Figure 4-7, was used to attach the Shuttle's Remote Manipulator System (RMS, also known as the Canadarm) to Hubble [125].



**Figure 4-7 - Hubble Space Telescope grapple fixture [126]**

The grapple fixture used on Hubble is part of a family of grapple fixtures, shown in Figure 4-8. These are now used extensively on the ISS by the Space Station Remote Manipulator System (SSRMS), also known as Canadarm2, as points to attach to the station and to grapple visiting vehicles. For example, SpaceX's Dragon capsule uses a Flight-Releasable Grapple Fixture (FRGF) [127], while

Northrop Grumman's Cygnus cargo spacecraft uses a Power and Video Grapple Fixture (PVGF) [128], with both being captured by the Latching End Effector (LEE) on the end of Canadarm2.

Once a visiting vehicle has been grappled by the SSRMS, it is rotated and berthed to the ISS. The interface used for this by Dragon and Cygnus, as well as Japan's H-II Transfer Vehicle (HTV), is the Common Berthing Mechanism (CBM) [129] [130]. The HTV also uses the SSRMS to berth to the ISS [131].

### SSRMS Interface Hardware

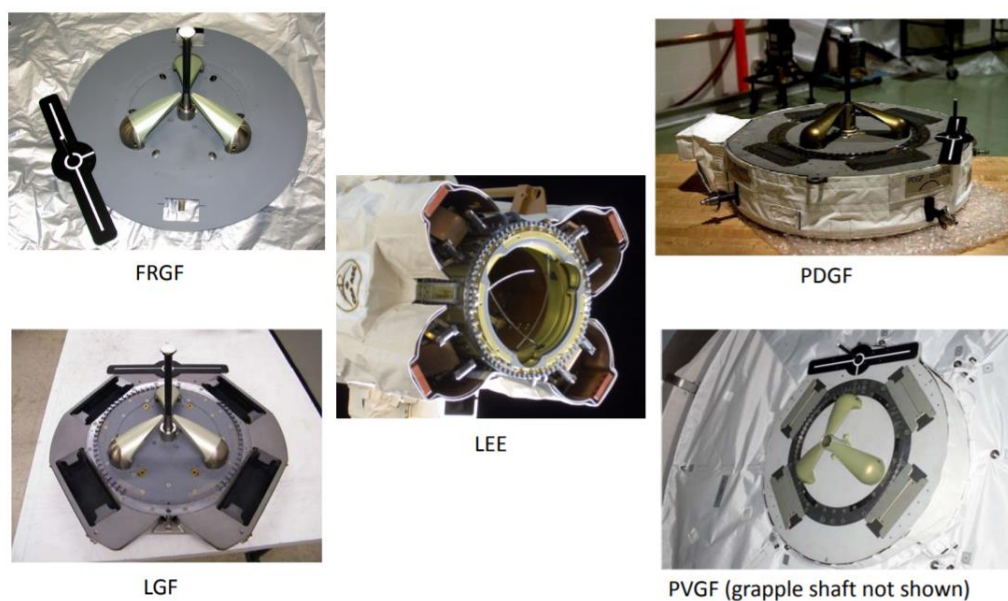


**Figure 4-8 - Screenshot of a slide showing NASA's grapple fixture family and, in the centre, Canadarm2's Latching End Effector (LEE). Top left: Flight-Releasable Grapple Fixture (FRGF), top right: Power and Data Grapple Fixture (PDGF), bottom left: Latchable Grapple Fixture (LGF), bottom right: Power and Video Grapple Fixture (PVGF) [132]**

SpaceX's Crew Dragon and Boeing's CST-100 Starliner vehicles operating under NASA's Commercial Crew program will use the ISS's new International Docking Adapters for docking, with the adapter being based on the International Docking System Standard (IDSS) [133] [134]. However, no similar standard exists for small satellite docking fixtures. Crew Dragon achieved its first docking with IDSS on March 3<sup>rd</sup>, 2019, completing the docking autonomously [135]. Starliner failed

to reach the ISS during its debut Orbital Flight Test in December 2019 due to an error in the programming of its Mission Elapsed Timer [136]. However, Boeing have announced that there will be a second attempt at the mission to “demonstrate the quality of the Starliner system” [137].

American company Altius Space Machines is developing a grappling fixture called DogTag, shown in Figure 4-10. The DogTag is a “completely passive, ferromagnetic grappling fixture” [138] that uses a “honeycomb AlSiC composite panel” [139, p. 6] and has five possible grappling modes: magnetic, mechanical, gecko gripping, electro-static and harpoon [140]. The preferred method of attachment to the DogTag is via a magnetic grappling head [140]. While ASM is not currently publishing many details of the magnetic grappling head due to its commercial sensitivity, it is known that the head will be based on electropermanent magnets (EPMs) that do not require continuous power to hold their state but rather need a short electrical pulse to switch on or off.

As discussed in Section 5.1 Background, DogTags have now been fitted to OneWeb’s satellites and will as a result be used as the baselined grappling fixture for this report’s mission. The impact of this on servicer design is discussed in Section 9.1 Grappling Fixture.

In Astroscale’s ELSA-d mission, the client is equipped with a “flat, disc-shaped docking plate... on top of a supporting stand-off structure” [79, p. 5]. The docking plate includes optical markers to aid navigation and is made of a ferromagnetic material to enable magnetic grappling [79]. The servicer will use a magnetic docking mechanism to capture the client. This will use a “set of small concentric permanent magnets which are extended and retracted using a mechanism to allow connection with the docking plate on the client” [79, p. 5]. An internal mechanism can be used to push the docking plate away to release it.

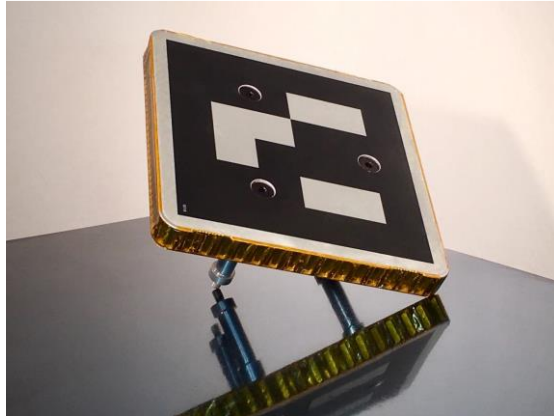


**Figure 4-9 - Altius Space Machines' DogTag grapple fixture [139]**

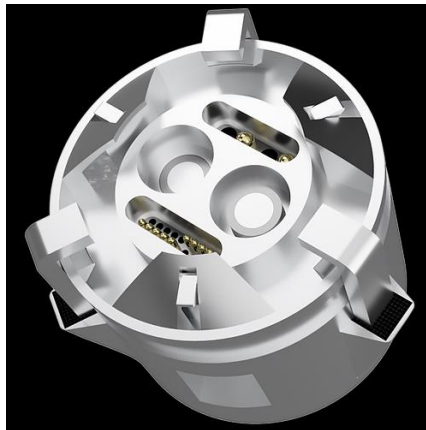


**Figure 4-10 - Obruta Space Systems' Puck docking interface [141]**

Canadian start-up company Obruta Space Systems is developing an androgynous docking interface called Puck, which includes passive and active forms [141]. The passive version would be fitted to a spacecraft seeking to be serviced, with the active version, shown in Figure 4-10, being used on a servicer spacecraft. The interface enables docking, fuel transfer (although whether it has cryogenic capability is unclear), data and electrical power transfer. Very little data is currently available on the Puck design, but its androgyny, whereby two identical Pucks could be attached together, would be useful to servicer and client spacecraft designers. This is because it makes the requirements on both vehicles the same and removes the need for two different designs of interface to be developed and proven, reducing risk for the spacecraft designers. The company is also developing a “tethered-net” system for ADR [142], although as discussed previously a tethered system would be unsuitable for other types of servicing.

ASM also produces a device called MagTag, shown in Figure 4-11. The MagTag is a square interface with sides 100 mm long and a mass of less than 350 g [143]. It uses EPMs like those in the grapple head used with the DogTag but is designed as a modular interface to transfer power or fluid between large satellites or space facilities [143]. The EPMs give a mechanical connection with a maximum load of around 600-800 N [143], making the MagTag suitable as a method of attaching to hardware modules that could then be pulled from a target satellite by a robot arm and placed into the servicing tug before the fitting of replacements. The MagTag is currently TRL 5, with a flight demonstration being targeted for the end of 2021 [143].

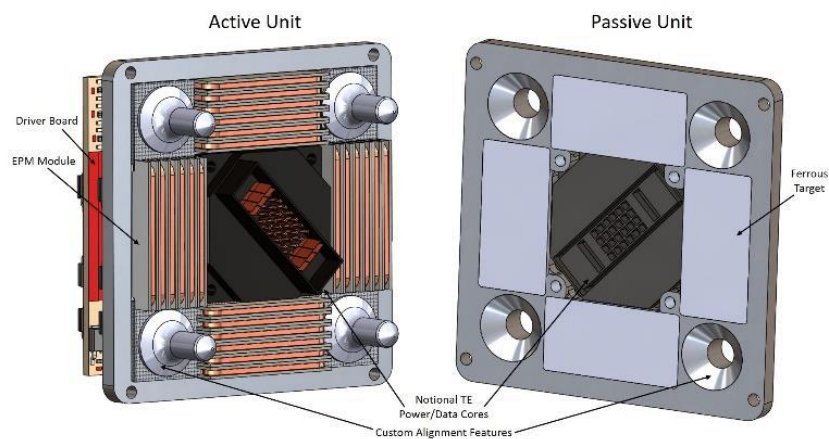


**Figure 4-11 – Altius Space Machines MagTag active and passive half configurations [143]**

German company iBOSS has produced an interface similar to the MagTag, called the intelligent Space System Interface (iSSI). This is shown in Figure 4-12 and is designed to transfer power and data as well as acting as a grapple fixture for moving spacecraft modules [144]. Both Altius Space Machines and iBOSS are sustaining members of CONFERS [145]. The iSSI is currently TRL 6, with an in-orbit demonstration planned for 2021 [146]. The interface has a diameter of 119 mm and a mass of 0.9 kg [144].

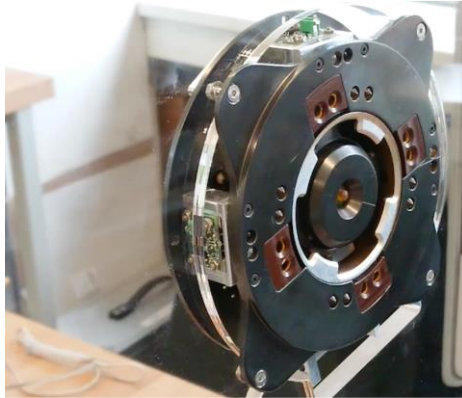


**Figure 4-12 - iBOSS iSSI [144]**

Considering more traditional forms of grappling, MDA previously produced the grappling fixture used on DARPA's Orbital Express mission. This fixture is shown in Figure 4-13 and uses a shaft inserted into a clamp. It is also to be used on DARPA's Payload Orbital Delivery (POD) system for their Robotic Servicing of Geosynchronous Satellites (RSGS) program [63].



**Figure 4-13 - The MDA grapple fixture used on DARPA's Orbital Express Mission [65]**

Considering probe attachment methods, Northrop Grumman's MEV uses a probe mechanism that is inserted into the target satellite's engine bell, as shown in Figure 4-14 [147]. Once the probe is firmly attached to the target, it is retracted, pulling the MEV in towards the target until three arms on the MEV are resting against the target's base. This mechanism has now been successfully used during the MEV-1 mission and will be used for the upcoming MEV-2 (see Section 4.4.1 Missions). The mechanism can attach to a variety of liquid apogee engines

but an increasing number of GEO satellites are now using fully electric propulsion, which will necessitate the development of a new attachment method [72].



**Figure 4-14 - Testing of the MEV's probe attachment mechanism [147]**

The University of Surrey's RemoveDEBRIS ADR technology demonstration mission successfully demonstrated its net and harpoon for capture of debris in 2018 [148] [149]. These validated the technology, although use of these methods for target capture in ADR is somewhat controversial.

ESA has studied net technology and tested it in parabolic flight [150]. They also researched harpoon technology for their e.Deorbit mission to deorbit Envisat, but found that it “doesn't offer enough advantages over a net or robotic arm”, according to a member of the e.Deorbit team [59]. An advantage of a net or harpoon system over a robotic solution is that they allow greater separation from the target. A robot arm gives a very rigid connection but requires the servicer to come within 2-3 m of the target and perform a ‘synchronised motion’ if the target is tumbling, requiring complex and highly accurate GNC [26].

However, it was found that if using a net or harpoon, control after capture would be extremely challenging, especially to ensure the tether did not become wrapped around both satellites [26]. A collision between the two spacecraft would also be a significant risk [59].

## 5 Mission Analysis and Design

This section describes the example OOS mission that will be used as the baseline throughout the report. Firstly, the decisions leading to definition of the architecture, such as the targeting of ‘mega-constellations’ for servicing, will be discussed, followed by the selection of a specific orbit. This will then be followed by description of the processes undertaken to gain an initial baseline for the size of the servicing spacecraft.

### 5.1 Background

Although the various types of OOS have already been discussed in Section 4.1 OOS types, a mission architecture to implement these services still needs to be defined. For this, the author referred to the MEV-1 and MEV-2, ESLA-d and ELSA-OW missions described in Section 4.4.1 Missions, as well as an OOS ontology paper from the Consortium for Execution of Rendezvous and Servicing Operations (CONFERS) [151]. CONFERS is a consortium of companies from around the world that seeks to “research, develop, and publish non-binding, consensus-derived technical and operations standards for OOS and RPO” [152]. A figure taken from the CONFERS ontology paper, shown in Figure 5-1, gives a good overview of a typical OOS mission architecture.

In the architecture used in this report, a single servicer spacecraft is used to provide services to a single target spacecraft. The servicer is launched into an initial orbit where a checkout of its systems is carried out by the spacecraft software, potentially with support from ground controllers. This would include calibration of sensors and actuators (see Sections 7 Guidance, Navigation and Control (GNC) System and 8 Relative Navigation System (RNS))

Once commissioning is complete, the servicer enters a parking orbit. When a client satellite requires servicing, the servicer rendezvouses and docks with it and then performs the required servicing operations. This could include de-orbiting the client if necessary. Once servicing is complete, the servicer undocks and

returns to its parking orbit to await the next client. This is the basic architecture used by MEV-1 but MEV-2, ELSA-d and ELSA-OW skip the initial parking orbit and immediately rendezvous with their clients after commissioning [80]. The reasoning behind this for MEV-2 is described in Section 4.4.1 Missions.

However, while it is a valid OOS type, this report’s mission will not be designed for active debris removal. This is because the uncontrolled and uncooperative nature of the target satellite in ADR means it is often spinning. For example, when ESA studied the ADR of Envisat (see Section 4.4.1 Missions), its maximum rotation rate was estimated as 2.8 °/s. This is a roughly average value, with some objects reaching over 10 °/s [26].

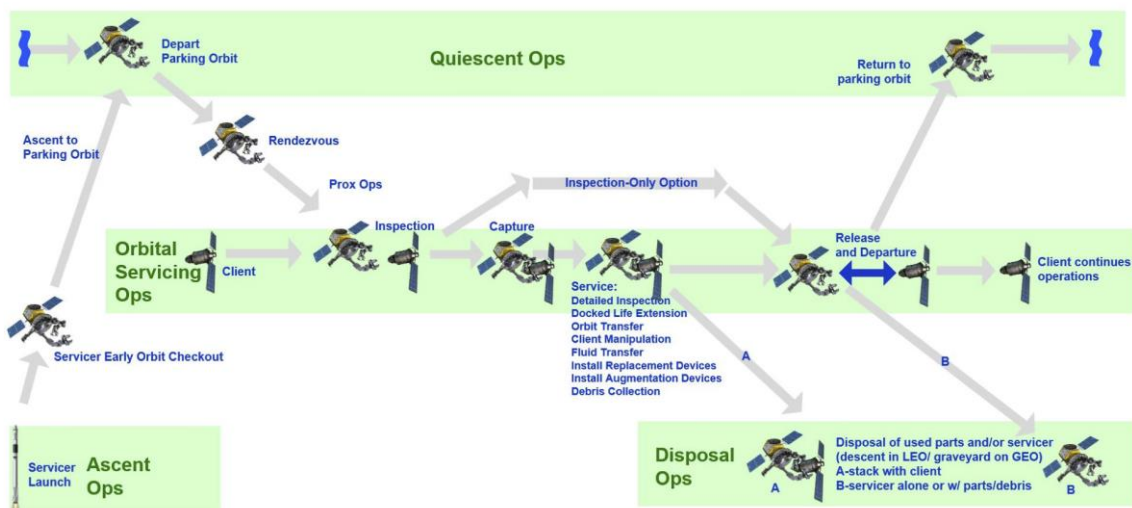


**Figure 5-1 - OOS architecture [151]**

Once the basic mission architecture had been defined, the client needed to be selected. This could either be a single satellite of high importance (for example Envisat was chosen for ESA’s e.Deorbit ADR mission – see Section 4.4.1 Missions) or multiple satellites such as in a constellation that would provide a continuous revenue stream for the servicer operator. In order to make the servicing economically viable, a group of satellites was desired that could all be serviced using the same hardware. This meant that any standardised grapple/docking fixture present on the spacecraft would place them at a major advantage relative to other satellite groups that would potentially have different structural designs and require different docking mechanisms.

'Mega-constellations' are currently growing in popularity, with the author's GDP report finding at least six large constellations currently under development to provide internet services to customers [20]. According to the ESA Technology Strategy, "The advent of constellations with similar satellites sharing orbits/orbital spots and requiring regular replenishment allows the consideration of servicing vehicles that, by means of suitable interfaces, can solve the issue of satellite de-orbiting, replacement of early aging payload, and refuelling" [19, p. 64].

At the time of writing the GDP report, SpaceX's Starlink and Amazon's Kuiper constellations were the largest planned constellations, with requests submitted to the US' Federal Communications Commission (FCC) for 42,000 and 3,236 satellites respectively. However, in May 2020, OneWeb asked the FCC for permission to increase its constellation to 48,000 satellites [153] from 720 [154], making it the largest constellation currently under development. However, Ars Technica reported that this large increase was likely strategic rather than technical in nature, as it being granted would make it more difficult for OneWeb's competitors, particularly Kuiper, to achieve similarly large constellations [154]. This is because the FCC would be unlikely to grant a large license to a second company given the constraints on space in orbit given the issue of space traffic management (STM), and the limitations communications bandwidth available. It is believed SpaceX was attempting a similar tactic when it filed to increase its constellation's size by 30,000 (to 42,000) in October 2019 [155]. Despite the large constellation increases likely not being fulfilled in future, the OneWeb and Starlink constellations at 720 and 12,000 satellites respectively would, as well as Kuiper, still constitute major potential customers for a servicer spacecraft.

However, OneWeb's constellation stands out as a useful target not only due to its size. OneWeb announced in December 2019 that they had entered an agreement with Altius Space Machines (ASM) whereby ASM would fit their DogTag grappling fixture (see Section 4.4.4 Attachment methods) to every OneWeb satellite [156]. This makes the OneWeb satellites the only commercial satellites, other than those that visit the ISS, to be fitted with a grappling fixture. The presence of a reliable grappling fixture makes the OneWeb satellites an

excellent target for servicing as it eliminates the need for custom grappling tools that, for example, grapple the engine bell of the target spacecraft (see Section 4.4.4 Attachment methods). It also means that the dynamics of the combined target/servicer vehicle when docked can be more accurately defined, as the location of the interface between the two spacecraft will be known very precisely. Furthermore, the design of the OneWeb satellites is relatively well known and relatively typical of a satellite found in low Earth orbit (LEO). The satellites are in the 200 kg class [157], with one shown in Figure 5-2.



**Figure 5-2 - Render of a OneWeb satellite in its operational configuration [157]**

This similarity to other designs is opposed to the Starlink satellites, which use a flat design – a stack of 60 Starlinks is shown in their launch vehicle in Figure 5-3, while the design of Amazon’s Kuiper satellites is not currently widely known.

For these reasons, the author decided that OneWeb’s constellation would be a more suitable target than Starlink or Kuiper. However, as this report focuses on OOS of satellites generally, rather than on servicing of mega-constellations per se, it was also decided that the OneWeb constellation should be used as a baseline for the mission architecture rather than a particular target. In this way, the OneWeb satellite design can be used as a baseline for the target’s design, but the selection of orbits can be left open for the author to then select based on which orbits are most highly populated. The orbit selection process is discussed in the following section.



**Figure 5-3 - A stack of 60 Starlink satellites in their Falcon 9 launch vehicle's fairing prior to launch [158]**

The future of the OneWeb constellation was thrown into doubt in March 2020 after it filed for Chapter 11 bankruptcy in the US [159] but this was resolved in July of the same year when the company was purchased by the UK Government and Indian company Bharti Global Limited [160], with the Government paying £400m for their stake [161]. This ensures the future of the constellation, further validating its satellites' design as the mission's target.

## **5.2 Orbit selection**

Once the selection of the OneWeb satellites as a mission baseline had been made, the orbit(s) for the mission targets needed to be selected. The OneWeb satellites orbit at an altitude of 1200 km [162] but the author judged that the OOS mission's orbit should initially be left open to allow servicing of satellites from multiple operators. The author also judged that the client would most likely be found in one of the most populated orbits, so these orbits needed to be identified.

This was done by studying a database from the Union of Concerned Scientists (UCS) [29] and compiling the results in a document, Satellite Distribution Research and Orbit Selection [28], which is discussed briefly in Section 3.3.4 Orbit selection document and can be found in full in Appendix A Satellite Distribution Research and Orbit Selection.

The satellites were first sorted by apogee altitude, with this used rather than perigee so that satellites in geostationary transfer orbit (GTO) were shown in GEO, where they would spend most of their orbit. This found that of the 2,666 satellites in the database, approximately 1930 were in LEO (below 2000 km altitude) and 543 in or passing through GEO (at 35,786 km altitude), as shown in Figure 5-4. 98 of those in LEO were at or below 300 km altitude, making their lifetimes too short for servicing to be practical or useful, so these were discarded from further analysis. Furthermore, communications satellites found in GEO are typically much larger than the OneWeb satellites, so this dissimilarity combined with the far greater population in LEO led to GEO being discarded.

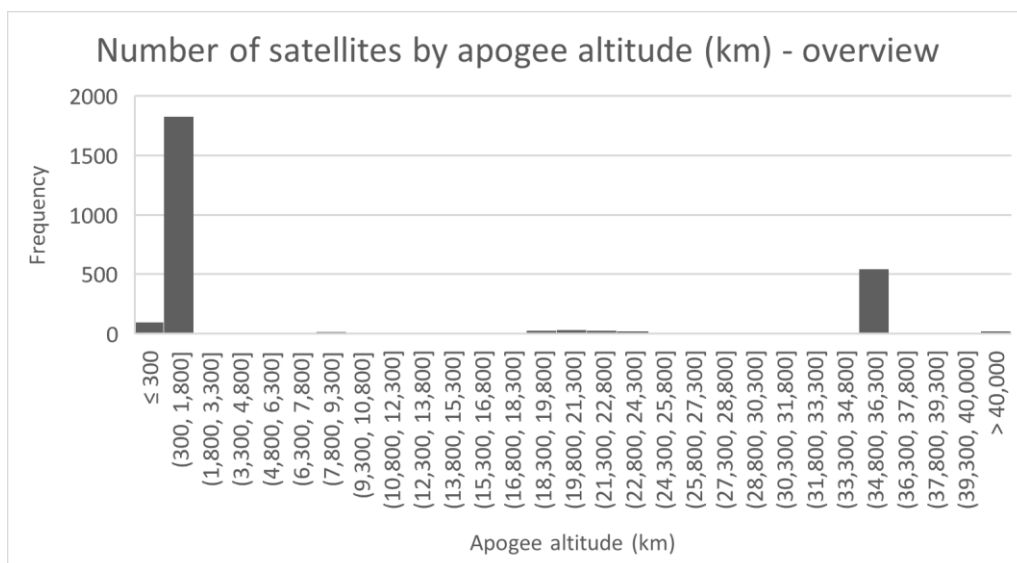


**Figure 5-4 - Chart showing the distribution of satellites in the UCS database by apogee altitude [28]**

A further chart, shown in Figure 5-5, showed that most of the LEO population is focussed around the 500-600 altitude region, with the population tapering off in approximately in a bell curve to either side of this altitude band. Using 550 km as

the new centre of the search and analysing a band 150 km to either side, the 400-700 km band, shown in Figure 5-6, shows a distinct peak between 503 and 523 km, with a smaller peak between 543 and 563 km.

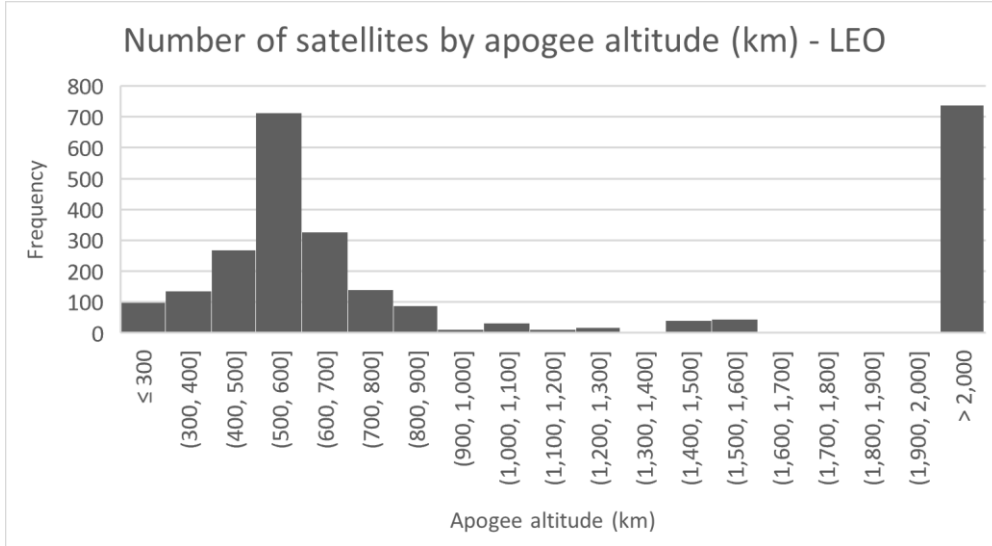


**Figure 5-5 - Chart showing the distribution of satellites in LEO according to the UCS database [28]**

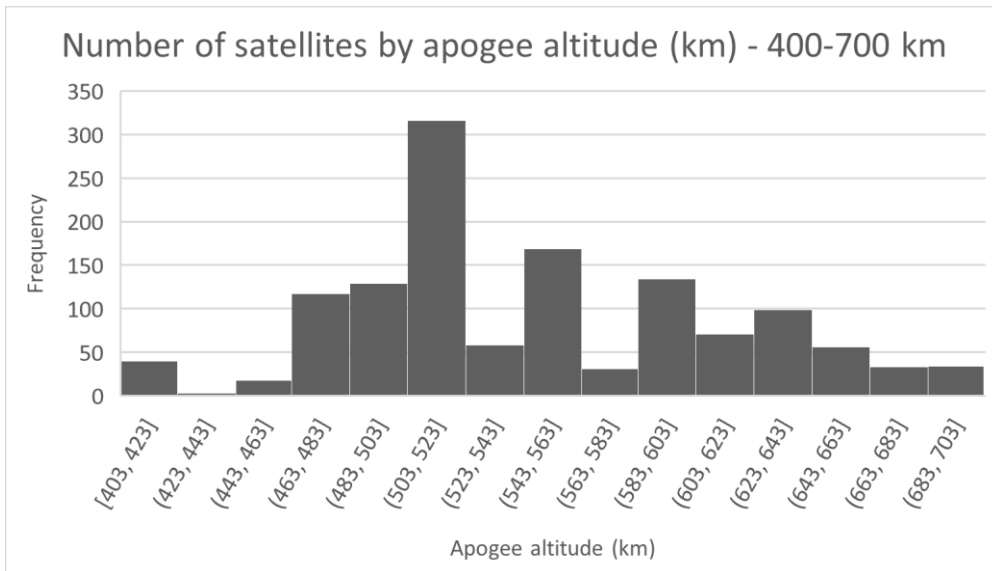


**Figure 5-6 - Chart showing the distribution of satellites in the 400-700 km altitude band according to the UCS database [28]**

Once the population distribution by altitude was understood, the eccentricity distribution needed to be analysed. The author suspected that the vast majority

of the population were in circular orbits, with this being confirmed by the data as shown in Figure 5-7.

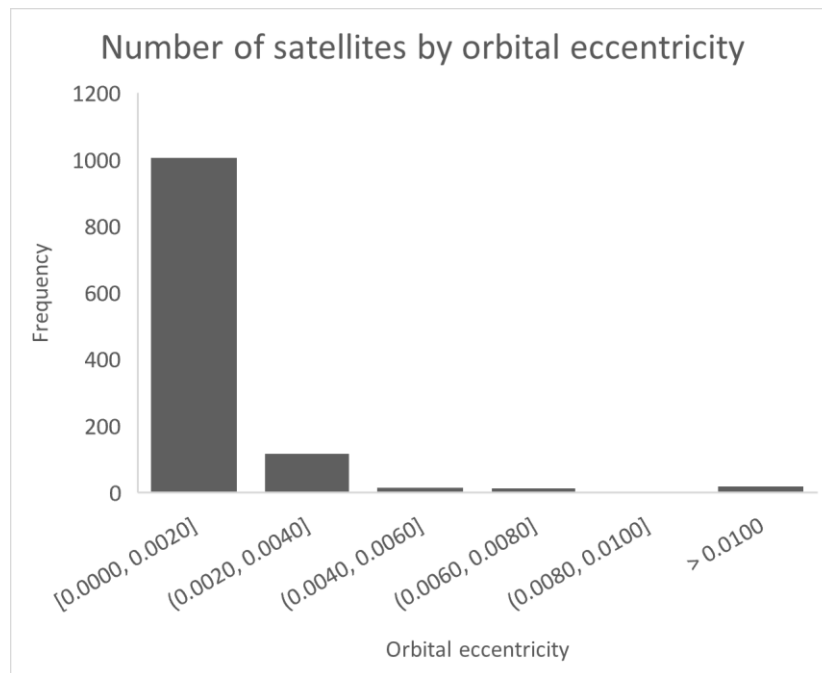


**Figure 5-7 - Chart showing the distribution of satellites in the UCS database by orbit eccentricity [28]**

Orbital inclination then needed to be analysed and the relationship between this and altitude understood so that the proportion of spacecraft in Sun synchronous orbits (SSO) could be determined. The previously selected 400-700 km altitude region was again analysed, with a plot of apogee versus inclination produced, which is shown in Figure 5-8. Three distinct bands were revealed, with the large top band at approximately 97.5 ° inclination corresponding to SSO, the middle band at 87.4 ° and between 460 and 582 km altitude being the OneWeb satellites launched to date, and the satellites at 53.0 ° inclination between 449 and 571 km being the SpaceX Starlink constellation [28]. Plotting inclination versus frequency, shown in Figure 5-9, highlighted the high proportion of spacecraft in this altitude range that reside in SSO. This meant that SSO was selected, with a final chart plotted (shown in Figure 5-10) depicting apogee versus inclination for the 500-700 km altitude and 97.2-97.8 ° inclination region. This was done to decide which specific orbits within SSO should be targeted. This revealed that

the lower altitude, medium inclination region, around 510 km altitude and 97.4 ° inclination, was most highly populated and thus used as the servicer spacecraft's mission target.

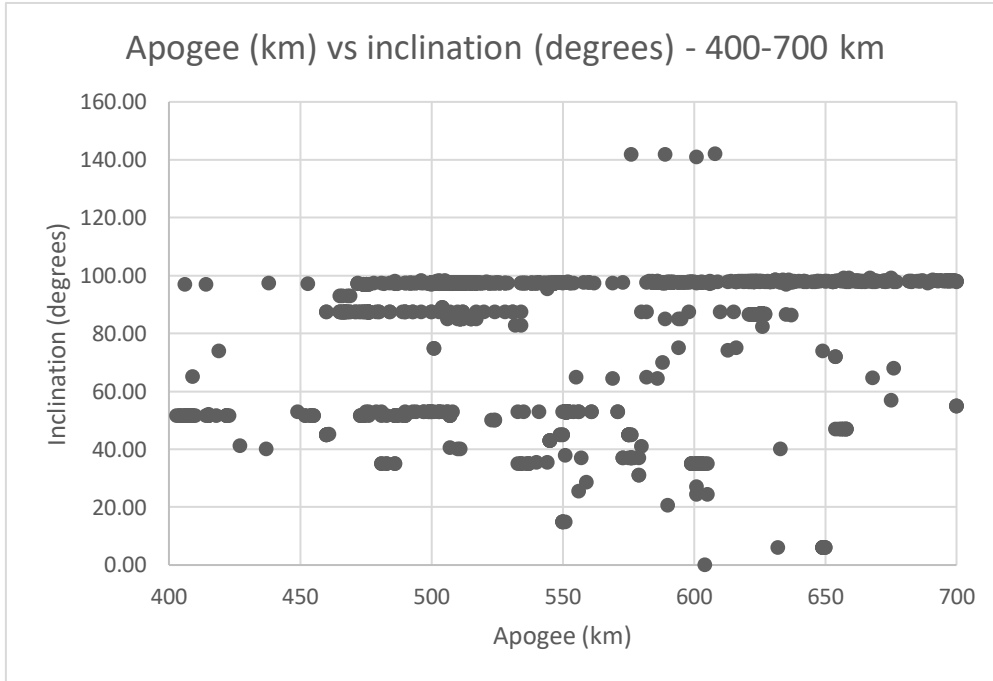


**Figure 5-8 - Chart showing the distribution of satellites in the UCS database by apogee and inclination [28]**

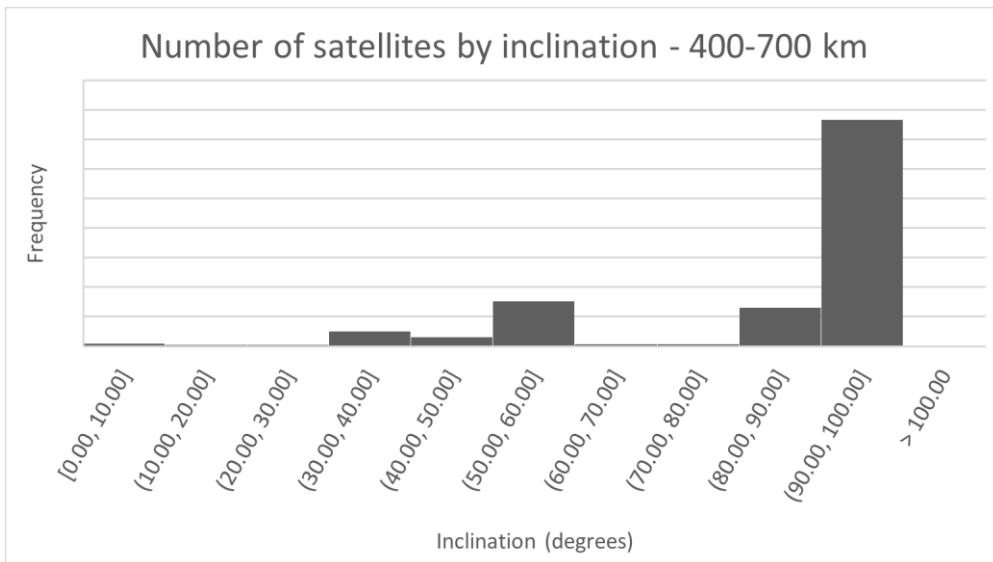


**Figure 5-9 - Chart showing inclination versus frequency for the satellites in the UCS database [28]**

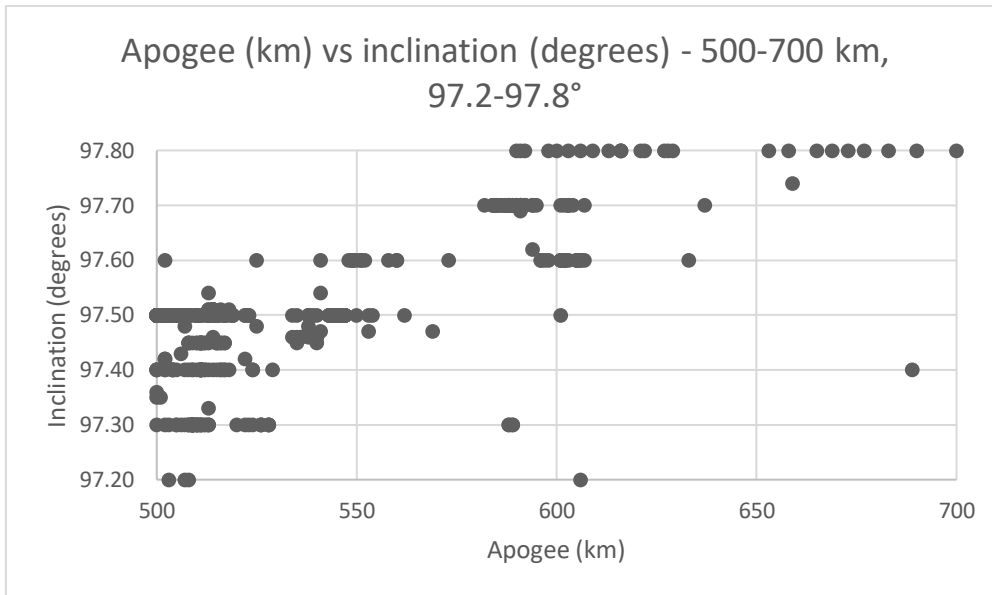


**Figure 5-10 – Chart of apogee versus inclination for satellites in the 500-700 km altitude and 97.2-97.8 ° inclination region, according to the UCS database [28]**

To summarise, the orbit selection was carried out by considering the size of the population in various regions, with LEO selected initially, then narrowed to 400-700 km altitude. A study of eccentricity revealed the vast majority of orbits to be circular, with further research revealing SSO to be a particularly highly populated area. Thus, SSO, and in particular the region of it around 510 km altitude and 97.4 ° inclination, was selected as the OOS mission’s target orbit.

When selecting the servicer’s orbit, it was also important to consider the effect of atmospheric drag on its operations. However, 510 km altitude is sufficiently high for natural decay to take around 1-5 years depending on the solar cycle [163, p. 218], giving more than enough time for the servicer to perform its operations. To compare, Astroscale’s proposed ELSA-OW mission (see Section 4.4.1 Missions) uses 550 km as its nominal altitude after completion of its disposal of a OneWeb satellite [80].

### 5.3 Servicer sizing

When performing an initial sizing of the servicer, two main factors needed to be considered: the mass of dry components such as the spacecraft structure, GNC,

relative navigation system (RNS) and robotics; and the mass of the fuel required to complete the necessary orbital transfers. The former could be estimated based on a review of literature and existing components, while the latter could be estimated by calculating the total  $\Delta v$  requirement then factoring in the specific impulse ( $I_{sp}$ ) of the selected propellant. These are discussed in the following two sections. By adding these two elements and determining the volume of propellant required, estimates of the spacecraft's total mass and volume could be found.

### **5.3.1 Dry mass estimation**

To estimate the total spacecraft mass, its dry mass first needed to be estimated. The servicer's mass budget is shown in Table 5-1, taken from MCC [25]. The spacecraft was split into its various subsystems, with the mass of each component estimated individually. Margins were then applied as per requirements MAR-MAS-020, MAR-MAS-030 and MAR-MAS-040 of ESA's guidelines for concurrent design facility (CDF) studies [164]. In the table, the margins relate to the components they appear below, with Margin (1) indicating MAR-MAS-020, Margin (2) for MAR-MAS-030 and Margin (3) for MAR-MAS-040.

MAR-MAS-020 is a design maturity mass margin, with 20 % used in the servicer's mass budget as it is assumed that products will be newly designed and developed. While the servicer will use COTS components where possible, this assumption ensures that the overall spacecraft mass will not be underestimated. MAR-MAS-030 is a payload level mass margin with 20 % used in this case. MAR-MAS-040 is a 20 % system level mass margin applied to the total dry mass. This is factored in when using the dry mass to calculate the required fuel mass (see the following section).

Component masses were estimated either as a proportion of the overall mass or using data on selected components where available. For example, the DST-13 selected in Section 7.4.2 Orbit determination methods and selection has a mass of 0.64 kg [165], with the 12 of these required giving a total thruster mass of 7.68 kg. This was then rounded to 10 kg to account for any additional components

required to support the thrusters. The robotics mass was estimated from the mass of the FRIEND arm, as discussed in Section 9.2.2 Servicing arm selection.

**Table 5-1 - Servicer mass budget [25]**

<b>System</b>	<b>Component</b>	<b>Mass (kg)</b>
<b>Bus</b>	Structure	30.00
	Margin (1)	6.00
<b>GNC</b>	GNC sensors	20.00
	Margin (1)	4.00
	Reaction wheels	5.00
	Margin (1)	1.00
<b>Payload</b>	Robotics	75.00
	Margin (1)	15.00
	Payload margin (2)	18.00
<b>Propulsion</b>	Thrusters	10.00
	Margin (1)	2.00
	Tanks	10.00
	Margin (1)	2.00
	Fuel	120.67
<b>Totals</b>	Dry mass	198.00
	Margin (3)	39.60
	<b>Total dry</b>	<b>237.60</b>
	<b>Total wet</b>	<b>323.97</b>

### 5.3.2 Fuel requirement estimation

The first step towards estimating the fuel requirement was to understand the orbital transfers that would be needed throughout the mission. Reviewing the mission architecture (see Figure 5-1 in Section 5.1 Background), for each servicing of a target, two transfers would be required: from the parking orbit to rendezvous with the target, then after servicing from the target back into the parking orbit. Fuel would also need to be allocated for manoeuvres while docking and undocking.

While modelling the transfers, it could not be assumed that the servicer would always begin the manoeuvre in an ideal position to rendezvous. This meant that a phasing orbit had to be considered. Therefore, a noncoplanar phasing algorithm from Vallado [166] was used and is shown in Figure 5-12, with the transfer geometry shown in Figure 5-11. The inclination difference between the servicer and target would likely be sufficiently small that the orbits could reasonably be considered coplanar, but the high  $\Delta v$  requirement for LEO inclination changes encouraged the author to model the transfer as noncoplanar to gain a better understanding of the inclination difference's effect on the overall  $\Delta v$  budget.

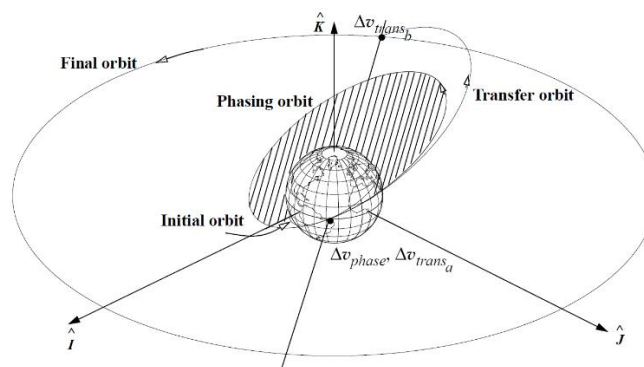


Figure 6-19. Alternate Geometry for a Circular, Noncoplanar, Orbit Transfer. An intermediate phasing orbit is useful to permit a quicker time to rendezvous. The size of the phasing orbit is calculated so the satellite returns to the node in time for the transfer into the final orbit. Both burns ( $\Delta v_{phase}$  and  $\Delta v_{trans_a}$ ) occur at the same point.

Figure 5-11 - Geometry for the mission's noncoplanar rendezvous [166, p. 366]

**ALGORITHM 46: Noncoplanar Phasing**

$$\begin{aligned}
 & (\vartheta_i, a_{int}, a_{igt}, k_{igt}, u_{int}, \Omega_{int}, \lambda_{true0}, \Delta i \Rightarrow \\
 & \quad \tau_{trans}, \tau_{phase}, \Delta v_{phase}, \Delta v_{trans1}, \Delta v_{trans2}, a_{phase}) \\
 & \omega_{igt} = \sqrt{\frac{\mu}{a_{igt}^3}} \quad \omega_{int} = \sqrt{\frac{\mu}{a_{int}^3}} \\
 & a_{trans} = \frac{a_{initial} + a_{final}}{2} \\
 & \tau_{trans} = \pi \sqrt{\frac{a_{trans}^3}{\mu}} \\
 & \alpha_L = \omega_{igt} \tau_{trans} \\
 & \text{Find } \Delta \vartheta_{int} \text{ to reach a node (180}^\circ \text{ or 360}^\circ - u_{int}) \\
 & \Delta t_{node} = \frac{\Delta \vartheta_{int}}{\omega_{int}} \\
 & \lambda_{true_{igt1}} = \lambda_{true0} + \omega_{igt} \Delta t_{node} \\
 & \text{Find } \lambda_{true} \text{ for interceptor at } t_1 \quad \lambda_{true_{int1}} = \Omega + \pi \\
 & \vartheta_{new} = \lambda_{true_{int1}} - \lambda_{true_{igt1}} \\
 & \alpha_{new} = \pi + \vartheta_{new} \\
 & \beta_{phase} = \frac{\alpha_{new} - \alpha_L + 2\pi k_{igt}}{\omega_{igt}} \\
 & a_{phase} = \left( \mu \left( \frac{\beta_{phase}}{k_{int} 2\pi} \right)^2 \right)^{1/3} \\
 & \Delta v_{phase} = \left| \sqrt{\frac{2\mu}{a_{int}} - \frac{\mu}{a_{phase}}} - \sqrt{\frac{\mu}{a_{int}}} \right| \\
 & \Delta v_{trans1} = \left| \sqrt{\frac{2\mu}{a_{int}} - \frac{\mu}{a_{trans}}} - \sqrt{\frac{2\mu}{a_{int}} - \frac{\mu}{a_{phase}}} \right| \\
 & \Delta v_{trans2} = \sqrt{\left( \frac{2\mu}{a_{igt}} - \frac{\mu}{a_{trans}} \right) + \left( \frac{\mu}{a_{igt}} \right) - 2 \sqrt{\frac{2\mu}{a_{igt}} - \frac{\mu}{a_{trans}}} \sqrt{\frac{\mu}{a_{igt}} \cos(\Delta i)}} \\
 & \tau_{total} = 2\pi \sqrt{\frac{a_{phase}^3}{\mu}} + \tau_{trans} + \Delta t_{node}
 \end{aligned}$$

**Figure 5-12 - Noncoplanar phasing rendezvous manoeuvre algorithm [166, pp. 368-369]**

The transfer algorithm was implemented in the Main Central Control spreadsheet (see Section 3.3.2 Main Central Control spreadsheet). The target's altitude was assumed to be 520 km, based on the orbit selection research described in Section 5.2 Orbit selection, with a 600 km parking orbit used as an estimate for the servicer's initial orbit. An inclination difference of 0.3 ° was modelled to simulate the servicer being positioned to access a range of SSOs. The transfer includes three manoeuvres:

- 1) A burn in the initial orbit to transfer into the phasing orbit. This phasing orbit is used to achieve the correct phasing angle between the servicer and target

- 2) A burn to change the phasing orbit into the transfer orbit. The transfer orbit is used to raise or lower the servicer's altitude to meet the orbit of the target
- 3) A final burn during rendezvous to match the orbit of the target, so the distance to it is maintained.

The model predicted a total  $\Delta v$  requirement of 190 m/s for the overall transfer, with 25 m/s being added to account for fuel used while docking. A one-way transfer has a total duration of 188 minutes. Margin was added to the  $\Delta v$  figure per requirement MAR-DV-010 of ESA's CDF guidelines [164, p. 11], giving a total of 225.8 m/s or 451.5 m/s for a return journey [25]. It was assumed that two servicing journeys would be required to make the servicer economical, so a total  $\Delta v$  of 903.1 m/s was used.

While the noncoplanar transfer successfully overcomes differences in altitude and inclination between the servicer and target, it cannot be used for differences in right ascension of the ascending node (RAAN). The line of nodes of a spacecraft's orbit regresses over time due to the J2 perturbation. However, this happens very slowly, for example around  $1 \times 10^{-3}$  rad/orbit for a spacecraft in SSO [167, p. 31]. Spacecraft at different altitudes have different rates of regression of their lines of nodes but the net effect for spacecraft with similar altitudes is very small.

This RAAN drift of one spacecraft (the servicer) relative to another (the tug) was modelled in another page of the Main Central Control spreadsheet, with the scenario established with the target in a 520 km altitude SSO (97.083 ° inclination) and the servicer initially in a 600 km altitude orbit with the same inclination as the target. A 10 ° difference in RAAN was used as an initial optimistic guess, with the model giving a drift time of 16719 days [25]. This means that if the servicer were to rely on natural precession of its line of nodes to match the RAAN of the target, it would have to wait for over 45 years. This is clearly impractical. Therefore, for the servicer to access targets with RAANs to its own, it would have to use its orbital manoeuvring system at the points the orbits cross to eliminate the angle between the orbits. However, this would use a large amount of propellant. The requirement on and feasibility for the servicer to access targets

with different RAANs will need to be researched further, as discussed in Section 10.1 Mission design and dynamics analysis.

Returning to the noncoplanar transfer, this transfer will need to be completed twice for each servicing mission – once on the way to the target from the parking orbit and back to the parking orbit once the servicing has been completed. The dry mass of the vehicle remains the same throughout as no manoeuvres are required while the servicer and target are docked. The total  $\Delta v$  is therefore simply twice the one-way  $\Delta v$ , with suitable margins added as per the ESA CDF guidelines [164]. The mass of the required fuel can then be found by taking the dry mass of 237.60 kg from the previous section and using the rocket equation shown in Equation (5-1) [168, p. 8], giving the servicer wet mass.

$$\Delta v = I_{sp} g_0 \ln \left( \frac{m_0}{m_f} \right) \quad (5-1)$$

where:

- $\Delta v$  is the change in velocity in m/s
- $I_{sp}$  is the specific impulse in s
- $g_0$  is the standard gravity of 8.81 m/s<sup>2</sup>
- $m_0$  is the servicer wet mass in kg
- and  $m_f$  is the servicer dry mass in kg.

Rearranging to find the wet mass gives Equation (5-2):

$$m_0 = m_f e^{\frac{\Delta v}{I_{sp} g_0}} \quad (5-2)$$

The thrusters selected in Section 7.4.2 Orbit determination methods and selection have an  $I_{sp}$  of 302 s. Therefore,

$$m_0 = 237.60 \times e^{\frac{903.1}{302 \times 9.81}}$$

$$\therefore m_0 = 322.28 \text{ kg}$$

This gives a fuel mass of  $322.28 - 237.60 = 84.68$  kg. Adding fuel residuals to this per requirement MAR-MAS-080 of the ESA CDF guidelines [164] gave a total

wet mass of 323.97 kg. This gives a propellant mass fraction of 26.7 %. The 1.17 kg/L density of the MMH/MON [169] used in the thrusters [165, p. 2] was used to calculate the fuel volume. Factoring in a volume margin per requirement MAR-CP-010 of the ESA guidelines [164, p. 13] gave a total tank volume of 81.2 L [25].

As a first approximation, the servicer bus was estimated as a 1 m cube, as this would provide 1000 L of volume, giving a substantial amount for the payload and other components. This approximation was supported by visual inspection of pictures of the ELSA-d satellite (such as Figure 4-4), which, judging by the size of its individual solar cells and people next to it, appears to be around a metre in length but shorter on the other two sides.

Under an alternative mission architecture, the servicer (also known in this case as the tug) could be required to tow the target back to an on-orbit servicing station for repairs or other operations to be completed there. The tug may refuel at this point. Once the servicing was completed, the tug would tow the target back to its operational orbit, before returning to the servicing station itself to refuel and await the next towing task. This servicing station concept is under active investigation by ESA (see Section 4.1 OOS types), but as it is not the architecture being used for this report's mission, detailed analysis of its  $\Delta v$  impact is beyond the report's scope. However, the significantly larger mass being manoeuvred when towing would increase the fuel use significantly and may necessitate the use of electric propulsion (EP) due to its high  $I_{sp}$ . The trade-off of EP against chemical propulsion for the tug is discussed in Section 7.6.2 Orbit control methods and selection and Section 10 Areas for Future Development.



## 6 Requirements Definition

The requirements for the OOS mission were formalised in their own document, entitled Space Servicer Requirements Specification [27], which is shown in full in Appendix C Space Servicer Requirements Specification. For the sake of brevity, only key top-level requirements contained within the document are discussed in this section. These requirements will be described and validated against the mission architecture. Requirements pertaining to particular subsystems such as the GNC system will be discussed in their relevant later sections.

Requirements were broken down into several sections. The first section listed general requirements pertaining to the overall mission, which included top-level requirements that cut across multiple systems. For example, spacecraft wet mass was included among the top-level requirements in the general section (as **TLR-0010**).

Subsequent requirement sections handled requirements relating only to one of five operations that were defined in the CONOPS (see Section 3.3.5 CONOPS and Appendix B CONOPS). The five operations were: undocking, rendezvous, final approach and docking, orbital manoeuvring, and hardware replacement/refuelling. Separation of requirements in this way allowed the author, acting as systems engineer, to quickly see which part of the mission the requirements related to. In a wider industry scenario, this would also allow other engineers to more easily concentrate only on requirements relating to their particular system.

Each requirement was given a unique identification number denoting the system related to and giving it a number that could be referred to later. These requirement identifiers were also printed in bold text throughout so the reader could find them easily. Each requirement was also given a short title summarising what it described. For example, **ROB-0010 Autonomy** was the first requirement relating to the servicer's robotics system and described the system's required level of autonomy.

## 6.1 Main requirements

Key physical requirements on the spacecraft were **TLR-0010** and **TLR-0020**, relating to wet mass and dimensions respectively. The servicer is required to have a wet mass of no more than 400 kg and no dimension greater than 1.5 m. This is to ensure it can be launched on a variety of launch vehicles to enable quicker and more flexible access to its customers. These limits constrain the spacecraft mass and volume budgets, setting limits on the sizes of components that can be used. These requirements were based on the mass and size of the Astroscale ELSA-d spacecraft (see Section 4.4.1 Missions).

One of the driving requirements for the mission was **TLR-0030**, which states that the spacecraft must be capable of fully autonomous operations. This will improve efficiency by enabling the servicer to perform more tasks between commands sent by ground operators [42, p. 71]. Autonomy gives the spacecraft the highest possible level of independence, above automatic and tele-operated systems. An automatic vehicle would require specific commands from ground controllers to define its operations, while a tele-operated spacecraft would be controlled directly by human operators. Autonomy means the spacecraft can be issued a general command such as “move to a 520 km altitude” and can interpret this to determine the tasks required to complete it. This requirement most heavily impacts the selection of sensors for the GNC system and RNS.

A final top-level driving requirement was **OPS-0010**, which specified a minimum 10-year mission lifetime. This means the spacecraft will have sufficient lifetime to service multiple targets, improving its financial viability. This was based on MEV-1, which will service IS-901 for five years before moving onto a new customer (see Section 4.4.1 Missions).

## 6.2 Requirements verification and validation

The requirements were verified by reading each in turn and checking that it met the SMART criteria, meaning every requirement should be Specific, Measurable, Attainable, Realisable and Time bounded [170]. These ensured that every

requirement was unambiguous and specific to a particular characteristic (e.g. mission lifetime).

Validation of requirements against the mission architecture was also performed to check that the requirements were accurately defining the mission needs, as driven by the OOS market and customer types as discussed in Section 5.1 Background. Some requirements were also taken from existing best practices, such as the GNC stability margin requirement (**GNC-0100**) that was defined from ESA's guidelines for Concurrent Design Facility (CDF) studies [164].



## **7 Guidance, Navigation and Control (GNC) System**

This section describes the design of the GNC system, which is used for absolute navigation before the servicer's computer hands over to the relative navigation system described in Section 8 Relative Navigation System (RNS) once within range of the target. This technique will also be used by the ELSA-d mission [79].

### **7.1 GNC architecture**

The overall function of the GNC is to perform absolute navigation for the servicer. This means it does not measure its position and attitude relative to the target like the RNS but instead uses 'fixed' targets such as the Sun and stars. The GNC must provide orbit determination and attitude determination information at regular intervals to the spacecraft's on-board computer, as well as to ground controllers. This will include information such as the orbit state vector and the heading of the spacecraft.

The system will work independently from the Relative Navigation System (RNS, described in Section 8 Relative Navigation System (RNS)). While both will use feedback loops to continuously receive and update their information, different sensors will be used for each to feed different information to the servicer's on-board computer (OBC).

The system is designed to operate autonomously, removing the need for ground controllers to remain in constant contact with the vehicle. This has the advantage that, in a scenario where multiple servicers are carrying out operations, the ground controllers do not have to track them all simultaneously and can instead cycle contact between them to periodically verify that they are still functioning as expected. Ground controllers can instead issue the servicer commands such as to move to a different orbit, with the servicer autonomously firing its thrusters at the correct point in its current orbit and for the correct duration, then validating the new orbit once manoeuvres are completed. This reduces workload on the controllers significantly, although oversight would still be required to ensure the

GNC is not operating on incorrect data. Autonomy is also useful when on final approach to and docking with the target, as the time delay on a video feed back to ground controllers can become too great to allow real time manual control. For example, the ETS-VII satellite had a six to seven second return delay in its robot arm control loop, which made teleoperation of the arm challenging [56, p. 420].

The GNC will use a three-axis stabilisation approach rather than spin stabilisation. This is because the spacecraft must be able to change its attitude freely to perform orbital manoeuvres and because it is not required to point in a particular direction such as Earth-facing during normal operations. Use of a three-axis architecture also enables larger solar arrays than the body-mounted cells that would be necessitated by a spin-stabilised design, increasing the electrical power available to the spacecraft systems [163, p. 406].

The spacecraft will be Sun-pointing by default, changing to inertial pointing when performing orbital manoeuvres, to point its antenna towards the ground and when handing control to the RNS. This and similar details are encapsulated by the spacecraft operational modes, which can be found in the CONOPS in Appendix B CONOPS.

## 7.2 GNC requirements

The GNC design is mostly driven by the requirements for orbit and attitude determination accuracy (**GNC-0060** and **GNC-0070**), pointing accuracy (**GNC-0080**), stability margins (**GNC-0090**) and slew rate (**GNC-0110**). These are shown in full in Appendix C Space Servicer Requirements Specification.

The stability margins requirement was taken from the ESA CDF guidelines [171, p. 22]. The accuracy requirements were based on the author's best estimates of reasonable values, with the slew rate requirements being scaled down from those given for an Earth observation mission in a paper by Votel and Sinclair [172].

### 7.3 Control Loop

The function of the GNC control loop is to continuously adjust the spacecraft's attitude and orbit to match the desired values. To do this at the start of each loop iteration it takes input from the attitude and orbit sensors, described in Section 7.4 Sensors. These feed into a controller, which processes the inputs from the sensors to determine the current attitude and orbit and compares these measured values against the demanded values supplied by the spacecraft's on-board computer (OBC).

With the use of a three-axis architecture and no mission requirement for fast slew manoeuvres (as may be required during an Earth observation (EO) mission), the attitude rates of the spacecraft can be assumed to remain low throughout the mission. This is particularly true when the tug is docked to the target spacecraft, with their combined mass reducing the angular acceleration that can be achieved by the GNC actuators with a given amount of propellant or momentum exchange. The assumption that the attitude rate remains low means that cross-coupling effects between spacecraft axes can be ignored and thus a Single-Input, Single-Output (SISO) controller can be used rather than a more complex and hence costly Multiple-Input, Multiple-Output (MIMO) controller.

Although a simple controller would be advantageous to enable rapid implementation and to avoid failure modes, a relatively complex controller such as a proportional-integral-derivative (PID) controller may be required to deal with controlling attitude and orbit simultaneously. A PID controller would also likely be required for the RNS due to the high precision and accuracy requirements when approaching the target. Further analysis of the required controller type for the servicer would be a key element of future work (described in Section 10.2 Systems engineering considerations).

## 7.4 Sensors

### 7.4.1 Sensor requirements

The selection of the GNC's orbit and attitude determination sensors was primarily driven by the requirements for orbit (**GNC-0070**) and attitude determination (**GNC-0080**) accuracy. These requirements are shown in full in Appendix C Space Servicer Requirements Specification.

For both sensor types, the highest degree of accuracy, 0.5 °, is needed when performing orbital manoeuvres. For the orbit determination sensors, this is to have accurate knowledge of the tug orbit prior to and after the burn to determine the  $\Delta v$  required for it and to verify that it has been completed within tolerance. For the attitude determination sensors, accurate and precise attitude knowledge is required pre-burn to ensure that the spacecraft's thrusters are oriented correctly so that the imparted  $\Delta v$  places the tug in the correct orbit.

The accuracy requirement is lowered at the start of the rendezvous phase, as it is at this point that the tug switches from using its absolute navigation GNC system described in this section to using the relative navigation system described in Section 8. For the entire RPOD phase of the mission, the RNS is providing the primary data set for navigation, although the GNC will still operate in the background as a method of detect any large errors in the RNS values.

If the RNS fails in some way, such as losing lock on the target, the tug may revert to using its absolute navigation sensors. These contingency operations are described in the CONOPS, shown in Appendix B CONOPS.

The GNC and RNS are also required (**GNC-0030**) to take up no more than 15 % of the spacecraft volume combined, although this is a preliminary estimate. A volume rather than mass requirement was specified due to the relatively small volume of the spacecraft bus. In terms of power, the GNS and RNS combined shall use no more than 75 % of the total power budget (**GNC-0040**), although this is again an estimated figure.

## 7.4.2 Orbit determination methods and selection

A key requirement for the servicer (**TLR-0030**, see Appendix C Space Servicer Requirements Specification) is for it to perform its operations autonomously. This requirement does not necessarily limit the tug's ability to use data from external systems for its navigation, but independence from these systems reduces the number of systems whose failures could affect tug operations.

Global navigation satellite systems (GNSS) use constellations of satellites to provide position and timing information to users. The most commonly used GNSS is the US Global Positioning System (GPS), although other systems such as Russia's GLONASS and Europe's Galileo are also available. GNSS systems use a receiver on the user spacecraft to detect the signals from multiple GNSS satellites to determine the user's orbit. Many receivers are available for GPS [173] [174] [175], with some receivers able to use multiple GNSS systems [176] [177].

Other available systems for orbit determination include the ground-based Space Surveillance Network (SSN) and Doppler Orbitography and Radiopositioning Integrated by Satellite (DORIS), and the space-based Tracking and Data Relay Satellite System (TDRSS).

The SSN collects around 500,000 measurements per day and is used to maintain the active space catalogue, particularly to provide orbit data for space debris [163, p. 593].

DORIS uses a network of 60 ground beacons whose signals are received by the satellite, with the Doppler shift between them allowing an orbit determination to be made. The system has previously been used on spacecraft such as TOPEX/Poseidon and Envisat [163, p. 596].

TDRSS uses a constellation of eight GEO satellites that provide "100 % visibility... from 1,200 km to 10,000 km altitude, decreasing to 85 % visibility at 300 km" [178, p. 67]. The spacecraft to be tracked is fitted with a transponder, with range and range-rate information with respect to the TDRSS satellites being used to periodically determine the orbit. Orbit information is passed from the

TDRSS ground segment directly to the user’s ground station [163, p. 594], so for this mission would then need to be uploaded to the servicer.

A system called the TDRSS On-board Navigation System (TONS) uses the TDRSS space segment, but also relays a signal from the TDRSS satellites to the user and measures the Doppler shift on this to accurately determine the orbit. The system requires more hardware on-board than the simpler TDRSS system but enables autonomy and higher accuracy.

**Table 7-1 - Orbit determination method trade-off table**

<b>Method</b>	<b>Can determine orbit independent of ground?</b>	<b>Hardware required on-board?</b>	<b>Accuracy</b>	<b>References</b>
SSN	No	No	~ 130-440 m	[179, p. 320]
TDRSS	No	Yes	50 m $3\sigma$	[163, p. 595]
TONS	Yes	Yes	10 m $1\sigma$	[163, p. 596] [180, p. 78]
DORIS	Yes	Yes	A few cm	[163, p. 596] [181]
GNSS	Yes	Yes	~ 10 m	[163, p. 595] [182]

The aforementioned orbit determination methods are summarised in Table 7-1. Trading off the systems, only TONS, DORIS and GNSS are able to determine the spacecraft’s orbit independently of the ground. While DORIS has the best accuracy of these, it would also require equipment on-board with a significant!9y greater mass and power draw. Envisat’s DORIS unit had a mass of 91 kg and power draw of 42 W [181], while a common GPS unit from General Dynamics has a mass of 1.1 kg and draws 7 W [183]. The additional accuracy from DORIS is not required and TONS also requires more advanced equipment than GNSS, making GNSS the optimal choice for orbit determination.

If the spacecraft were equipped with a receiver for a single GNSS, most likely GPS, it could use SSN data relayed from the ground as a backup, removing its independence. However, use of a multi-GNSS system would mean that even if an unlikely failure of, say, GPS did occur, the spacecraft could fall back on one of the other GNSS constellations it could receive, allowing it to continue operations unhindered.

### **7.4.3 Attitude determination methods and selection**

This section will discuss the various types of attitude determination sensors available that can then be selected from for the mission's GNC design.

A wide variety of sensors exist that can be used for attitude determination. These include: Sun sensors, Earth horizon sensors, star trackers, gyroscopes and accelerometers (often combined in an inertial measurement unit (IMU)), magnetometers and Global Positioning System (GPS) receivers. A description of each of these is given below.

Sun sensors come in analogue or digital forms. Digital Sun sensors use a small image sensor with a grating to determine the angle of the Sun relative to the sensor plane's normal. An analogue Sun sensor will have two image sensors inclined with respect to each other, with the difference in output between the two cells providing a measurement of the Sun incidence angle [184]. A spacecraft's solar cells can also be used as coarse Sun sensors as a backup or if the main Sun sensor fails, with this method determining the Sun's angle in much the same way as a normal analogue Sun sensor [185].

Earth horizon sensors use infrared sensors to detect the difference in temperature between the Earth and deep space. Three-axis stabilised spacecraft use scanning Earth horizon sensors that measure the horizon chord length [184]. Their power use can be fairly high, up to around 10 W, with masses ranging between approximately 1 and 4 kg for scanning Earth horizon sensors [163, p. 583].

Star trackers combine an imaging sensor with a built-in star map. A processor within the tracker then compares the images taken by the sensor to the star map, allowing attitude determination to be performed with accuracies as low as 1 arcsecond. However, the image sensor and computation required mean star trackers have relatively high power usage and are also very expensive [163].

The US's Global Positioning System (GPS), while traditionally used for position or time information, can also be used to find a spacecraft's attitude. Multiple receivers are used to receive the signal transmitted by the GPS satellites, with the phase difference of the received signals used to determine the spacecraft attitude, to accuracies as good as  $0.25^\circ$  for a 1 m baseline between the receivers [163, p. 584]. This makes GPS accurate enough to be used in spacecraft with low attitude determination accuracy requirements or as a backup for other systems such as star trackers. GPS receivers also have little impact on the spacecraft's power or data budgets and are fairly low cost [186] [183].

A gyroscope can be used to measure the rotation speed of a spacecraft or its angle relative to an initial reference [163, p. 584]. If combined with a high accuracy system such as a star tracker, that system can be used to get an initial fix of the attitude with the low power and negligible data production gyroscope then used for attitude determination. However, gyroscopes do exhibit drift over time, meaning another system is occasionally needed as a new initial angle reference. Gyroscopes are often grouped together to form an inertial reference unit (IRU) that provides three-axis information, with accelerometers sometimes added to an IRU to also give position information. This combined gyroscope and accelerometer system is referred to as an inertial measurement unit (IMU) [163, p. 585].

Finally, magnetometers can provide attitude information when combined with an accurate on-board model of the Earth's magnetic field and knowledge of the spacecraft's position in its orbit. These sensors are reliable and lightweight (around 0.3-1.2 kg) but due to uncertainty in the magnetic field model have relatively poor accuracies of around  $0.5\text{-}3^\circ$  [163, p. 583].

The various sensor types and their typical accuracies, masses and power draws are summarised in Table 7-2. From these data, a trade-off can be performed to select the attitude determination sensor configuration.

The highest attitude accuracy while under absolute navigation ( $0.05^\circ$  per **GNC-0080**) will be required when performing orbital manoeuvres to ensure the thrust vector is correctly aligned. The spacecraft also needs a reliable way of determining the position of the Sun for solar array pointing.

Earth horizon sensors can be ruled out because the spacecraft will change its attitude and altitude frequently. As Sun sensors are the only sensor type that directly determines the position of the Sun, they are the best choice for solar array pointing. The spacecraft's solar cells can also be used as coarse Sun sensors as a backup, for example when the spacecraft is in safe mode. The Sun sensors would need to be mounted on different faces of the spacecraft to any optical instruments such as cameras to avoid blinding the instruments when determining Sun position.

Magnetometers, while low power, offer significantly worse accuracy than GPS for a similar amount of mass and would require an accurate model of the Earth's magnetic field to be stored on-board.

To meet **GNC-0080**, a high accuracy solution is required. However, the high power consumption and data production of star trackers should be avoided where possible. To accomplish this, a star tracker and gyroscope combination can be implemented. The star tracker will be used periodically to achieve a precise attitude determination, with low power and data rate gyroscopes then used to update this until their drift becomes excessive and calibration by the star tracker is needed again.

GPS's low mass and power requirement and reasonable accuracy make it a good choice for a backup system. While it would not be accurate enough to support orbital manoeuvres, it would allow the solar arrays to be pointed towards the Sun in the event of a Sun sensor failure. Also, as GPS or another GNSS system is already being used for orbit determination as described in the previous section,

its use for attitude determination will only require one additional receiver unit so that a baseline can be formed. The baseline should be as long as possible to maximise accuracy, so the receivers should be mounted on opposite faces of the spacecraft if possible.

To summarise the attitude sensor selection, Sun sensors will provide pointing information for the solar arrays, with the arrays themselves being used as coarse Sun sensors when in safe mode. A star tracker combined with gyroscopes will provide accurate determination to support orbital manoeuvres with GPS used as a backup system in case of failure of one of the other determination methods.

**Table 7-2 – Attitude determination sensor trade-off table**

Sensor type	Accuracy (°)	Mass (kg)	Power (W)	References
Gyroscopes	Drift rate 0.003-1 °/hr	~ 1 to 2	< 12	[163, p. 583] [187] [188]
Sun sensors	0.005-3	0.1 to 2	0 to 3	[163, p. 583]
Star trackers	0.0003-0.01	< 2	< 12	[163, p. 583] [189] [190]
Scanning Earth horizon sensors	0.05-1 ° (0.1 ° best for LEO)	1 to 4	5 to 10	[163, p. 583]
Magnetometer	0.5-3 °	0.3 to 1.2	< 1	[163, p. 583]
GPS	0.25-0.5 ° for 1 m baseline	~ 1.1	~ 7	[183]

## 7.5 Plant

The function of the plant within the GNC control loop is to model the spacecraft's dynamics and the effect on them from external torques. When considering attitude control alone, the output from the plant is the attitude quaternion and body rate vector [191, p. 4]. For a full GNC system, orbital information such as

state vectors or Keplerian elements (depending on the plant's implementation) will also be outputted. These give the OBC current true data on the spacecraft's dynamics.

Examples of external torques modelled by the GNC plant include effects on attitude such as solar radiation pressure (SRP), magnetic torque and gravity gradient torque, and orbital perturbations such as atmospheric drag, SRP, the J2 perturbation and Earth triaxiality [192]. Actuators such as thrusters that exert an external torque – one that adds momentum to the spacecraft in the inertial frame – will also be included in the total external torque.

Another crucial element of the plant is its model of the spacecraft's moment of inertia matrix, both when on its own and when docked to the target. Although under this mission architecture no orbital manoeuvres will be carried out while the vehicles are docked, the combined inertia matrix is still required so the attitude dynamics can be understood. For example, the inertia matrix was used along with total torque calculations (see Section 7.6 Actuators) to find the maximum angular acceleration that the spacecraft could achieve.

To find the inertia matrices, the locations of the centres of mass of the servicer and target were also required. Calculations were carried out in the Main Central Control spreadsheet (see Section 3.3.2 Main Central Control spreadsheet) that determined the following centre of mass locations and inertia matrices. Derivations of these and the definitions of the various reference frames are shown in Appendix E Centres of Mass and Moment of Inertia Matrices Calculations.

- Servicer centre of mass in the servicer body frame:  $[0 \ 0 \ 0^T] \text{ m}$
- Target centre of mass in the target body frame:  $[0 \ 0 \ 0^T] \text{ m}$
- Target centre of mass in the docked body frame:  $[1.2792 \ 0 \ 0^T] \text{ m}$
- Combined centre of mass in the docked body frame:  $[0.4883 \ 0 \ 0]^T \text{ m}$
- $I_{\text{servicer}} = \begin{bmatrix} 53.99 & 0 & 0 \\ 0 & 53.99 & 0 \\ 0 & 0 & 53.99 \end{bmatrix} \text{ kg m}^2$
- $I_{\text{target}} = \begin{bmatrix} 28.23754 & 0 & 0 \\ 0 & 39.99213 & 0 \\ 0 & 0 & 44.57873 \end{bmatrix} \text{ kg m}^2$

- $I_{docked} = \begin{bmatrix} 82.23 & 0 & 0 \\ 0 & 296.34 & 0 \\ 0 & 0 & 300.92 \end{bmatrix} \text{ kg m}^2$

## 7.6 Actuators

When designing the architecture for the actuators, their use for both attitude and orbit control needed to be considered. Due to the three-axis stabilisation architecture (see Section 7.1 GNC architecture) and the need to perform orbital manoeuvres throughout the mission, the actuators were required to control the spacecraft in all six degrees of freedom (DOF). The author also decided that to reduce spacecraft complexity, the same actuators would be used by the RNS when approaching the target.

An actuator architecture first had to be defined. While systems such as reaction wheels (RWs) or control moment gyroscopes (CMGs) can provide attitude control (and are evaluated in Section 7.6.3 Attitude control methods and selection), only thrusters are able to translate the spacecraft. Thrusters would also be needed to desaturate any reaction wheels or CMGs as magnetorquers would provide insufficient torque given the mass of the spacecraft. It was therefore decided that the thrusters would provide 6DOF capability, with a smoother system such as RWs or CMGs used when required, such as during approach to docking.

Eight thrusters were found to be the minimum to achieve 6DOF control [193], with the ELSA-d mission (see Section 4.4.1 Missions) using 12 thrusters – one on each corner of the spacecraft and two each on the face with the docking fixture and the opposing face to aid translation [194]. The ELSA-d configuration was baselined and modelled in the Main Central Control spreadsheet (see Section 3.3.2 Main Central Control spreadsheet), as shown in Figure 7-2.

A basic CAD model of the servicer, shown with thruster numbering labels in Figure 7-1, was first produced to aid understanding while modelling the thrusters. This included the spacecraft bus, the DogTag grapple fixture (see Section 9.1 Grappling Fixture) and the 12 thrusters.

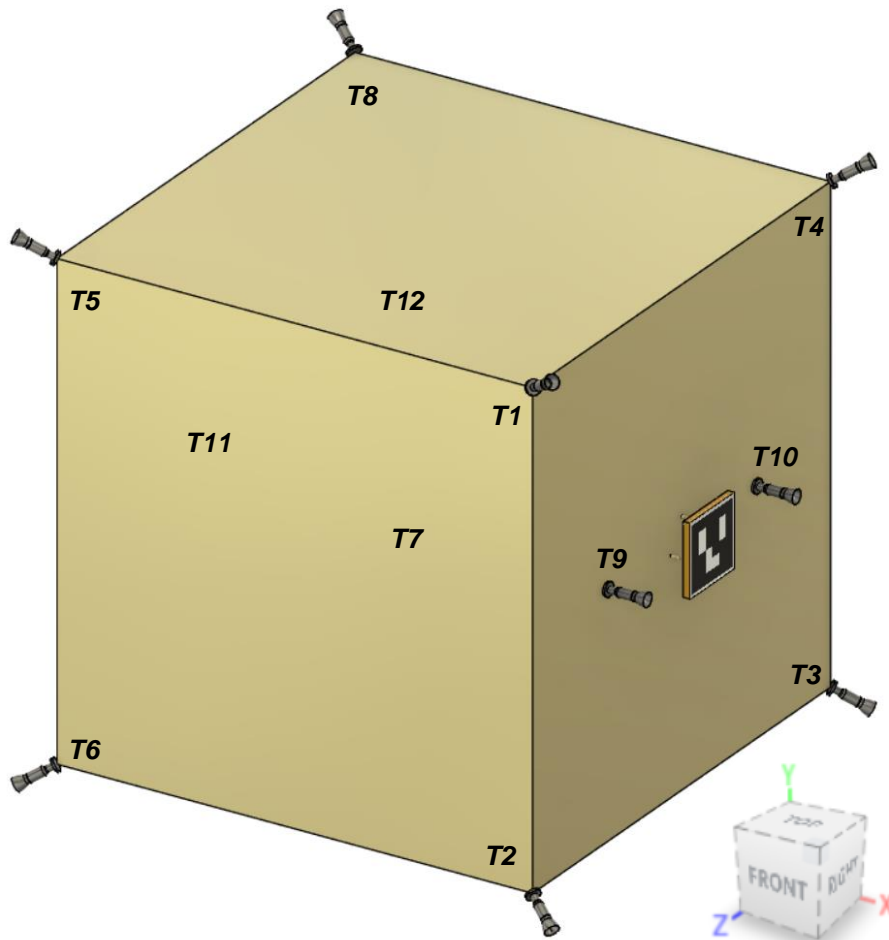


**Figure 7-1 - Basic servicer CAD model with labels showing thruster numbering and inset showing axes definitions**

While eight thrusters are the minimum for 6DOF control, if their thrust vectors were at 45 ° relative to the adjacent faces, the cube shape of the servicer bus would mean the thrust vectors would all point through the spacecraft's centre of mass (assuming a homogenous cube). This would mean no torque could be produced and attitude control could not be achieved. Main Central Control was therefore used to determine suitable pointing for each thruster.

When the CAD model of a thruster was imported into the servicer model, it would initially be pointing (i.e. have its thrust vector pointing) in the +Z direction, or  $[0 \ 0 \ 1]^T$ . The author then translated the thruster into position on the corner where it was rotated by 30 ° around the X-axis followed by 60 ° around the Y-axis. The angles were modified appropriately for each thruster to point the

thruster in the correct direction, but the magnitude of the resulting direction vector for each thruster was the same. The direction vectors were found by using direction cosine matrices (DCMs) as shown below.

The Euler 123 sequence DCM shown in Equation (7-1) was used [195], where  $\phi$  is the angle rotated around the X-axis,  $\theta$  is the angle rotated around the Y-axis and  $\psi$  is the angle rotated around the Z-axis.

$$R = \begin{bmatrix} c\psi c\theta & c\psi s\theta s\phi + s\psi c\phi & -c\psi s\theta c\phi + s\psi s\phi \\ -s\psi c\theta & -s\psi s\theta s\phi + c\psi c\phi & s\psi s\theta c\phi + c\psi s\theta \\ s\theta & -c\theta s\phi & c\theta c\phi \end{bmatrix} \quad (7-1)$$

The initial thruster vector of  $[0 \ 0 \ 1]^T$  was then multiplied by this as shown in Equation (7-2) [195] to give the output direction vector (denoted  $\underline{d_{output}}$ ) for each thruster, considering any changes that needed to be made to the angles to point the thruster in the correct direction for its location. For example, thruster 1 used angles of  $-30^\circ$  around the X-axis and  $60^\circ$  around the Y-axis, while thruster 8 used  $30^\circ$  around the X-axis (the negative of T1's value) and  $-120^\circ$  around the Y-axis (T1's value minus  $180^\circ$ ). The angles were verified by inspection for each thruster by examining the CAD model.

$$\underline{d_{output}} = R[0 \ 0 \ 1]^T \quad (7-2)$$

This translation and rotation procedure produced the position and direction vector data shown in the spreadsheet model in Figure 7-2.

	A	B	C	D	E	F	G	H	I	J	K	L	M	N	O	P	Q	R	S	T	
1			Direction vector (-)			Position vector (m)				Torque (Nm)						Thrust (N)					
2		Thruster	X	Y	Z	X	Y	Z		X	Y	Z				X	Y	Z	Enabled?		
3		Attitude control	1	0.866	0.250	0.433	0.500	0.500	0.500		-4.575	-10.825	15.401			43.301	12.500	21.651	y		
4			2	0.866	-0.250	0.433	0.500	-0.500	0.500		4.575	-10.825	-15.401			43.301	-12.500	21.651	y		
5			3	0.866	-0.250	-0.433	0.500	-0.500	-0.500		0.000	0.000	0.000			0.000	0.000	0.000	n		
6			4	0.866	0.250	-0.433	0.500	0.500	-0.500		0.000	0.000	0.000			0.000	0.000	0.000	n		
7			5	-0.866	0.250	0.433	-0.500	0.500	0.500		0.000	0.000	0.000			0.000	0.000	0.000	n		
8			6	-0.866	-0.250	0.433	-0.500	-0.500	0.500		0.000	0.000	0.000			0.000	0.000	0.000	n		
9			7	-0.866	-0.250	-0.433	-0.500	-0.500	-0.500		-4.575	-10.825	15.401			-43.301	-12.500	-21.651	y		
10			8	-0.866	0.250	-0.433	-0.500	0.500	-0.500		4.575	-10.825	-15.401			-43.301	12.500	-21.651	y		
11		Translation	9	1.000	0.000	0.000	0.500	0.000	0.250		0.000	0.000	0.000			0.000	0.000	0.000	n		
12			10	1.000	0.000	0.000	0.500	0.000	-0.250		0.000	0.000	0.000			0.000	0.000	0.000	n		
13			11	-1.000	0.000	0.000	-0.500	0.000	0.250		0.000	0.000	0.000			0.000	0.000	0.000	n		
14			12	-1.000	0.000	0.000	-0.500	0.000	-0.250		0.000	0.000	0.000			0.000	0.000	0.000	n		
15																					
16		Thrust	50 N							X	Y	Z				X	Y	Z			
17									$T_{total}$	0.000	-43.301	0.000	Nm		$Thrust_{tot}$	0.000	0.000	0.000	N		
18			Thruster angles						$\alpha$	0.000	-0.138	0.000	rad.s <sup>-2</sup>		$a$	0.000	0.000	0.000	m.s <sup>-2</sup>		
19			X	Y	Z				$Torque\ mag$	43.301 Nm				$Thrust\ mag$	0.000 N						
20			-30	60	0°				$\alpha\ mag$	7.926 deg.s <sup>-2</sup>				$a\ mag$	0.000 m.s <sup>-2</sup>						
21	Default		-30	60	0																
22			-0.524	1.047	0.000	radians															
23																					
24			Initial vector																		
25			X	Y	Z																
26			0	0	1																
27																					
28	Thruster 1		Thruster angles			DCM				Output vector											
29			Y	X	Z	X	Y	Z		X	Y	Z									
30			60	-30	0°	0.500	-0.433	0.750		0.866	0.250	0.433									
31			1.047	-0.524	0.000	0.000	0.866	-0.500													
32						0.866	0.250	0.433													
33																					
34	Thruster 2		Thruster angles			DCM				Output vector											
35			Y	X	Z	X	Y	Z		X	Y	Z									
36			60	30	0°	0.500	0.433	0.750		0.866	-0.250	0.433									
37			1.047	0.524	0.000	0.000	0.866	0.500													
38						0.866	-0.250	0.433													
39																					
40	Thruster 3		Thruster angles			DCM				Output vector											
41			Y	X	Z	X	Y	Z		X	Y	Z									
42			60	-210	0°	0.500	0.433	-0.750		0.866	-0.250	-0.433									
43			1.047	-3.665	0.000	0.000	-0.866	0.500													
44						0.866	-0.250	-0.433													
45																					
46	Thruster 4		Thruster angles			DCM				Output vector											
47			Y	X	Z	X	Y	Z		X	Y	Z									
48			60	210	0°	0.500	-0.433	-0.750		0.866	0.250	-0.433									
49			1.047	3.665	0.000	0.000	-0.866	-0.500													
50						0.866	0.250	-0.433													
51																					
52	Thruster 5		Thruster angles			DCM				Output vector											
53			Y	X	Z	X	Y	Z		X	Y	Z									
54			-60	-30	0°	0.500	0.433	-0.750		-0.866	0.250	0.433									
55			-1.047	-0.524	0.000	0.000	0.866	-0.500													
56						-0.866	0.250	0.433													
57																					

**Figure 7-2 - Screenshot of the Main Central Control spreadsheet showing modelling of the servicer thrusters [25]**

Once the direction and position vectors had been found, the cross product was taken and multiplied by the thrust of an individual thruster to find the torque vector produced by each thruster. Summing the results then gave the spacecraft's total torque vector. The diagonal elements of the spacecraft inertia matrix (see Section 7.5 Plant) were multiplied by their respective elements of the torque vector to give the angular acceleration vector. The torque and angular acceleration magnitudes were also calculated to aid mission planning.

The thrust vector for each thruster was found by multiplying the thrust of a single thruster by each thruster's direction vector. These were then summed to find the

spacecraft's thrust vector. Using the spacecraft wet mass (see Section 5.3.2 Fuel requirement estimation) to give a worst case, the linear acceleration of the vehicle could then be found, as well as the thrust and acceleration magnitudes.

An additional column on the end of the thruster table allowed each thruster to be turned on or off individually. This assumed that a thruster would produce its maximum torque when on and zero torque when off. By switching thrusters on and off, the author could determine factors such as the maximum thrust and torque and the effect on these if a thruster became inoperable.

An additional option in the spreadsheet specified whether the servicer was docked to the target. If not, only the servicer's calculated mass and moment of inertia matrix would be used to find the linear and angular accelerations. However, if the docked option were set, the calculations would use the combined mass found in Section 5.3.2 Fuel requirement estimation and the combined moment of inertia from Section 7.5 Plant. This enabled the author to see the vehicle dynamics throughout all mission phases.

### **7.6.1 Actuator requirements**

The requirements discussed in this section can be found in full in Appendix C Space Servicer Requirements Specification. The main requirements affecting the actuators were linear acceleration (**GNC-0230**) to ensure the servicer's orbital manoeuvres could be considered impulsive, and angular acceleration (**GNC-0020**) to stabilise and control the attitude of the combined spacecraft when docked.

Impulsive manoeuvres were desired to reduce the mission time spent on orbital manoeuvres, as this would be time where the target had degraded functionality so could not maintain full operations for its owner, or where the servicer was not actually servicing targets so was not earning money for its owner. To calculate the minimum acceleration needed for impulsive manoeuvres, it was first assumed that a manoeuvre could be considered impulsive if its duration was no more than 5 % of the orbit period. The required  $\Delta v$  for the orbital manoeuvres for the non-

coplanar phasing (see Section 5.3.2 Fuel requirement estimation) were already known, as were the orbital periods for each part of the transfer. As a first approximation, it was assumed that the acceleration during the manoeuvres would be linear. This allowed the minimum acceleration for each manoeuvre to be found. The highest of these raw figures then had a 20 % margin added as per the ESA CDF guidelines [164] to give the minimum for the spacecraft. This gave a raw acceleration of  $0.296 \text{ m/s}^2$  and a minimum for the spacecraft of  $0.356 \text{ m/s}^2$  once margin had been added [25]. The figure with margin was then rounded to  $0.36 \text{ m/s}^2$  for the requirement, **GNC-0230**.

Regarding the angular acceleration requirement, the spacecraft had no need to slew quickly as would be the case, for example, for an Earth observation mission. A minimum acceleration of  $0.25 \text{ }^\circ/\text{s}^2$  was chosen to avoid heavily driving the actuator selection while ensuring the spacecraft could successfully control its attitude during orbital manoeuvres and while docked to the target. The highest theoretical torque would be required when the servicer and target were docked and attempting to rotate, although in reality the servicer would have expended some fuel to reach the target so its mass and the required torque would be less.

### **7.6.2 Orbit control methods and selection**

As discussed previously, only thrusters can be used for spacecraft translation. They can and will however be used by the RNS (see Section 8 Relative Navigation System (RNS)) during RPO. They can be separated into chemical and electric propulsion (EP) systems and then further into particular types such as hydrazine or Hall effect thrusters (HETs).

However, EP has far lower thrust than chemical propulsion, for example in 2017, the X3 thruster set a new thrust record for plasma thrusters of 5.4 Newtons [196]. A thrust of 71 N would be required to meet the acceleration requirement (**GNC-0230**) considering the servicer's 198 kg dry mass alone. For this reason, the author quickly determined that EP could not meet the acceleration requirement. However, the MEV-1 and -2 missions discussed in Section 4.4.1 Missions use

EP as their main system for orbit raising (in addition to a small hydrazine system) [73], so further analysis of its impact on mission duration and whether this is problematic will be required.

Examples of available chemical thrusters are shown in Table 7-3 for the purposes of performing a trade-off analysis. Using the spreadsheet thruster model and enabling the thruster configuration that gave the highest linear acceleration, the author determined that a minimum thrust per thruster of 24.2 N would be required to meet **GNC-0230** in full. However, assuming an  $I_{sp}$  of 220 s, a thrust of 22 N would give an acceleration of  $0.331 \text{ m/s}^2$  (an 8 % reduction), which may be acceptable from a mission design point of view. This will require further analysis and is discussed in Section 10.1 Mission design and dynamics analysis. It will be assumed for the trade-off that this reduced acceleration would not be acceptable.

Firstly, the NG MRE-4.0 thruster can be eliminated due to insufficient thrust, and the MT-6, MR-107T and 50N HPGP thrusters due to excessive thrust. The Dawn Aerospace thruster also has low thrust, but its 285 s  $I_{sp}$  means it still achieves an acceleration of  $0.331 \text{ m/s}^2$ . However, it is ruled out due to its low maximum impulse bit of 150 N-s [197], which only allows it to run at full thrust for 7.5 s at a time, while the orbital manoeuvres require burns of approximately five minutes. Low TRL is another disadvantage of the 50N HPGP and Dawn Aerospace thrusters.

The 22N HPGP Thruster can then be eliminated due to insufficient throughput lifetime – calculations in MCC showed that for an  $I_{sp}$  of 250 s, approximately 108 kg of propellant would be required for a single servicing return journey [25], exceeding its limit of 50 kg. It also has a low TRL.

275 s  $I_{sp}$  was found in MCC to be the lower limit for the acceleration requirement to be met with a set of 22 N hydrazine thrusters, as a lower  $I_{sp}$  would lead to more fuel being needed that would increase the servicer's mass. The MR-106L and two Moog MONARC thrusters were therefore eliminated due to their low  $I_{sp}$ .

**Table 7-3 - Examples of available chemical thruster systems**

Manufacturer	Model	Thrust (N)	Propellant	I <sub>sp</sub> (s)	Lifetime			TRL	References
					No. pulses	Throughput (kg)	Total Impulse (N-s)		
Aerojet Rocketdyne	MR-106L	22	Hydrazine	235-228	120,511	Unknown	561,388	9	[198]
Aerojet Rocketdyne	MR-107T	110	Hydrazine	222-225	36,500	Unknown	162,360	9	[198]
Bradford Space	22N HPGP Thruster	22	LMP-103S	243-255	2,000	50	Unknown	4	[199]
Bradford Space	50N HPGP Thruster	50	LMP-103S	243-255	2,000	50	Unknown	4	[200]
Dawn Aerospace	SmallSat Propulsion Thruster – 20N	20	N <sub>2</sub> O and propene (C <sub>3</sub> H <sub>6</sub> )	>285	Unknown	Unknown	93,000	~4 <sup>2</sup>	[197]

<sup>2</sup> The TRL for this thruster has been assessed by the author by judging available information on completed testing against the ESA TRL scale in Appendix D Technology Readiness Levels.

IHI AeroSpace	MT-6	50	Hydrazine	215-225	14,800	>120	Unknown	9	[201]
Moog	DST-11H	22	Hydrazine/ MON	310	Unknown	907	Unknown	9	[165]
Moog	DST-12	22	MMH/MON	302	Unknown	1073	Unknown	9	[165]
Moog	DST-13	22	MMH/MON	298	Unknown	637	Unknown	9	[165]
Moog	5 lbf	22	MMH/MON	288/292	Unknown	484	Unknown	9	[165]
Moog	MONARC- 22-6	22	Hydrazine	229.5	230,000	Unknown	533,784	9	[202]
Moog	MONARC- 22-12	22	Hydrazine	228.1	160,000	Unknown	1,173,085	9	[202]
Northrop Grumman	MRE-4.0	18	Hydrazine	217	507,000	249	Unknown	9	[203]
Northrop Grumman	MRE-5.0	28 (36 max)	Hydrazine	232	28,512	456	Unknown	9	[204]

Any of the five remaining thrusters (DST-11H, DST-12, DST-13, 5 lbf, MRE-5.0) seem to meet the requirements. The 28 N (or 36 N with high inlet pressure [204]) NG MRE-5.0 thruster would meet the acceleration requirement, but its low  $I_{sp}$  means the spacecraft would have a higher wet mass and hence a higher launch cost. It was therefore eliminated. The 5lbf thruster was eliminated due to its low throughput; for this thruster approximately 91 kg of fuel would be required for a return journey, meaning only five could be achieved before the thrusters would need replacing.

Examining the throughputs and  $I_{sp}$ s of the remaining three thrusters, the DST-11H could do 10 full servicing journeys, the DST-12 12 journeys and the DST-13 7 journeys. The DST-13 was therefore eliminated. While the DST-11H thruster has a slightly higher  $I_{sp}$ , this only saves 2.58 kg or 3 % of the propellant. The extra journeys gained by the DST-12's higher throughput are judged to be more advantageous. The DST-12 thruster was therefore selected.

### **7.6.3 Attitude control methods and selection**

The thrusters described previously will also be used for attitude control. However, the deadband needed for a thruster control system means their operation is not as smooth and hence not as accurate as a continuously adjustable system such as a reaction wheel or CMG. When performing orbital manoeuvres or on final approach to dock with the target, high pointing accuracy will be required. This necessitates a set of continuously adjustable actuators.

Aside from thrusters, four main types of actuator are available for attitude control: magnetorquers, RWs and CMGs. Magnetorquers cannot provide a high enough torque for attitude control of a spacecraft the size of the servicer though, so could quickly be eliminated from the trade-off. For example, the NCTR-M012 magnetorquer from NewSpace Systems has a magnetic moment of  $1.19 \text{ Am}^2$  [205]. The torque produced by a magnetorquer is given by Equation (7-3) [206], where  $\tau$  is the torque in Nm,  $M$  is the magnetorquer's magnetic moment in Amps-metre squared ( $\text{Am}^2$ ) and  $B$  is the flux density of the Earth's magnetic field in

Webers per metre squared ( $\text{Wb/m}^2$ ).  $\underline{B}$  is approximately  $3 \times 10^{-5}$  Tesla (T) at the Earth's surface [207]. While the flux density varies with altitude, this is sufficiently accurate for a first approximation. From this, the torque is approximately 0.0357 mNm, which would be far too little to be useful on the servicer.

$$\underline{T} = \underline{M} \times \underline{B} \quad (7-3)$$

$$\underline{T} = 1.19 \times 3 \times 10^{-5} = 3.57 \times 10^{-5} \text{ Nm} = 0.0357 \text{ mNm}$$

Once magnetorquers had been discarded, three options remained: RWs, CMGs and momentum wheels. A momentum wheel spins at a constant non-zero rate, giving the spacecraft gyroscopic stiffness around two axes [163, p. 579]. However, this would not be desirable when on final approach to the target, as the servicer needs to be able to use its thrusters to adjust its attitude in all three rotational degrees of freedom to counter any unexpected disturbance torques or, for example, in the event of a thruster failure. This leaves RWs and CMGs.

Both types can supply the torque and momentum capacity needed for the servicer. However, a CMG's extra axis of rotation and the resulting complexity relative to a RW means it tends to be more expensive and less reliable [208, p. 7]. The controller of a CMG-based system also has to avoid singularities caused by the torque axes of two or more CMGs aligning, which would prevent a three-axis torque from being generated. This makes the controller more algorithmically and computationally complex than for a RW system [172, p. 2]. The singularity can be overcome though by using variable speed CMGs [209, p. 2].

One of the key issues facing CMGs is availability. Four CMGs have been used successfully on the ISS for several years [210, p. 2], but these are far too large for the servicer. CMG technology is currently under development for CubeSats by Cranfield University [211]. Only a handful of other models are available [209] [212]. One example was developed at the Surrey Space Centre around 2009 as a variable speed CMG system for attitude control as well as energy storage. CMGs were also used on the 120 kg BIILSAT-1 satellite, giving it the capability to slew  $40^\circ$  in around 20 s, although these were custom parts for the mission

[208, p. 7]. Airbus Defense & Space produce a COTS CMG with a torque capability of 45 Nm, but it has a power draw of around 25 W [212].

CMGs, at least large models, do tend to be significantly more power efficient than RWs [210, p. 2], but for the servicer with its low torque requirement this is not a major concern.

The author judged that due to the disadvantages listed above, RWs would be a more promising technology for the attitude control actuators. The availability of a selection of COTS models with flight heritage is a major advantage as it speeds up system development and ensures reliability. Collins Aerospace are a leading manufacturer of RWs. The company sells six different models of wheel that can be used as RWs or momentum wheels, with 7,300 years of flight heritage across the range [213] [214]. Collins' RSI 12 wheel is a strong candidate as it has been designed for satellites in the 200-1,000 kg mass range, has a mass of less than 4.85 kg and has an angular momentum capacity of 12 Nms [215, p. 2]. However, the wheel's torque is only 75 mNm [215, p. 2], meaning for situations where relatively fast slews are required such as in case of a misalignment during final approach to the target, the servicer's thrusters may have to be used instead.

The momentum capacity of a RW (or momentum wheel) is limited, with the wheel eventually needing to be desaturated. This will have to be accounted for in the spacecraft  $\Delta v$  budget. The momentum capacity of a thruster system is limited only by the available propellant, but the non-reusability of the fuel means it should be saved for times when it is definitely required.

## 8 Relative Navigation System (RNS)

### 8.1 RNS requirements

The relative navigation system is used by the servicer for RPO, including approaching the target to a point where it can be grappled. The main requirements on the RNS are to provide the following accuracies in target range, range rate, pose and pose rate respectively to the servicer's OBC: 1 cm, 1 cm/s, 1 °, 1 °/s. These are codified in requirements **GNC-0190** to **GNC-00220** (see Appendix C).

The RNS must be ready to take over from the GNC as the primary navigation system as soon as the target comes within the RNS' outer range limit. This limit is baselined as 80 km as this is the figure used for AstroScale's ADRAS-J mission [84]. However, this will need refining as sensor limitations become better understood. The OBC will switch from using an orbit state vector and servicer attitude estimation for navigation and will instead use the target range and range rate data provided by the RNS. This will later be supplemented by pose and pose rate data as the servicer approaches the target.

### 8.2 RNS concept and component selection

Before selecting components for the relative navigation system, its architecture must be understood. This section describes the chosen concept for the mission's RNS and the rationale behind it.

When defining the RNS architecture, the decision was made early on to include several layers of sensors. This is because no single sensor type can provide relative pose, range, pose rate and range rate data from tens of kilometres range all the way to docking. This also follows the multi-layer approach taken by AstroScale for ADRAS-J, which uses three layers of sensing as described in Section 4.4.2 Rendezvous, proximity operations & docking (RPOD) sensors. For example, at 80 km range, the target would be too small in the field of view (FoV) of a Light Detection and Ranging (LIDAR) sensor to be resolved within the

LIDAR's point cloud. At this range, a long focal length optical sensor would be more appropriate.

Table 8-1, from a paper by Opromolla et al. [98], describes various types of relative navigation system and how they can be used across the full range of target cooperation levels. A variety of mission types are also mentioned, although the ADR, formation flight (FF) and comet/asteroid exploration categories are out of scope of this research.

Under this report's mission architecture, the OneWeb-like target satellite (see Section 5.1 Background) can be considered passively cooperative [98]. This is because its Altius Space Machines DogTag grappling fixture (see Section 9.1 Grappling Fixture) features an optical fiducial marker on its front face that can inform the servicer of the target's relative pose, range and rate of change of these [139]. The fiducial is based on an open source Aruco code to enable tracking by any servicer [140]. It can be used for tracking at "distances between 0.5 m to 5 m and can maintain tracking up to a  $\pm 45^\circ$  offset, relative to fiducial normal, as well as through a full  $360^\circ$  roll" [140, p. 1]. However, the 0.5 m to 5 m range is simply the range the fiducial has been tested at. Some testing has been performed at closer ranges with no issues found, although beyond 5 m steep fiducial angles can cause ambiguity in the tracking software, leading it to be unsure in which direction the fiducial is facing. This could be solved by adding a second camera or through software modifications [216]. It is also worth considering that some of the 0 to 0.5 m range will be taken up by the length of the magnetic head used to grapple the DogTag.

**Table 8-1 - Taxonomy of spaceborne relative navigation approaches and scenarios [98]**

<b>Target type</b>	<b>Relative navigation approach</b>	<b>Relative navigation hardware (chaser)</b>	<b>Relative navigation hardware (target)</b>	<b>Possible mission scenario</b>
Actively cooperative	RF-based	RF transmitting/receiving antennas	RF transmitting/receiving antennas	FF, OOS
	GNSS-based	GNSS receiver and communication link	GNSS receiver and communication link	
Passively cooperative	EO-based	Monocular/stereo camera, LIDAR	Artificial markers e.g. LEDs, corner cube reflectors (CCRs)	FF, OOS
Uncooperative known	EO-based	Monocular/stereo camera, LIDAR	N/A	OOS, ADR
Uncooperative unknown	EO-based	Monocular/stereo camera, LIDAR	N/A	ADR, comet/asteroid exploration

Due to the fiducial on the DogTag being optical in nature, a camera is required to track it. This is supported by Table 8-1 that specifies an electro-optical- (EO) based system for tracking a passively cooperative target. The 5 m maximum tracking range limits the ability to track the fiducial but not the overall spacecraft.

A single (monocular) camera would be sufficient for fiducial tracking, avoiding the added complexity and power requirement of a stereo camera system or LIDAR [98]. Use of the camera within the final 5 m before docking means the target can fill the field of view, avoiding issues with objects unexpectedly entering the frame. The short amount of time that this camera will be used for also avoids large changes in illumination, as long as docking is not being performed very close to sunrise or sunset. However, beta angle, which is the angle between the spacecraft's orbital plane and the vector from the centre of the Earth to the Sun [217], will still need to be analysed to determine acceptable beta angle ranges in terms of illumination of the target. This is discussed further in Section 10.1 Mission design and dynamics analysis.

Next, consider a range of distance to target of approximately 250 m to 5 m, with the fiducial-tracking camera taking over at 5 m range. Throughout this range, the selected sensor must output pose, range, pose rate and range rate data to allow the OBC and thrusters to guide the servicer towards the target. At the upper end of this range, the target may be relatively small in the field of view, so a sensor is needed that can discriminate the target from the background. A LIDAR sensor is well suited to this [98].

A stereo camera system could also be used to produce the necessary output data. The effectiveness of this could be limited in poorly illuminated scenarios, but this could be counteracted by adding a light source to the servicer. This would increase the power requirement (although this would likely still be below the power requirement for LIDAR [98]) and its effect would be limited at 250 m range. Stereo cameras can output images with a greater level of texture than a LIDAR but have a depth accuracy that depends on the baseline between the two cameras, whereas a LIDAR's accuracy will be constant across its operational range [98]. Resolving the surface texture of the target is not a significant factor for this report's mission, with depth accuracy being far more important to ensure the two spacecraft do not collide. For this reason, a LIDAR system is favoured for the 250 m to 5 m range.

Considering the LIDAR systems in Table 4-1 in Section 4.4.2 Rendezvous, proximity operations & docking (RPOD) sensors, most have a maximum range in the multi-kilometre range. This sets the outer limit for the LIDAR layer of the RNS concept. In particular, the LARS LIDAR has a maximum range of 10 km using its triangulation mode, with other advantages being discussed below.

Trading off the sensors in Table 4-1, the LCS, RVS-3000 and LDRI can be eliminated due to low maximum range. The DragonEye sensor also has a low range relative to the remaining sensors so is eliminated. While the table does not provide any accuracy data for the Neptec TRIDAR, a paper by Zhu et al. states the sensor can achieve pose accuracy of “less than 1 cm in translation and less than 1 ° of rotation” [218, p. 4]. The other sensors, apart from the LARS, tend to have an accuracy in the tens of cm range, which would be limiting when close to the target.

The LARS though, according to the table, has sub-mm accuracy below 10 m range and 3 cm accuracy between 10 m and 10 km. This is supported by Laurin et al., who report that LARS uses triangulation for 0.5 to 20 m range and time-of-flight (TOF) for 20 m to 10 km, with sub-millimetre accuracy below 1 m range that drops gradually with distance, achieving 2 cm accuracy at 10 m range. The sensor has a constant  $\pm 3$  cm accuracy when in the long range TOF mode. The sensor has a 30 ° by 30 ° FOV and a refresh rate of up to 137 Hz for a single target, although the whole point cloud refresh rate is not specified [219, p. 278]. These characteristics make the LARS LIDAR a strong selection for the servicer’s intermediate range sensor.

At ranges beyond 10 km, only range and range rate data are required. A long focal length camera is ideal for this role due to its low power and simplicity relative to a LIDAR system. For example, the narrow field of view variant of Neptec’s VisCam could be used for this [105]. The range limit of this sensor is not known, but for comparison Astroscale’s ADRAS-J will use a visible camera from 80 km range [84]. This is therefore used as the baseline outer limit of the RNS.

To summarise the RNS concept, at 80 km range to the target, the servicer’s OBC would switch from using the GNC system to the RNS. It would then use a long

focal length visible light camera for range and range rate data, until at a range of 10 km. At this point it would switch to using the LARS LIDAR, initially in TOF mode, to collect range, range rate, pose and pose rate data, although pose data would not be required at the long-range end of this phase. The LARS would switch to triangulation mode when within 20 m range, achieving steadily greater accuracy as it approaches the target. Once within 5 m range, the optical camera would be used to track the DogTag fiducial, with this being used until contact is made by the servicer’s magnetic grappling head. The LARS would also be used as a backup sensor during this final approach phase. This is summarised in Figure 8-1.

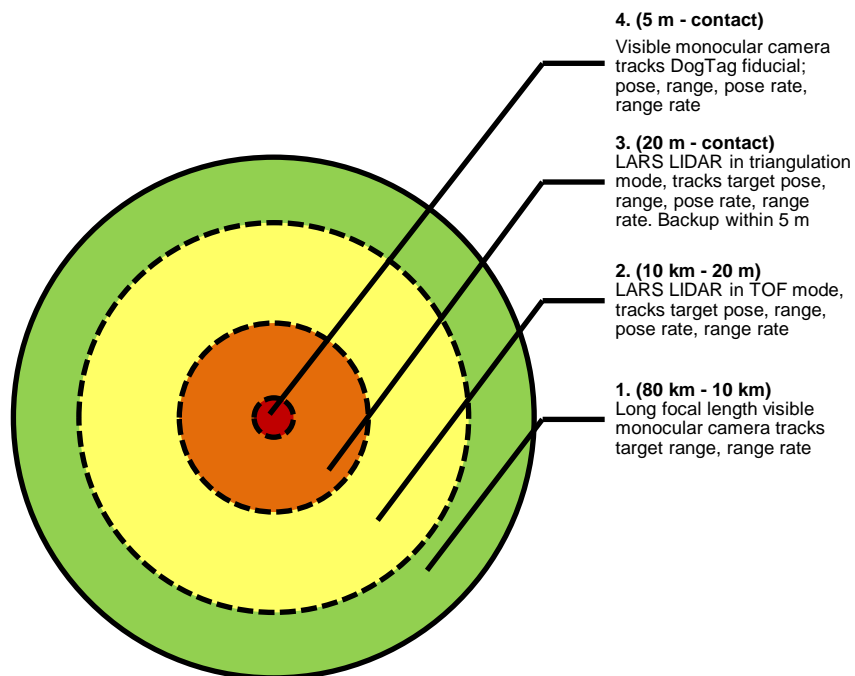


**Figure 8-1 - Relative navigation sensor concept**

### 8.3 Safety

For spacecraft that perform proximity operations, manoeuvring safety and collision avoidance are of critical importance. When approaching its target, a rendezvousing vehicle should do so along a trajectory that gives passive safety. For example, the Space Shuttle most often used an “r-bar” method where it rendezvoused with the ISS from below and behind [220]. As the Shuttle’s altitude

increased to match that of the ISS, its orbital velocity would mean it would fall behind the space station without thruster firings to keep it on the radial vector. This meant that in the event of a thruster failure, the distance between the vehicles would naturally increase, giving passive safety. An r-bar approach to Hubble was used during the 1999 SM3A servicing mission [125, p. 533].

ISS operations also use the concepts of an approach ellipsoid (AE) and keep out sphere (KOS). A visiting vehicle is defined to have begun its approach when it performs a manoeuvre that will bring it inside the 4x2x2 km AE, with the KOS having a 200 m radius and being centred at the ISS centre of mass [221, p. 4]. The Orion capsule will also use a KOS and passive safety when approaching the Lunar Gateway [100]. These definitions give RNS designers, mission controllers and managers clarity regarding the approach limits, ensuring safe procedures are designed into the system and carried out successfully.

During rendezvous with their targets, Astroscale's ELSA-d and ADRAS-J missions (see Section 4.4.1 Missions) will use walking safety ellipses [194] [84] to ensure they approach in a way that respects keep out zones and is passively safe due to not crossing the target's velocity vector [222, p. 17] [42, p. 59]. ELSA-d will also use evacuation points that it will fall back to in case of a problem, and will use "ground segment oversight during critical phases" [79, p. 5].

Aside from operational aspects, technical factors also need to be considered. For example, fault tolerance computing should be used within the RNS to ensure that any sensor or processor failures or errors are detected and corrected [223, p. 1]. This avoids a situation where the RNS makes incorrect decisions based on bad data, which could lead to a collision with the target.

While detailed analysis of these considerations is beyond the scope of this report, they would form the core of the design of mission operations and RNS risk management. A detailed data budget would also need to be constructed to ensure the servicer's computer has enough bandwidth and processing capability to handle the data from the various GNC and RNS sensors.

## 9 Grappling and Robotics

This section details the hardware that would be required on the tug for it to attach itself to the target spacecraft and for the tug to be able to perform servicing operations on the spacecraft. This report will mostly consider robot arms and grappling fixtures, although other target capture methods will also be described.

### 9.1 Grappling Fixture

The OneWeb constellation's satellite design was baselined as the design of a typical target satellite (see Section 5.1 Background). The OneWeb satellites are each equipped with a DogTag grappling fixture (shown in Figure 4-9) from Altius Space Machines so the DogTag is baselined as the grappling fixture that the target will be equipped with. This requires a DogTag-compatible magnetic grappling head on the servicer, as discussed in Section 4.4.4 Attachment methods.

The servicer's grappling head will have to be attached to the servicer bus in such a way that it can access the DogTag. It will also need a reliable power source. However, the mass and volume impact of the grappling head should be low, allowing it to be implemented on the servicer without a large detriment to other systems. While the grappling head could be fixed to the end of a robot arm, a simpler solution would be to mount the head on a simple boom or set of stand-offs. This would enable it to protrude from the servicer for easy access to the DogTag, without the mass and power budget penalty and control system complexity associated with a robot arm. For initial sizing and design of the grappling system, the outer size of the DogTag, 150 mm by 150 mm, can be used as a "good approximation" [138] for the size of the EPM element used in the magnetic head.

An initial concern regarding the DogTag was that the absorptivity,  $\alpha$ , and emissivity,  $\epsilon$ , of the fiducial's image would change during the mission lifetime and lead to a loss of contrast that would make tracking the fiducial more challenging.

However, the fiducial uses a photo development process to place the image on specially treated aluminium. The company that makes the fiducial, Metalphoto, have qualified the coating for 20 years of outdoor exposure [224], with the technology having been used successfully on the ISS since 1997 [225].

While the DogTag is being baselined for this mission architecture, this report section will also analyse other available grappling fixtures to assess their suitability for other future OOS missions. As discussed in Sections 4.4.4 Attachment methods and 5.1 Background, the grappling fixture selection process assumes that the target is to be cooperative and therefore not tumbling. This allows a connection between the spacecraft to be achieved without the use of a complex manoeuvre to match the target's tumble.

Astroscale's ELSA-d mission (see Section 4.4.1 Missions) uses a magnetic capture system to capture the client spacecraft. This was chosen as it avoids difficulties with tethered systems such as "tether dynamic issues, complexity/jamming of a reeling mechanism, difficulty in controlling client attitude" and robotic system issues such as "degree of complexity [and] cost" [226, p. 5]. ESA's research on tethered capture for e.Deorbit (described in Section 4.4.1 Missions) found that "any tether-based capturing procedure comes with a problem: it is very difficult to control the pulling of the target" [59].

Grappling fixtures such as those used by ISS visiting vehicles (see Section 4.4.4 Attachment methods) are at TRL 9 and provide a reliable connection between the vehicles but are too large for this mission's uses. For example, the Cygnus cargo spacecraft, for which MDA supply the Power and Video Grapple Fixture (PVGf) [128], has a cargo mass alone of 1,700 kg [227], compared to the 321.39 kg wet mass of the servicer [25].

The impact of the grappling fixture on the target should be considered. The DogTag simply requires a solid face on the target that the DogTag's three standoffs can be fixed to. This would make part of or the whole face unavailable to other components such as solar panels or cameras, but the ability to service the satellite would be a substantial benefit.

While the availability of the DogTag on the OneWeb satellites makes docking relatively simple, the presence of a similar docking interface on other satellites would be far from guaranteed. If no docking interface were available, the target would have to be grappled or captured using an alternative method. ESA's research for e.Deorbit and Airbus's O.CUBED spacecraft (see Section 4.4.1 Missions for details of both) suggest a robot arm would be the best capture method, rather than a net or harpoon, for example. The Obruta Space Systems Puck could also be used for docking, but as very limited information is currently on that system, a reliable assessment of it is not possible. More details of the trade-offs between capture mechanisms are given in Section 4.4.4 Attachment methods.

For hardware replacement, both Altius' MagTag and iBOSS' iSSI are valid options, but as the MagTag uses a similar magnetic grappling head to that used to capture the DogTag, this may be preferred. The iSSI is slightly larger and significantly heavier than the MagTag, with a diameter of 119 mm and a mass of 0.9 kg [144]. While this may make the iSSI less suitable than the MagTag for hardware replacement, the lack of public information on the MagTag makes an informed trade-off currently impossible. Trade-off of these and other options will therefore form part of the project's future work (see Section 10 Areas for Future Development).

## **9.2 Servicing arm**

To perform refuelling and hardware replacement operations on the target once docked, the tug requires a system with which it can perform high dexterity tasks such as connecting to a refuelling nozzle and grasping hardware to be replaced. The only type of machinery able to do this with sufficient freedom is a robot arm. Other systems such as a grabbling end effector that could slide along a rail lack the necessary degree of freedom to complete complex tasks.

### **9.2.1 Servicing arm requirements**

Due to high complexity, particularly when designed for space applications, the servicing arm was a component where a commercial off the shelf (COTS) solution was particularly desired. This is formalised in requirement ROB-0020. Other key requirements for the arm are its support of automatic and autonomous operation (ROB-0010), its reach of 2 m (ROB-0030), maximum stowed volume of 2 m<sup>3</sup> (ROB-0040), maximum load of 25 kg (ROB-0060) and maximum mass of 55 kg (ROB-0070). These requirements are shown in greater detail in Section 6.1 Main requirements and in full in Appendix C Space Servicer Requirements Specification. They ensure that the arm can fit within the volume and mass constraints imposed by the spacecraft bus and that it has the reach and load capacity to support hardware replacement of components inside a target spacecraft.

### **9.2.2 Servicing arm selection**

As discussed in the literature review in Section 4.4.3 Robotics, various COTS robot arms of a size appropriate for dexterous OOS applications are already available. These include the NGC Small [112] (shown in Figure 9-1), OSAM-1's SPIDER arm [228], DARPA's FREND [118] and the TALISMAN arm [120]. The NGC Small, SPIDER and FREND arms have been specifically designed for OOS, with the TALISMAN arm designed to be appropriate for a variety of applications. The NGC Small, SPIDER and FREND arms are sufficiently small and dexterous for operations such as hardware replacement, but the TALISMAN arm has instead been designed for grappling of a target spacecraft while it is being serviced.

While further arms may become available before the space tug design is frozen, a design similar to the NGC Small, SPIDER and FREND represents a good baseline for this point in the design process. Alternatively, any of the arms would likely satisfy the system requirements, so could be used 'off the shelf'. Any other arm options that become available later could be traded off against the baseline

and the existing arms specifically to determine the best selection for the final tug design.

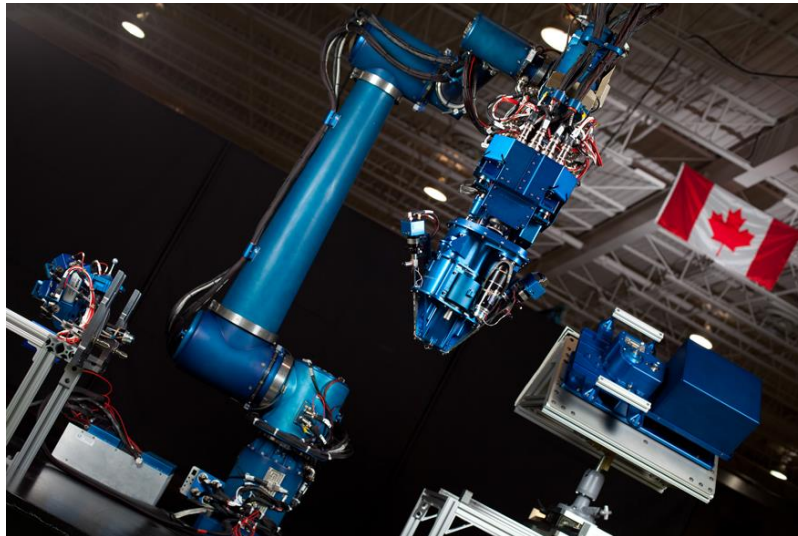


**Figure 9-1 - The Next Generation Small Canadarm [229]**

Little information is available on the physical properties of the SPIDER arm or the mass of the NGC Small. For the purposes of the spacecraft mass budget (see Section 5.3.1 Dry mass estimation), the mass of the servicer's servicing arm can be estimated as 75 kg, as the FRENDA arm has a mass of 77 kg [118, p. 6] and is of a similar size to that required for this mission. To compare, the 8.5 m long Canadarm3 will have a mass of approximately 715 kg [110].

The SPIDER arm is heavily based on the FRENDA design [115], showing that FRENDA's foundation can be adapted to suite requirements of individual missions. FRENDA's extensive testing and TRL of around 6 (see Section 4.4.3 Robotics) also make it a strong candidate.

The author recommends that the servicer be baselined to include an arm based on the FRENDA design, but which could also factor in lessons learned from NGC Small and SPIDER once the latter has been used on orbit for the OSAM-1 mission.

### 9.3 Tooling and sensing

Tooling for OOS is currently an area of technology immaturity. Generic tools such as grippers have been used in space for some time and specialist tools have been developed and tested for operations such as unscrewing fuelling caps. However, there is currently no standard tool set or tool specification for tools designed to work with a variety of target spacecraft.

Autonomous grappling using the FRIEND robot arm (see Section 4.4.3 Robotics) has been tested at the US Naval Research Laboratory (NRL) for DARPA's RSGS program (see Section 4.4.1 Missions) [230]. This is shown in Figure 4-6.

Tooling for refuelling is an area that has been researched extensively by NASA, with the series of Robotic Refuelling Mission (RRM) demonstrations on the ISS. Example of tools used for RRM are shown in Figure 9-2. However, RRM's tools have limited applicability beyond refuelling operations.

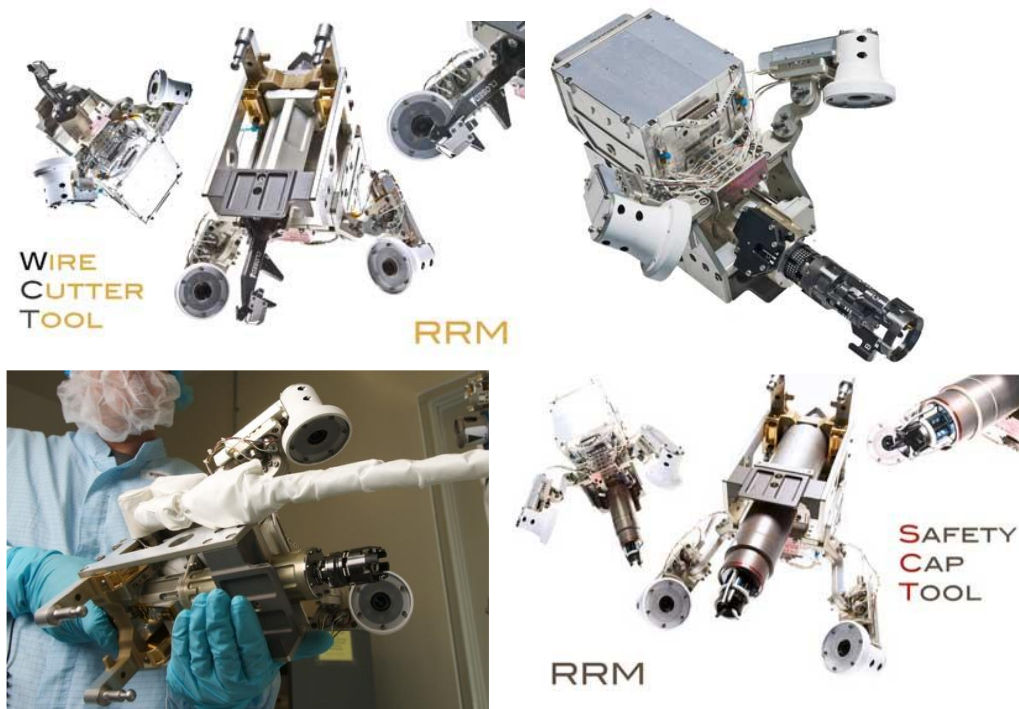


**Figure 9-2 - Tools for RRM. Clockwise from top left: Wire Cutter and Blanket Manipulation Tool, Multifunction Tool, Safety Cap Tool, Nozzle Tool [231]**

To demonstrate use of the tools, the RRM Task Board 3 and Task Board 4, shown in Figure 9-3, were created. During operations in May 2015, ground controllers

manually used the ISS's Dextre robot arm to simulate tasks on the Task Boards [232].

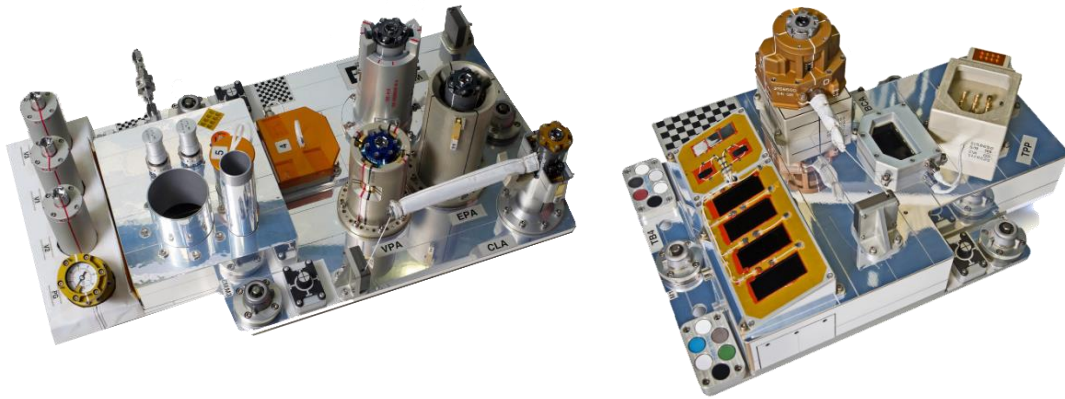


**Figure 9-3 – RRM Task Boards 3 (left) and 4 (right) [233]**

The RRM3 mission was used to develop technology for OSAM-1 (see Section 4.4.1 Missions) including transfer of cryogenic propellant [234]. It was attached to the ISS in 2018 [235]. Some tooling operations were completed successfully but a cryocooler failure meant that the experiment lost the ability to transfer its liquid methane [236], leading it to be vented to space in 2019 [237]. The experiment had however “demonstrated the longest storage of a cryogen” without boil off, keeping the methane cold for four months [236].

It is worth considering that refuelling requires a tool that allows a fluid connection to be established between the two spacecraft. This contrasts against the tools required for, for example, hardware replacement, where only a mechanical connection is required. This increases the degree of robotics precision required for refuelling tools.

As well as its tools, the servicing arm will require some sort of sensor to avoid collisions with surrounding objects and to allow the tug’s onboard computer or ground controllers to grapple the target object. This is often achieved using cameras, for example the 8.5 m long Canadarm3 that will be installed on the Lunar Gateway will include six colour cameras at 4K resolution, with “one 360-degree camera on each side of the elbow, one on each boom on swivel mounts and the other two on the “hands”” [110].

## 10 Areas for Future Development

### 10.1 Mission design and dynamics analysis

25 m/s is currently estimated as the  $\Delta v$  required when docking. This figure will need to be refined to allow a more accurate and precise estimate of the total  $\Delta v$  and fuel mass required for the mission. The total fuel estimate will also give the effective total momentum capacity for the thruster system, which will be much higher than a RW/CMG system, although the RW chosen in Section 7.6.3 Attitude control methods and selection will still be used where possible to avoid wasting fuel. To refine the docking  $\Delta v$  estimate, the Clohessy-Wiltshire equations [166, p. 397] can be used for a first approximation, with this later being refined using an n-body simulation.

As discussed in Section 5.3.2 Fuel requirement estimation, changing the servicer's RAAN once in orbit would require a large amount of fuel. This fuel requirement should be modelled accurately so that a cost-benefit analysis of changing the RAAN can be performed. The ability to change the RAAN would be beneficial as it would allow the servicer to reach new targets in different orbits.

Further analysis is needed of the effect that using EP would have on the mission. Its greatly reduced thrust relative to chemical propulsion means orbital manoeuvres would take significantly longer and could no longer be considered impulsive, requiring different  $\Delta v$  models to be used. For example, Vallado has discussed an algorithm for low thrust noncoplanar transfers, so this could be implemented in the MCC spreadsheet [238]. The longer transfer times for EP would be disadvantageous, as they would mean the servicer spends less of its lifetime actively servicing customers. However, the fuel mass savings could be significant due to EP's higher  $I_{sp}$ , and Northrop Grumman's MEVs make use of EP as their main propulsion system [73]. If EP is found to be acceptable, this would impact the discussion in Section 7.6.2 Orbit control methods and selection.

In Section 5.3.2 Fuel requirement estimation, it was assumed that the servicer would need to be able to complete two missions to make it economically viable. This needs to be further assessed both from a financial and technical standpoint

to understand whether it is required and what impact it would have on the mission and spacecraft design. For example, if only one servicing mission is required, fuel could be saved that could instead be used for more payload or could allow a smaller launch vehicle or a ride share slot to be used. This could lower the launch cost and potentially make more launch opportunities available. If more than two missions would be needed, the opposite would be true, with the servicer potentially being forced to switch to EP to maintain a reasonable fuel mass.

Another concern regarding chemical propulsion is fuel sloshing. This will be particularly important for the servicer given its relatively high propellant mass fraction of 26.7 % that was found in Section 5.3.2 Fuel requirement estimation. As the fuel is used, there will be a significant change in the spacecraft's moment of inertia and hence how it responds to the sloshing of the fuel within the tank. Ideally, this would be modelled within the control loop plant to enable the spacecraft to counteract the effect.

During RPOD, illumination from the Sun will be an important factor. The beta angle – the angle between the spacecraft's orbital plane and the Earth-Sun vector – will need to be analysed to determine the range of allowable beta angles during RPOD. Angles should be avoided where the Sun will be within the field of view of any optical sensors during the approach and docking. The analysis could take the form of a simulation in software such as MATLAB, or a laboratory experiment with satellite mock-ups and a powerful spotlight to simulate the Sun. Similarly, the fields of view of the various optical sensors should be understood so Sun keep out zones can be built into the spacecraft control software to avoid blinding the sensors.

## **10.2 Systems engineering considerations**

When docking, the DogTag grappling fixture will have limits on maximum misalignment in terms of rotation and translation, as well as a maximum velocity at contact. These will need to be quantified so the grappling head and servicer control system can be designed to ensure the limits are respected during docking.

To ensure flowdown of this to the systems' design, the limits are formalised in requirement **GNC-0230**, shown in Appendix C Space Servicer Requirements Specification.

The GNC and RNS control loops will need to be modelled and simulated, for example in MATLAB and Simulink, to validate the control system design. This should include aspects such as sensor noise and minimum thruster on time. To simulate the relative motion of the servicer towards the target, a Clohessy-Wiltshire model could be used as discussed previously, with this also being used for  $\Delta v$  analysis.

Moving forward, a detailed spacecraft power budget that includes the GNC, RNS and robotics will be required to ensure the systems do not draw more power than the spacecraft's power sources (batteries and solar arrays) can provide. This will be built around the framework of the operational modes found in Appendix B CONOPS.

The distribution of mass within the spacecraft bus will need to be calculated once the rest of the servicer's configuration is known. This will allow calculation of an accurate inertia matrix so that the spacecraft dynamics model and control loops can be refined. For example, the new inertia matrix will mean the linear and angular accelerations imparted by the thrusters will need to be updated.

The thruster plumes will also need to be modelled to ensure they do not obscure any of the GNC or RNS sensors or impinge on the target and damage it. Heat shielding may also be required around the thrusters to protect delicate components.

A more detailed trade-off and selection process will be required to choose the type of controller for the GNC and RNS control loops. For example, PI or PID controllers could be used. The controller selection will impact the computational complexity of the system.

Finally, radiation will be an important factor in the design of the spacecraft electronics. For example, the total ionising dose (TID) will need to be calculated so the necessary shielding can be designed in to avoid single-event upsets

(SEUs). Tools such as the Space Environment Information System (SPENVIS) [239] can be used to analyse the radiation environment.

### **10.3 Other areas**

While SSO was chosen as the target orbit in Section 5.2 Orbit selection due to its large population, commercial analysis should be performed to ensure there is a market for servicing in this region. This will consider factors such as the lifetime and applications of satellites in SSO, with the analysis being carried out by a dedicated business development specialist.

The current RNS system described in Section 8 Relative Navigation System (RNS) was not designed to approach noncooperative tumbling targets. If the mission were to be expanded in future to also encompass ADR, the RNS and docking mechanism would have to be updated so that tumbling targets could be captured. This would increase the complexity of the systems significantly as the spacecraft would have to perform a manoeuvre to match the target's tumble before grappling and detumbling it.

## 11 Conclusion

The importance and applications of OOS have been discussed, while a literature review has revealed that technology maturity is now sufficient to enable autonomous OOS. Previous OOS missions and those currently under development have been studied to gain an understanding of mission architectures and servicing types.

The mission's target satellite was defined as being similar to those in the OneWeb constellation as these have a DogTag grappling fixture installed that simplifies capture. SSO was used as the target orbit as this is currently the most densely populated region so will have the most satellites accessible to a single servicer.

Various top-level requirements for the servicer have been discussed, such as fully autonomous operations and a 10-year lifetime.

Investigation of GNC and RNS technologies revealed that existing COTS parts can be used to produce fully autonomous systems that can also meet the mission requirements. Selected component types included GNSS for orbit determination and a star tracker and gyroscopes for attitude determination.

A variety of robotic arms have been developed for OOS, but these are not available off the shelf. However, DARPA's FRENDA arm in particular has shown great potential for OOS use, having been adapted into the SPIDER arm for OSAM-1. Grappling fixtures are an area with a large amount of ongoing development, from large companies and start-ups alike. No standard currently exists for small satellite grappling but systems such as the DogTag fixture on the OneWeb satellites are enabling new types of grappling to be performed.

Various areas of future development will need to be pursued to increase the number of OOS missions. These include mission design topics such as trade-off of electric versus chemical propulsion, and systems engineering aspects such as thruster plume and radiation modelling.

## REFERENCES

- [1] Xilinx, Inc, "Triple Modular Redundancy Design Techniques for Virtex FPGAs," Xilinx, Inc, 2006.
- [2] P. Rincon, "Nasa SpaceX launch: What is the Crew Dragon?," BBC News, 31 May 2020. [Online]. Available: <https://www.bbc.co.uk/news/science-environment-52840482>. [Accessed 28 July 2020].
- [3] European Space Agency, "ESA Is Looking Into Futuristic In-Orbit Services: Recycling Satellites," European Space Agency, [Online]. Available: <https://blogs.esa.int/cleanespace/2019/09/09/esa-is-looking-into-futuristic-in-orbit-services-recycling-satellites/>. [Accessed 31 July 2020].
- [4] National Aeronautics and Space Administration, "NASA, ULA Launch Mars 2020 Perseverance Rover Mission to Red Planet," National Aeronautics and Space Administration, 30 July 2020. [Online]. Available: <https://mars.nasa.gov/news/8724/nasa-ula-launch-mars-2020-perseverance-rover-mission-to-red-planet/>. [Accessed 31 July 2020].
- [5] National Aeronautics and Space Administration, "Brains," National Aeronautics and Space Administration, [Online]. Available: <https://mars.nasa.gov/mars2020/spacecraft/rover/brains/>. [Accessed 28 July 2020].
- [6] BAE Systems, "RAD750® radiation-hardened PowerPC microprocessor," BAE Systems.
- [7] EveryMac.com, "Apple Power Macintosh G3 233 Desktop Specs," [Online]. Available:

- [https://everymac.com/systems/apple/powermac\\_g3/specs/powermac\\_g3\\_233\\_dt.html](https://everymac.com/systems/apple/powermac_g3/specs/powermac_g3_233_dt.html). [Accessed 28 July 2020].
- [8] techradar, "AMD Ryzen 5 3600 review," Future Publishing Limited, 7 October 2019. [Online]. Available: <https://www.techradar.com/uk/reviews/amd-ryzen-5-3600>. [Accessed 28 July 2020].
- [9] Advanced Micro Devices, Inc, "AMD Ryzen™ 5 3600," Advanced Micro Devices, Inc, [Online]. Available: <https://www.amd.com/en/products/cpu/amd-ryzen-5-3600>. [Accessed 28 July 2020].
- [10] Inter-Agency Space Debris Coordination Committee, "IADC Space Debris Mitigation Guidelines," United Nations Office for Outer Space Affairs, 2007.
- [11] D. J. Kessler and B. G. Cour-Palais, "Collision Frequency of Artificial Satellites: The Creation of a Debris Belt," *Journal of Geophysical Research*, vol. 83, no. A6, pp. 2637-2646, 1978.
- [12] D. J. Kessler, N. L. Johnson, J.-C. Liou and M. Matney, "The Kessler Syndrome: Implications to Future Space Operations," in *33rd Annual AAS Guidance and Control Conference*, Breckenridge, 2010.
- [13] Northrop Grumman, "James Webb Space Telescope Launch and Deployment," YouTube, 24 January 2017. [Online]. Available: <https://www.youtube.com/watch?v=v6ihVeEoUdo>. [Accessed 31 July 2020].
- [14] SpaceX, "Falcon User's Guide," SpaceX, 2019.
- [15] Arianespace, "Ariane 5 User's Manual," Arianespace, Évry-Courcouronnes, 2016.

- [16] Arianespace, "Ariane 6 User's Manual," Arianespace, Évry-Courcouronnes, 2018.
- [17] National Aeronautics and Space Administration, "Space Launch System (SLS) Mission Planner's Guide," National Aeronautics and Space Administration, 2018.
- [18] A. Rivolta, P. Lunghi and M. Lavagna, "GNC & robotics for on orbit servicing with simulated vision in the loop," *Acta Astronautica*, vol. 162, pp. 327-335, 2019.
- [19] European Space Agency, "ESA's Technology Strategy," European Space Agency, 2019.
- [20] W. Easdown, "Mission ORCA: Orbit Refinement for Collision Avoidance," William Easdown, Cranfield, 2020.
- [21] Trello, "Trello Boards," Trello, [Online]. Available: <https://trello.com/williamneasdown/boards>. [Accessed 25 July 2020].
- [22] elegantt.com, "Elegantt | The leading Gantt Chart for Trello," Google, [Online]. Available: <https://chrome.google.com/webstore/detail/elegantt-the-leading-gantt/jdongfcbejkjibhkbekkjckkophhjccj>. [Accessed 25 July 2020].
- [23] Microsoft, "OneDrive," Microsoft, [Online]. Available: <https://www.microsoft.com/en-gb/microsoft-365/onedrive/online-cloud-storage>. [Accessed 25 July 2020].
- [24] W. Easdown, "General Running Notes," William Easdown, Cranfield, 2020.
- [25] W. Easdown, "Main Central Control," William Easdown, Cranfield, 2020.
- [26] European Space Agency, "FROM ACTIVE DEBRIS REMOVAL TO IN-ORBIT SERVICING: THE NEW TRAJECTORY OF E.DEORBIT, PART

- TWO,” European Space Agency, 18 December 2018. [Online]. Available: <https://blogs.esa.int/cleanspace/2018/12/18/from-active-debris-removal-to-in-orbit-servicing-the-new-trajectory-of-e-deorbit-part-two/>. [Accessed 2 August 2020].
- [27] W. Easdown, “Space Servicer Requirements Specification,” William Easdown, Cranfield, 2020.
- [28] W. Easdown, “Satellite Distribution Research and Orbit Selection,” William Easdown, Cranfield, 2020.
- [29] Union of Concerned Scientists, “UCS Satellite Database,” 1 April 2020. [Online]. Available: <https://www.ucsus.org/resources/satellite-database>. [Accessed 21 July 2020].
- [30] W. Easdown, “Space Tug Concept of Operations,” William Easdown, Cranfield, 2020.
- [31] W. Easdown, “Space Tug Design Definition File,” William Easdown, Cranfield, 2020.
- [32] European Cooperation for Space Standardization, “ECSS-E-ST-10C Rev.1 - System engineering general requirements,” European Cooperation for Space Standardization, Noordwijk, 2017.
- [33] O. Hagolle, J. Inglada, S. Valero, M. Arias, D. M. M. Savinaud, A. Mondot, A. Bricier, S. Bontemps, G. S. Canto, N. Matton, C. Cara and C. Udroui, “Sentinel-2 Agriculture Design Definition File,” UCL Geomatics, 2016.
- [34] G. I. S. S. Z.o.o., “Design Definition File BIBLOS,” GMV Innovating Solutions Sp. Z.o.o., 2016.
- [35] T. Nagler, M. Heidinger, R. Solberg, J. Amlien, B. Wangensteen and K. Luoju, “Global Snow Monitoring for Climate Research Design Definition File,” GlobSnow Consortium, 2010.

- [36] Moog Inc., "Small Launch Orbital Maneuvering Vehicle," Moog Inc., [Online]. Available: <https://www.moog.com/markets/space/omv/slomv.html>. [Accessed 31 July 2020].
- [37] Firefly Aerospace, "Firefly's Orbital Transfer Vehicle (OTV)," Firefly Aerospace, [Online]. Available: <https://firefly.com/launch-otv/>. [Accessed 31 July 2020].
- [38] Momentus Space, "Rides Giving You A Boost From Orbit To Orbit," Momentus Space, [Online]. Available: <https://momentus.space/rides/>. [Accessed 31 July 2020].
- [39] B. Bernus, G. Trinh, C. Gregg, O. Formoso and K. Cheung, "Robotic Specialization in Autonomous Robotic Structural Assembly," in *IEEE Aerospace Conference*, Big Sky, 2020.
- [40] European Space Agency, "Statement of Work ESA Express Procurement - EXPRO+ Preliminary Design of On-Orbit Servicing Station for Satellite Manufacture, Refurbish and Recycle," European Space Agency, Noordwijk, 2019.
- [41] P. D. Ans-Meador, J. N. Opiela, D. Shoots and J.-C. Liou, "History of On-Orbit Satellite Fragmentations 15th Edition," Orbital Debris Program Office, National Aeronautics and Space Administration, 2018.
- [42] National Aeronautics and Space Administration Goddard Space Flight Center, "On-Orbit Satellite Servicing Study Project Report," National Aeronautics and Space Administration, Greenbelt, 2010.
- [43] C. F. Lillie, "On-Orbit Assembly and Servicing for Future Space Observatories," in *Space Telescope and Instrumentation I Optical, Infrared, and Millimeter*, 2006.

- [44] Space Forge Limited, "Space Forge," Space Forge Limited, [Online]. Available: <https://spaceforge.co.uk/>. [Accessed 8 August 2020].
- [45] Made In Space, "The Future Will Be Made In Space," Made In Space, [Online]. Available: <https://madeinspace.us/>. [Accessed 19 August 2020].
- [46] National Aeronautics and Space Administration, "Astronauts, Robots and the History of Fixing and Building Things in Space," National Aeronautics and Space Administration, 23 April 2020. [Online]. Available: <https://www.nasa.gov/feature/goddard/2020/astronauts-robots-and-the-history-of-fixing-and-building-things-in-space>. [Accessed 19 August 2020].
- [47] National Aeronautics and Space Administration, "Skylab 2: Mission Accomplished!," National Aeronautics and Space Administration, 22 June 2018. [Online]. Available: <https://www.nasa.gov/feature/skylab-2-mission-accomplished>. [Accessed 19 August 2020].
- [48] J. Young, R. Crippen, W. Hale, H. Lane, C. Chapline and K. Lulla, *Wings In Orbit: Scientific and Engineering Legacies of the Space Shuttle 1971-2010*, Washington, DC: National Aeronautics and Space Administration, 2010.
- [49] B. Evans, *Tragedy and Triumph in Orbit: The Eighties and Early Nineties*, Springer Science & Business Media, 2012.
- [50] National Aeronautics and Space Administration, "STS51A-46-057," [Online]. Available: <https://eol.jsc.nasa.gov/SearchPhotos/photo.pl?mission=STS51A&roll=46&frame=057>. [Accessed 26 June 2020].
- [51] Our Space Heritage 1960-2000, "Retrievals of Westar VI, Palapa B-2: An Epic Adventure From a Special Commemorative Issue of SCG

- Journal, December 1984,” 23 August 2013. [Online]. Available: <https://www.hughescgheritage.com/retrievals-of-westar-vi-palapa-b-2-an-epic-adventure-from-a-special-commemorative-issue-of-scg-journal-december-1984/>. [Accessed 26 June 2020].
- [52] National Aeronautics and Space Administration, “35 Years Ago: STS-51A – “The Ace Repo Company”,” National Aeronautics and Space Administration, 12 November 2019. [Online]. Available: <https://www.nasa.gov/feature/35-years-ago-sts-51a-the-ace-repo-company>. [Accessed 19 August 2020].
- [53] National Aeronautics and Space Administration, “Facts About Spacesuits and Spacewalking,” Internet Archive, [Online]. Available: <https://web.archive.org/web/20130603133402/http://www.nasa.gov/audience/foreducators/spacesuits/facts/facts-index.html>. [Accessed 19 August 2020].
- [54] NASA on The Commons, “Three Crew Members Capture Intelsat VI,” flickr, 13 May 1992. [Online]. Available: <https://www.flickr.com/photos/nasacommons/9458306767/in/photolist-fpNfet-fpNi5B-8PLv3N-fgBW55-qcvNcr-fp1pQe-fpfEYu-oX8fju-qRL7w1>. [Accessed 19 August 2020].
- [55] NASA Langley Research Center, “Hubble Space Telescope Returned Hardware,” Internet Archive, [Online]. Available: [https://web.archive.org/web/20130219022932/http://setas-www.larc.nasa.gov/HUBBLE/HARDWARE/hubble\\_ORU.html](https://web.archive.org/web/20130219022932/http://setas-www.larc.nasa.gov/HUBBLE/HARDWARE/hubble_ORU.html). [Accessed 19 August 2020].
- [56] M. Oda, “Summary of NASDA's ETS-VII robot satellite mission,” *J. Robotics Mechatronics*, vol. 12, pp. 417-424, 2000.

- [57] I. Kawano, M. Mokuno, T. Suzuki, H. Koyama and M. Kunugi, "Approach Trajectory Design for Autonomous Rendezvous of ETS-VII," vol. 49, no. 575, pp. 432-437, 2001.
- [58] European Space Agency, "REMOVING DEBRIS TO DEMONSTRATE COMMERCIAL IN-ORBIT SERVICING," European Space Agency, 6 September 2018. [Online]. Available: <https://blogs.esa.int/cleanspace/2018/09/06/removing-a-debris-to-demonstrate-commercial-in-orbit-servicing/>. [Accessed 2 August 2020].
- [59] European Space Agency, "FROM ADR TO IN-ORBIT SERVICING: THE SHIFTED TRAJECTORY OF E.DEORBIT, PART THREE," European Space Agency, 9 January 2019. [Online]. Available: <http://blogs.esa.int/cleanspace/2019/01/09/from-adr-to-in-orbit-servicing-the-shifted-trajectory-of-e-deorbit-part-three/>. [Accessed 2 August 2020].
- [60] University of Surrey, "RemoveDEBRIS deploys from the International Space Station to begin its mission," University of Surrey, 20 June 2018. [Online]. Available: <https://www.surrey.ac.uk/news/removedebris-deploys-international-space-station-begin-its-mission>. [Accessed 14 August 2020].
- [61] Defense Advanced Research Projects Agency, "Orbital Express," Defense Advanced Research Projects Agency, [Online]. Available: <https://www.darpa.mil/about-us/timeline/orbital-express>. [Accessed 14 August 2020].
- [62] C. J. Dennehy and J. R. Carpenter, "A Summary of the Rendezvous, Proximity Operations, Docking and Undocking (RPODU) Lessons Learned from the Defense Advanced Research Project Agency (DARPA) Orbital Express (OE) Demonstration System Mission," National Aeronautics and Space Administration, Hampton, 2011.

- [63] M. J. Parrish, "Robotic Servicing of Geosynchronous Satellites," Defense Advanced Research Projects Agency, [Online]. Available: <https://www.darpa.mil/program/robotic-servicing-of-geosynchronous-satellites>. [Accessed 9 August 2020].
- [64] Defense Advanced Research Projects Agency, "In-space Robotic Servicing Program Moves Forward with New Commercial Partner," U.S. Department of Defense, 4 March 2020. [Online]. Available: <https://www.darpa.mil/news-events/2020-03-04>. [Accessed 27 July 2020].
- [65] D. B. Sullivan, D. Barnhart, D. L. Hill, P. Oppenheimer, D. B. Benedict, G. v. Ommering, L. Chappell, J. Ratti and D. P. Will, "DARPA Phoenix Payload Orbital Delivery (POD) System: "FedEx to GEO"," in *AIAA SPACE 2013 Conference and Exposition*, 2013.
- [66] Northrop Grumman, "Space Logistics Services," Northrop Grumman, [Online]. Available: <https://www.northropgrumman.com/space/space-logistics-services/>. [Accessed 27 July 2020].
- [67] Airbus Defence & Space, "O.CUBED Services," Airbus Defence & Space, [Online]. Available: <https://www.airbus.com/space/Services/on-orbit-services.html>. [Accessed 14 August 2020].
- [68] Airbus Defence and Space, "Space Tug, an autonomous spacecraft," YouTube, 27 September 2017. [Online]. Available: <https://www.youtube.com/watch?v=Oe1Wrbz07Is>. [Accessed 2 August 2020].
- [69] Northrop Grumman Corporation, "Companies demonstrate groundbreaking satellite life-extension service," Northrop Grumman Corporation, 26 February 2020. [Online]. Available: <https://news.northropgrumman.com/news/releases/northrop-grumman->

- successfully-completes-historic-first-docking-of-mission-extension-vehicle-with-intelsat-901-satellite. [Accessed 29 July 2020].
- [70] Intelsat, "Intelsat 901 Satellite Returns to Service Using Northrop Grumman's Mission Extension Vehicle," Intelsat, 17 April 2020. [Online]. Available: <http://www.intelsat.com/news/press-release/intelsat-901-satellite-returns-to-service-using-northrop-grumman-mission-extension-vehicle/>. [Accessed 29 July 2020].
- [71] Spaceflight Now, "Launch Schedule," Spaceflight Now / Pole Star Publications Ltd, 11 August 2020. [Online]. Available: <https://spaceflightnow.com/launch-schedule/>. [Accessed 14 August 2020].
- [72] J. Foust, "Satellite servicing industry seeks interface standards," SpaceNews, 13 August 2020. [Online]. Available: <https://spacenews.com/satellite-servicing-industry-seeks-interface-standards/>. [Accessed 14 August 2020].
- [73] T. Corbett, "Ariane 5 scrubs launch of Mission Extension Vehicle, two communications satellites to orbit," NASASpaceflight.com, 31 July 2020. [Online]. Available: <https://www.nasaspaceflight.com/2020/07/ariane-5-launch-va253/>. [Accessed 2 August 2020].
- [74] Northrop Grumman, "Northrop Grumman's Second Mission Extension Vehicle and Galaxy 30 Satellite Begin Launch Preparations in French Guiana," Northrop Grumman, 30 June 2020. [Online]. Available: <https://news.northropgrumman.com/news/releases/northrop-grumman-second-mission-extension-vehicle-and-galaxy-30-satellite-begin-launch-preparations-in-french-guiana>. [Accessed 2 August 2020].
- [75] J. Foust, "Effective Space announces partnership with IAI for satellite servicing development," SpaceNews, 11 September 2018. [Online]. Available: <https://spacenews.com/effective-space-announces->

- partnership-with-iai-for-satellite-servicing-development/. [Accessed 14 August 2020].
- [76] Astroscale, "Astroscale U.S. Enters the GEO Satellite Life Extension Market," Astroscale, 3 June 2020. [Online]. Available: <https://astroscale.com/astroscale-u-s-enters-the-geo-satellite-life-extension-market/>. [Accessed 14 August 2020].
- [77] Astroscale, "Life Extension (LEX)," Astroscale, [Online]. Available: <https://astroscale.com/services/life-extension-lex/>. [Accessed 14 August 2020].
- [78] Astroscale, "End of Life (EOL)," Astroscale, [Online]. Available: <https://astroscale.com/services/end-of-life-eol/>. [Accessed 14 August 2020].
- [79] J. Forshaw and R. Lopez, "The ELSA-d End-of-Life Debris Removal Mission: Mission Design, In-flight Safety, and Preparations for Launch," in *Advanced Maui Optical and Space Surveillance Technologies Conference (AMOS)*, Maui, 2019.
- [80] J. Forshaw, R. d. V. v. Steenwijk, S. Wokes, S. Ainley, A. Bradford, J. Auburn, C. Blackerby and N. Okada, "Preliminary Design of an End-of-life ADR Mission for Large Constellations," in *70th International Astronautical Congress (IAC)*, Washington DC, 2019.
- [81] D-Orbit, "D-Orbit Signs Contract with OneWeb in the Frame of ESA Project Sunrise," iPress, 29 October 2019. [Online]. Available: <https://www.ipresslive.it/comunicates/26495/d-orbit-signs-contract-with-oneweb-in-the-frame-of-esa-project-sunrise>. [Accessed 15 August 2020].
- [82] Astroscale, "Astroscale Selected as Commercial Partner for JAXA's Commercial Removal of Debris Demonstration Project," Astroscale, 12 February 2020. [Online]. Available: <https://astroscale.com/astroscale->

- selected-as-commercial-partner-for-jaxas-commercial-removal-of-debris-demonstration-project/. [Accessed 15 August 2020].
- [83] Astroscale, "Active Debris Removal (ADR)," Astroscale, [Online]. Available: <https://astroscale.com/services/active-debris-removal-adr/>. [Accessed 15 August 2020].
- [84] Astroscale, "ADRAS-J ConOps video - Phase I," YouTube, 3 February 2020. [Online]. Available: [https://www.youtube.com/watch?v=5u\\_X33krhHY](https://www.youtube.com/watch?v=5u_X33krhHY). [Accessed 2 August 2020].
- [85] European Space Agency, "ESA commissions world's first space debris removal," European Space Agency, 9 December 2019. [Online]. Available: [https://www.esa.int/Safety\\_Security/Clean\\_Space/ESA\\_commissions\\_world\\_s\\_first\\_space\\_debris\\_removal](https://www.esa.int/Safety_Security/Clean_Space/ESA_commissions_world_s_first_space_debris_removal). [Accessed 15 August 2020].
- [86] European Space Agency, "RACE double CubeSat mission," European Space Agency, 5 June 2019. [Online]. Available: [https://www.esa.int/ESA\\_Multimedia/Images/2019/06/RACE\\_double\\_CubeSat\\_mission](https://www.esa.int/ESA_Multimedia/Images/2019/06/RACE_double_CubeSat_mission). [Accessed 15 August 2020].
- [87] United States Government Accountability Office, "NASA Assessments of Major Projects," United States Government Accountability Office, 2020.
- [88] NASA NExIS, "Mission Update: OSAM-1 Successfully Passes Key Decision Point-C," National Aeronautics and Space Administration, 29 May 2020. [Online]. Available: [https://nexis.gsfc.nasa.gov/05292020\\_osam1\\_update.html](https://nexis.gsfc.nasa.gov/05292020_osam1_update.html). [Accessed 15 August 2020].
- [89] J. Lymer, "Pioneering the Next Era of Space Operations and Exploration," Maxar Technologies, 8 April 2019. [Online]. Available: <https://blog.maxar.com/space-infrastructure/2019/pioneering-the-next->

- era-of-space-operations-and-exploration-through-on-orbit-servicing-assembly-and-manufacturing. [Accessed 7 August 2020].
- [90] National Aeronautics and Space Administration, "NASA's Restore-L Mission to Refuel Landsat 7, Demonstrate Crosscutting Technologies," National Aeronautics and Space Administration, 23 June 2016. [Online]. Available: <https://www.nasa.gov/feature/nasa-s-restore-l-mission-to-refuel-landsat-7-demonstrate-crosscutting-technologies>. [Accessed 15 August 2020].
- [91] RussianSpaceWeb.com, "The Kurs-NA docking system for Soyuz MS," RussianSpaceWeb.com, [Online]. Available: <http://www.russianspaceweb.com/soyuz-ms-kurs-na.html>. [Accessed 7 August 2020].
- [92] E. M. Hinman and D. M. Bushman, "Soviet automated rendezvous and docking system overview," The SAO/NASA Astrophysics Data System, [Online]. Available: <https://ui.adsabs.harvard.edu/abs/1991arcr.nasa...34H/abstract>. [Accessed 18 August 2020].
- [93] Space Servicing Capabilities Project, "On-Orbit Satellite Servicing Study," National Aeronautics and Space Administration Goddard Space Flight Center, Greenbelt, 2010.
- [94] J. A. Christian and S. Cryan, "A Survey of LIDAR Technology and its Use in Spacecraft Relative Navigation," in *AIAA Guidance, Navigation and Control (GNC) Conference*, Boston, 2013.
- [95] N. A. a. S. Administration, "Press Kit/April 2014 SpaceX CRS-3 Mission Cargo Resupply Services Mission," National Aeronautics and Space Administration, 2014.

- [96] S. Ruel and T. Luu, "STS-128 on-orbit demonstration of the TriDAR targetless rendezvous and docking sensor," in *IEEE Aerospace Conference Proceedings*, 2010.
- [97] D. W. Scott, "Meet Neptec, the newest weapon in the Maxar arsenal," Maxar Technologies, 15 November 2018. [Online]. Available: <https://blog.maxar.com/earth-intelligence/2018/meet-neptec-the-newest-weapon-in-the-maxar-arsenal>. [Accessed 7 August 2020].
- [98] R. Opromolla, G. Fasano, G. Rufino and M. Grassi, "A review of cooperative and uncooperative spacecraft pose determination techniques for close-proximity operations," *Progress in Aerospace Sciences*, vol. 93, pp. 53-72, 2017`.
- [99] J. A. Christian, H. Hinkel, C. N. D'Souza, S. Maguire and M. Patangan, "The Sensor Test for Orion RelNav Risk Mitigation (STORRM) Development Test Objective," in *AIAA Guidance, Navigation and Control Conference*, Portland, 2011.
- [100] P. Z. Schulte, P. T. Spehar and D. C. Woffinden, "GN&C Sequencing for Orion Rendezvous, Proximity Operations, And Docking," National Aeronautics and Space Administration, Houston, 2020.
- [101] University of Surrey, "RemoveDEBRIS completes reconnaissance and navigation test," University of Surrey, 30 October 2018. [Online]. Available: <https://www.surrey.ac.uk/news/removedebris-completes-reconnaissance-and-navigation-test>. [Accessed 2 August 2020].
- [102] B. J. Naasz, R. D. Burns, S. Z. Queen, J. V. Eepoel, J. Hannah and E. Skelton, "The HST SM4 Relative Navigation Sensor System: Overview and Preliminary Testing Results from the Flight Robotics Lab," in *AAS F. Landis Markley Astronautics Symposium*, Cambridge, 2008.

- [103] M. Strube, R. Henry, E. Skelton, J. V. Eepoel, N. Gill and R. McKenna, "Raven: An On-Orbit Relative Navigation Demonstration Using International Space Station Visiting Vehicles," in *AAS GN&C Conference*, Breckenridge, 2015.
- [104] NASA NExIS, "Raven Creating Autopilot for Spacecraft," National Aeronautics and Space Administration, [Online]. Available: <https://nexis.gsfc.nasa.gov/Raven.html>. [Accessed 28 July 2020].
- [105] Neptec, "Cameras," Neptec, [Online]. Available: <https://neptec.com/products/cameras/>. [Accessed 17 August 2020].
- [106] D. Patterson, "Source Selection Statement for the Restore-L Rendezvous Proximity Operations (RPO) Subsystem Visible Wavelength Spaceflight Cameras Contract," Goddard Space Flight Center, Greenbelt, 2017.
- [107] IEEE Canada, "The Shuttle Remote Manipulator System -- The Canadarm," IEEE Canada, [Online]. Available: [https://www.ieee.ca/millennium/canadarm/canadarm\\_technical.html](https://www.ieee.ca/millennium/canadarm/canadarm_technical.html). [Accessed 9 August 2020].
- [108] National Aeronautics and Space Administration, "Remote Manipulator System (Canadarm2)," National Aeronautics and Space Administration, 24 October 2018. [Online]. Available: [https://www.nasa.gov/mission\\_pages/station/structure/elements/remote-manipulator-system-canadarm2/Remote Manipulator System \(Canadarm2\)](https://www.nasa.gov/mission_pages/station/structure/elements/remote-manipulator-system-canadarm2/Remote%20Manipulator%20System%20(Canadarm2)). [Accessed 9 August 2020].
- [109] Canadian Space Agency, "About Canadarm3," Canadian Space Agency, [Online]. Available: <https://www.asc-csa.gc.ca/eng/canadarm3/about.asp>. [Accessed 9 August 2020].

- [110] Canadian Space Agency, "Canadarm, Canadarm2, and Canadarm3 - A comparative table," Canadian Space Agency, [Online]. Available: <https://www.asc-csa.gc.ca/eng/iss/canadarm2/canadarm-canadarm2-canadarm3-comparative-table.asp>. [Accessed 28 July 2020].
- [111] MDA, "Iconic Space Technology Firm Returns to Canadian Control As Sale of MDA to Northern Private Capital Closes," MDA, 8 April 2020. [Online]. Available: <https://www.mdacorporation.com/mdaSplash/DealClosingPressRelease-Final-ENG.pdf>. [Accessed 9 August 2020].
- [112] Canadian Space Agency, "The Next-Generation Canadarm," Canadian Space Agency, 5 July 2013. [Online]. Available: <https://www.asc-csa.gc.ca/eng/canadarm/ngc.asp>. [Accessed 23 July 2020].
- [113] Maxar, "SPIDER Revolutionizing the space ecosystem," Maxar.
- [114] Maxar Technologies, "NASA Selects Maxar to Build, Fly Innovative Robotic Spacecraft Assembly Technology on Restore-L," Maxar Technologies, 31 January 2020. [Online]. Available: <https://investor.maxar.com/investor-news/press-release-details/2020/NASA-Selects-Maxar-to-Build-Fly-Innovative-Robotic-Spacecraft-Assembly-Technology-on-Restore-L/default.aspx>. [Accessed 7 August 2020].
- [115] NASA NExIS, "Robotic Servicing Arm," National Aeronautics and Space Administration, [Online]. Available: [https://nexis.gsfc.nasa.gov/robotic\\_servicing\\_arm.html](https://nexis.gsfc.nasa.gov/robotic_servicing_arm.html). [Accessed 9 August 2020].
- [116] Maxar Technologies, "OSAM-1 (Formerly Restore-L) Continues to Make Progress, Fuel Tank Installed," Maxar Technologies, 23 April 2020. [Online]. Available: <https://blog.maxar.com/space->

- infrastructure/2020/osam-1-formerly-restore-l-continues-to-make-progress-fuel-tank-installed. [Accessed 7 August 2020].
- [117] U.S. Naval Research Laboratory, "NRL Engineers to Lead Payload Development for Robotic Servicing of Geosynchronous Satellites," U.S. Naval Research Laboratory, 11 April 2016. [Online]. Available: <https://www.nrl.navy.mil/news/releases/nrl-engineers-lead-payload-development-robotic-servicing-geosynchronous-satellites>. [Accessed 9 August 2020].
- [118] T. J. Debus and S. P. Dougherty, "Overview and Performance of the Front-End Robotics Enabling Near-Term Demonstration (FRIEND) Robotic Arm," in *AIAA Infotech @Aerospace Conference*, Seattle, 2009.
- [119] G. Roesler, P. Jaffe and G. Henshaw, "Inside DARPA's Mission to Send a Repair Robot to Geosynchronous Orbit," *IEEE Spectrum*, 8 March 2017. [Online]. Available: <https://spectrum.ieee.org/aerospace/satellites/inside-darpas-mission-to-send-a-repair-robot-to-geosynchronous-orbit>. [Accessed 9 August 2020].
- [120] NASA Technology Transfer Program, "Tension Actuated in Space MANipulator (TALISMAN)," National Aeronautics and Space Administration, [Online]. Available: <https://technology.nasa.gov/patent/LAR-TOPS-220>. [Accessed 4 August 2020].
- [121] K. Landzettel, A. Albu-Schäffer, C. Preusche, D. Reintsema, B. Rebele and G. Hirzinger, "Robotic On-Orbit Servicing - DLR's Experience and Perspective," in *2006 IEEE/RSJ International Conference on Intelligent Robots and Systems*, Beijing, 2006.
- [122] European Space Agency, "ESA OPENS THE RENEGADE ACTIVITY FOR SPACE SERVICING VEHICLE," European Space Agency, 1 June 2018. [Online]. Available:

- <https://blogs.esa.int/cleanspace/2018/06/01/esa-opens-the-renegade-activity-for-ssv/>. [Accessed 2 August 2020].
- [123] I. S. Paraskevas, G. Rekleitis, K. Nanos, O. Christidou, S. Andiappane and E. Papadopoulos, "Space Robotics Technologies for On-Orbit Servicing Missions," EROSS, [Online]. Available: <https://eross-h2020.eu/publications/publication-1>. [Accessed 10 August 2020].
- [124] EROSS, "Objective of the project," EROSS, [Online]. Available: <https://eross-h2020.eu/about-us/i3ds-building-blocks>. [Accessed 10 August 2020].
- [125] S. Lee, S. Anandkrishnan, C. Connor, E. Moy, D. Smith, M. Myslinski, L. Markley and A. Vernacchio, "Hubble Space Telescope Servicing Mission 3A Rendezvous Operations," National Aeronautics and Space Administration, 2001.
- [126] N. Atkinson, "Hubble Captured by Space Shuttle Crew," Universe Today, 13 May 2009. [Online]. Available: <https://www.universetoday.com/30782/hubble-captured-by-space-shuttle-crew/>. [Accessed 31 July 2020].
- [127] T. Rice, "Space station catches Dragon by the tail," WRAL.com, 4 March 2013. [Online]. Available: <https://www.wral.com/space-station-catches-dragon-by-the-tail/12180768/>. [Accessed 31 July 2020].
- [128] MDA, "MDA contract will enable robotic capture and mating of Orbital's Cygnus(TM) Cargo Delivery Spacecraft to the ISS," SpaceRef Interactive Inc., 19 January 2010. [Online]. Available: <http://www.spaceref.com/news/viewpr.html?pid=30051>. [Accessed 31 July 2020].
- [129] SpaceFlight101.com, "Dragon Cargo Craft successfully Captured by Space Station Crew after extended Rendezvous," SpaceFlight101.com, 23 February 2017. [Online]. Available:

- <https://spaceflight101.com/dragon-spx10/dragon-spx-10-cargo-craft-arrives-at-iss/>. [Accessed 31 July 2020].
- [130] M. Garcia, "The Cygnus craft from Northrop Grumman," National Aeronautics and Space Administration, 12 February 2019. [Online]. Available: <https://www.nasa.gov/image-feature/the-cygnus-cargo-craft-from-northrop-grumman-2>. [Accessed 31 July 2020].
- [131] National Aeronautics and Space Administration, "Press Kit/October 2010 Expedition 25 and 26 A New Decade Begins," National Aeronautics and Space Administration, 2010.
- [132] P. Callen, "Robotic Transfer and Interfaces for External ISS Payloads," in *3rd Annual ISS Research and Development Conference*, 2014.
- [133] National Aeronautics and Space Administration, "Meet the International Docking Adapter," National Aeronautics and Space Administration, 5 October 2015. [Online]. Available: <https://www.nasa.gov/feature/meet-the-international-docking-adapter>. [Accessed 31 July 2020].
- [134] International Space Station Partner Agencies, "International Docking Standard," [InternationalDockingStandard.com](http://InternationalDockingStandard.com), 16 July 2019. [Online]. Available: <https://www.internationaldockingstandard.com/>. [Accessed 31 July 2020].
- [135] T. Burghardt, "Crew Dragon successfully conducts debut docking with the ISS," [NASASpaceflight.com](http://NASASpaceflight.com), 3 March 2019. [Online]. Available: <https://www.nasaspaceflight.com/2019/03/crew-dragon-first-docking-iss-dm1/>. [Accessed 31 July 2020].
- [136] Marie Lewis, "NASA Update on Orbital Flight Test Independent Review Team," National Aeronautics and Space Administration, 6 March 2020. [Online]. Available: <https://blogs.nasa.gov/commercialcrew/2020/03/06/nasa-update-on-orbital-flight-test-independent-review-team/>. [Accessed 31 July 2020].

- [137] Boeing Space, "Boeing Statement on Starliner's Next Flight," Boeing, 6 April 2020. [Online]. Available: <https://boeing.mediaroom.com/2020-04-06-Boeing-Statement-on-Starliners-Next-Flight>. [Accessed 31 July 2020].
- [138] E. Kopp-DeVol, Interviewee, *Product Brochures [Email]*. [Interview]. 30 June 2020.
- [139] Altius Space Machines, "Interface Definition Document (IDD) for Altius DogTag™ Grapple Fixtures and Visiting Vehicles (VVs)," Altius Space Machines, Broomfield, 2020.
- [140] Altius Space Machines, "Altius DogTag™," Altius Space Machines, Broomfield.
- [141] Obruta Space Systems, "The Puck," Obruta Space Systems, [Online]. Available: <https://www.obruta.com/puck>. [Accessed 4 August 2020].
- [142] O. S. Systems, "Active Debris Removal Tethered-Net," Obruta Space Systems, [Online]. Available: <https://www.obruta.com/tethered-net>. [Accessed 4 August 2020].
- [143] Altius Space Machines, "MagTag™ Modular Interfaces for Palletized Subsystems and Satellites," Altius Space Machines, Broomfield.
- [144] iBOSS, "iSSI intelligent Space System Interface New Standard for Modular Plug-and-Play + More," iBOSS, 2020.
- [145] Consortium for Execution of Rendezvous and Servicing Operations (CONFERS), "Current Members," Consortium for Execution of Rendezvous and Servicing Operations (CONFERS), [Online]. Available: <https://www.satelliteconfers.org/members/>. [Accessed 27 July 2020].

- [146] iBOSS, "iSSI - intelligent Space System Interface," iBOSS, [Online]. Available: <https://www.iboss.space/products/#overview>. [Accessed 27 July 2020].
- [147] Northrop Grumman, "Northrop Grumman's Mission Extension Vehicle (MEV)," YouTube, 30 July 2018. [Online]. Available: <https://www.youtube.com/watch?v=vJZ3xmuom0M>. [Accessed 8 August 2020].
- [148] University of Surrey, "Net successfully snares space debris," University of Surrey, 19 September 2018. [Online]. Available: <https://www.surrey.ac.uk/news/net-successfully-snares-space-debris>. [Accessed 2 August 2020].
- [149] SSTL, "RemoveDEBRIS: success for harpoon experiment," Surrey Satellite Technology Ltd, 15 February 2019. [Online]. Available: <https://www.sstl.co.uk/media-hub/latest-news/2019/removedebris-success-for-harpoon-experiment>. [Accessed 10 August 2020].
- [150] European Space Agency, "Weightless net testing for derelict satellite capture," YouTube, 23 March 2015. [Online]. Available: <https://www.youtube.com/watch?v=mx9Fb5sixBU>. [Accessed 2 August 2020].
- [151] D. A. Barnhart and R. Rughani, "On-Orbit Servicing Ontology applied to Recommended Standards for Satellites in Earth Orbit," in *70th International Astronautical Congress*, Washington D.C., 2019.
- [152] Consortium for Execution of Rendezvous and Servicing Operations (CONFERS), "About," Consortium for Execution of Rendezvous and Servicing Operations (CONFERS), [Online]. Available: <https://www.satelliteconfers.org/about-us/>. [Accessed 27 July 2020].

- [153] OneWeb, "OneWeb Seeks to Increase Satellite Constellation Up to 48,000 Satellites, Bringing Maximum Flexibility to Meet Future Growth and Demand," OneWeb, 27 May 2020. [Online]. Available: <https://www.oneweb.world/media-center/oneweb-seeks-to-increase-satellite-constellation-up-to-48000-satellites-bringing-maximum-flexibility-to-meet-future-growth-and-demand>. [Accessed 2 August 2020].
- [154] J. Brodtkin, "Bankrupt OneWeb seeks license for 48,000 satellites, even more than SpaceX," Ars Technica, WIRED Media Group, 27 May 2020. [Online]. Available: <https://arstechnica.com/tech-policy/2020/05/spacex-and-oneweb-look-for-licenses-to-launch-78000-broadband-satellites/>. [Accessed 2 August 2020].
- [155] C. Henry, "SpaceX submits paperwork for 30,000 more Starlink satellites," SpaceNews, 15 October 2019. [Online]. Available: <https://spacenews.com/spacex-submits-paperwork-for-30000-more-starlink-satellites/>. [Accessed 2 August 2020].
- [156] OneWeb, "OneWeb and OneWeb Satellites bolster commitment to Responsible Space with advanced grappling technology from Altius Space Machines," OneWeb, 10 December 2019. [Online]. Available: <https://www.oneweb.world/media-center/oneweb-and-oneweb-satellites-bolster-commitment-to-responsible-space-with-advanced-grappling-technology-from-altius-space-machines>. [Accessed 30 July 2020].
- [157] eoPortal Directory, "OneWeb Minisatellite Constellation for Global Internet Service," European Space Agency, [Online]. Available: <https://directory.eoportal.org/web/eoportal/satellite-missions/o/oneweb>. [Accessed 2 August 2020].
- [158] E. M. (@elonmusk), "Tweet," Twitter, 12 May 2019. [Online]. Available: <https://twitter.com/elonmusk/status/1127388838362378241>. [Accessed 2 August 2020].

- [159] OneWeb, "OneWeb Files for Chapter 11 Restructuring to Execute Sale Process," OneWeb, 27 March 2020. [Online]. Available: <https://www.oneweb.world/media-center/oneweb-files-for-chapter-11-restructuring-to-execute-sale-process>. [Accessed 3 August 2020].
- [160] OneWeb, "OneWeb announces HMG and Bharti Global Limited consortium as winning bidders in court-supervised sale process," OneWeb, 3 July 2020. [Online]. Available: <https://www.oneweb.world/media-center/oneweb-announces-hmg-and-bharti-global-limited-consortium-as-winning-bidders-in-court-supervised-sale-process>. [Accessed 3 August 2020].
- [161] BBC News, "UK government takes £400m stake in satellite firm OneWeb," BBC News, 3 July 2020. [Online]. Available: <https://www.bbc.co.uk/news/science-environment-53279783>. [Accessed 3 August 2020].
- [162] OneWeb, "Our Vision & Values," OneWeb, [Online]. Available: <https://www.oneweb.world/our-vision-values>. [Accessed 2 August 2020].
- [163] J. R. Wertz, D. F. Everett and J. J. Puschell, Space Mission Engineering: The New SMAD, Microcosm Press, 2011.
- [164] European Space Agency, "Concurrent Design Facility Studies Standard Margin Philosophy Description," European Space Agency, Noordwijk, 2017.
- [165] Moog, "Bipropellant Attitude Control System (ACS) Thrusters," Moog, Inc., East Aurora, 2019.
- [166] D. A. Vallado, Fundamentals of Astrodynamics and Applications, Hawthorne: Microcosm Press, 2013.
- [167] J. P. S. Cuartielles, "Session 3 Orbit Perturbations," Cranfield University, Cranfield, 2020.

- [168] B. Parkinson, "Lecture 1 Introduction Tsiolkowski & Specific Impulse," Cranfield University, Cranfield, 2019.
- [169] M. Wade, "MON/MMH," Mark Wade, [Online]. Available: <http://www.astronautix.com/m/monmmh.html>. [Accessed 17 August 2020].
- [170] M. Mannion and B. Keepence, "SMART Requirements," Napier University, Edinburgh, 1995.
- [171] European Space Research and Technology Centre, Concurrent Design Facility Studies Standard Margin Philosophy Description, Noordwijk: European Space Agency, 2017.
- [172] R. Votel and D. Sinclair, "Comparison of Control Moment Gyros and Reaction Wheels for Small Earth-Observing Satellites," in *26th Annual AIAA/USU Conference on Small Satellites*, 2012.
- [173] satsearch, "Viceroy-4 GPS Spaceborne Receiver," satsearch, [Online]. Available: <https://satsearch.co/products/general-dynamics-viceroy-4-gps-spaceborne-receiver>. [Accessed 19 August 2020].
- [174] satsearch, "Sentinel™ M-Code GPS Receiver," satsearch, [Online]. Available: <https://satsearch.co/products/general-dynamics-sentinel-m-code-gps-receiver>. [Accessed 19 August 2020].
- [175] satsearch, "ANT-GPS Active GPS Antenna," satsearch, [Online]. Available: <https://satsearch.co/products/space-quest-ant-gps-active-gps-antenna>. [Accessed 19 August 2020].
- [176] satsearch, "ARGO-L1 GNSS Receiver Unit," satsearch, [Online]. Available: <https://satsearch.co/products/astrofein-argo-l1-gnss-receiver-unit>. [Accessed 19 August 2020].

- [177] satsearch, "GNSS All-bands Antenna," satsearch, [Online]. Available: <https://satsearch.co/products/anywaves-gnss-all-bands-antenna>. [Accessed 19 August 2020].
- [178] J. Teles, M. V. Samii and C. E. Doll, "Overview of TDRSS," *Advances in Space Research*, vol. 16, no. 12, pp. 67-76, 1995.
- [179] H. Klinkrad, "Meteoroid and Debris Protection," in *Safety Design for Space Systems*, Elsevier Ltd, 2009, pp. 319-340.
- [180] C. Gramling and A. C. Long, "Autonomous Navigation Using the TDRSS Onboard Navigation System (TONS)," *Advances in Space Research*, vol. 16, no. 12, pp. 77-80, 1995.
- [181] eoPortal Directory, "EnviSat (Environmental Satellite)," eoPortal Directory, [Online]. Available: <https://directory.eoportal.org/web/eoportal/satellite-missions/e/envisat>. [Accessed 19 August 2020].
- [182] T. P. Yunck, "Orbit Determination," in *Global Positioning System: Theory and Applications Vol. II*, American Institute of Aeronautics and Astronautics, 1996, pp. 559-592.
- [183] General Dynamics, "Viceroy-4 GPS Spaceborne Receiver," General Dynamics, 2015.
- [184] Cranfield University, "Attitude & Orbit Control Subsystem (AOCS)," Cranfield University, Cranfield, 2019.
- [185] M. B. A. Zahran and M. A. Moawad, "A Solar Cell Based Coarse Sun Sensor for a Small LEO Satellite Attitude Determination," *Journal of Power Electronics*, vol. 9, no. 4, pp. 631-642, 2009.
- [186] N. Prasad, "An overview of GPS receivers for small satellites," satsearch, 12 November 2019. [Online]. Available:

- <https://blog.satsearch.co/2019-11-12-an-overview-of-gps-receiver-products-for-small-satellites>. [Accessed 10 August 2020].
- [187] Astro- und Feinwerktechnik Adlershof GmbH, "Space Technology AOCS-Components Gyro-System AGS-1 for Small Satellites," satsearch, Berlin.
- [188] G. Solutions, "GS-IMU3000TA," satsearch, Hong Kong.
- [189] jenaoptronik, "Autonomous Star Sensor ASTRO APS," satsearch, Jena, 2015.
- [190] Sinclair Interplanetary, "Second Generation Star Tracker (ST-16RT2)," satsearch, 2016.
- [191] S. Hardacre, "Workshop 1 - Plant Modelling in Matlab / SIMULINK," Cranfield University, Cranfield, 2020.
- [192] J.-P. Sánchez, "Session 3 Orbit Perturbations," Cranfield University, Cranfield, 2020.
- [193] D. H. Collins, "Six-Degree-of-Freedom Control With Only Eight Thrusters," 1 December 2015. [Online]. Available: <https://www.techbriefs.com/component/content/article/tb/techbriefs/mechanics-and-machinery/23462>. [Accessed 11 August 2020].
- [194] Astroscale, "Astroscale's Space Debris Removal Mission, ELSA-d - ConOps Video," YouTube, 12 September 2019. [Online]. Available: <https://www.youtube.com/watch?v=HCWxdK7I0hI>. [Accessed 2 August 2020].
- [195] Cranfield University, "MSc in Astronautics & Space Engineering Spacecraft Attitude Dynamics & Control - Formulae," Cranfield University, Cranfield, 2019.

- [196] T. Pultarova, "Ion Thruster Prototype Breaks Records in Tests, Could Sent Humans to Mars," Space.com, 13 October 2017. [Online]. Available: <https://www.space.com/38444-mars-thruster-design-breaks-records.html>. [Accessed 11 August 2020].
- [197] Dawn Aerospace, "SmallSat Propulsion Thruster - 20N," Dawn Aerospace, [Online]. Available: <https://www.dawnaerospace.com/products/smallsat-propulsion>. [Accessed 13 August 2020].
- [198] Aerojet Rocketdyne, "In-Space Propulsion Data Sheets," Aerojet Rocketdyne, Redmond, 2020.
- [199] bradford ecaps, "22N HPGP Thruster," Bradford, [Online]. Available: <https://www.ecaps.space/products-22n.php>. [Accessed 12 August 2020].
- [200] bradford ecaps, "50N HPGP Thruster," Bradford, [Online]. Available: <https://www.ecaps.space/products-50n.php>. [Accessed 12 August 2020].
- [201] IHI AeroSpace, "Monopropellant Thrusters," IHI AeroSpace, Tomioka.
- [202] Moog, "Monopropellant Thrusters," Moog, Inc., Niagara Falls, 2018.
- [203] Northrop Grumman, "MRE-4.0 Monopropellant Thruster," Northrop Grumman, [Online]. Available: [https://www.northropgrumman.com/wp-content/uploads/MRE-40\\_MonoProp\\_Thruster.pdf](https://www.northropgrumman.com/wp-content/uploads/MRE-40_MonoProp_Thruster.pdf). [Accessed 13 August 2020].
- [204] Northrop Grumman, "MRE-5.0 Monopropellant Thruster," Northrop Grumman, [Online]. Available: [https://www.northropgrumman.com/wp-content/uploads/MRE-50\\_MonoProp\\_Thruster.pdf](https://www.northropgrumman.com/wp-content/uploads/MRE-50_MonoProp_Thruster.pdf). [Accessed 13 August 2020].
- [205] NewSpace Systems, "Magnetorquer Rod," NewSpace Systems, Somerset West.

- [206] L. J. Kamm, "Magnetorquer - a Satellite Orientation Device," *American Rocket Society*, vol. 31, no. 6, pp. 813-815, 1961.
- [207] University of Washington, "Earth's Magnetic Field," University of Washington, [Online]. Available: [https://courses.washington.edu/ess502/Lect2\\_EarthMagneticField.pdf](https://courses.washington.edu/ess502/Lect2_EarthMagneticField.pdf). [Accessed 13 August 2020].
- [208] L. M. Gomes, G. Yuksel, V. Lappas, A. d. S. Curiel, A. Bradford, C. Ozkaptan and P. S. M. Sweeting, "BILSAT: Advancing SmallSat Capabilities," in *17th AIAA/USU Conference on Small Satellites*, Logan, 2003.
- [209] D. J. Richie, V. J. Lappas and G. Prassinis, "A practical small satellite variable-speed control moment gyroscope for combined energy storage and attitude control," *Acta Astronautica*, vol. 65, no. 11-12, pp. 1745-1764, 2009.
- [210] L3, "CMG - Control Moment Gyroscope Double-Gimbal CMG," L3.
- [211] A. Gaude and V. Lappas, "Design and Structural Analysis of a Control Moment Gyroscope (CMG) Actuator for CubeSats," *Aerospace*, vol. 7, no. 5, p. 55, 2020.
- [212] Airbus Defense & Space, "CMG 15-45S," satsearch, 2014.
- [213] Collins Aerospace, "Space Wheels," Collins Aerospace, [Online]. Available: <https://www.collinsaerospace.com/what-we-do/Space/Space-Wheels>. [Accessed 18 August 2020].
- [214] Collins Aerospace, "RSI 68 Momentum and Reaction Wheels," Collins Aerospace, [Online]. Available: <https://www.collinsaerospace.com/what-we-do/Space/Space-Wheels/RSI-68-Momentum-And-Reaction-Wheels>. [Accessed 18 August 2020].

- [215] Rockwell Collins, "RSI 12 Momentum and Reaction Wheels 4 – 12 Nms with integrated Wheel Drive Electronics," Rockwell Collins, Heidelberg, 2007.
- [216] E. Kopp-DeVol, Interviewee, *Product Brochures [Email]*. [Interview]. 7 August 2020.
- [217] B. Castle, "Mission Control Answers Your Questions," National Aeronautics and Space Administration, 7 April 2002. [Online]. Available: [https://spaceflight.nasa.gov/feedback/expert/answer/mcc/sts-92/10\\_15\\_03\\_59\\_48.html](https://spaceflight.nasa.gov/feedback/expert/answer/mcc/sts-92/10_15_03_59_48.html). [Accessed 7 August 2020].
- [218] X. Zhu, I. C. Smith and F. Babin, "A hybrid 3D sensor (NEPTEC TriDAR) for object tracking and inspection," in *Laser Radar Technology and Applications XI*, Orlando, 2006.
- [219] D. Laurin, J.-A. Beraldin, F. Blais, M. Rioux and L. Cournoyer, "A three-dimensional tracking and imaging laser scanner for space operations," in *AeroSense '99*, Orlando, 1999.
- [220] T. Rickerl, S. R. Walker and C. M. Reichert, "Rendezvous STS-135," Lyndon B. Johnson Space Center, Houston, 2011.
- [221] D. S. Koons, C. Schreiber, F. Acevedo and M. Sechrist, "Risk Mitigation Approach to Commercial Resupply to the International Space Station," National Aeronautics and Space Administration, Houston, 2010.
- [222] D. E. Gaylor and B. W. Barbee, "Algorithms for Safe Spacecraft Proximity Operations," *Advances in the Astronautical Sciences*, vol. 127, pp. 133-152, 2007.
- [223] R. L. Ticker, F. Cepollina and B. B. Reed, "NASA's In-Space Robotic Servicing," in *AIAA SPACE 2015 Conference and Exposition*, Pasadena, 2015.

- [224] Metalphoto, "When to Use Metalphoto?," Metalphoto, [Online]. Available: <https://metalphoto.com/#whenAnchor>. [Accessed 7 August 2020].
- [225] Metalphoto, "Metalphoto Application Hall of Fame," Metalphoto, [Online]. Available: <https://metalphoto.com/metalphoto-hall-fame/>. [Accessed 7 August 2020].
- [226] C. Blackerby, A. Okamoto, S. Iizuka, Y. Kobayashi, K. Fujimoto, Y. Seto, S. Fujita, T. Iwai, N. Okada, J. Forshaw and A. Bradford, "The ELSA-d End-of-life Debris Removal Mission: Preparing for Launch," in *70th International Astronautical Congress (IAC)*, Washington DC, 2019.
- [227] National Aeronautics and Space Administration, "About the Northrop Grumman Cygnus," National Aeronautics and Space Administration, [Online]. Available: [https://www.nasa.gov/mission\\_pages/station/structure/elements/cygnus\\_about.html](https://www.nasa.gov/mission_pages/station/structure/elements/cygnus_about.html). [Accessed 16 August 2020].
- [228] NASA NExIS, "OSAM-1 On-Orbit Servicing, Assembly, and Manufacturing 1," [Online]. Available: <https://nexis.gsfc.nasa.gov/osam-1.html>.
- [229] Canadian Space Agency, "A suite of robotic technologies designed to help explore space further and longer," Canadian Space Agency, 5 July 2013. [Online]. Available: <https://www.asc-csa.gc.ca/eng/canadarm/ngc.asp>. [Accessed 22 July 2020].
- [230] D. Parry, "NRL Engineers to Lead Payload Development for Robotic Servicing of Geosynchronous Satellites," US Naval Research Laboratory, 11 April 2016. [Online]. Available: <https://www.nrl.navy.mil/news/releases/nrl-engineers-lead-payload-development-robotic-servicing-geosynchronous-satellites>. [Accessed 5 August 2020].

- [231] NASA NExIS, "RRM Phase 1," National Aeronautics and Space Administration, [Online]. Available: [https://nexis.gsfc.nasa.gov/rrm\\_phase1.html](https://nexis.gsfc.nasa.gov/rrm_phase1.html). [Accessed 25 July 2020].
- [232] NASA NExIS, "RRM Robotic Refueling Mission," National Aeronautics and Space Administration, 5 May 2015. [Online]. Available: [https://nexis.gsfc.nasa.gov/rrm\\_update2015spring.html](https://nexis.gsfc.nasa.gov/rrm_update2015spring.html). [Accessed 28 July 2020].
- [233] NASA NExIS, "RRM Phase 2," National Aeronautics and Space Administration, [Online]. Available: [https://nexis.gsfc.nasa.gov/rrm\\_phase2.html](https://nexis.gsfc.nasa.gov/rrm_phase2.html). [Accessed 25 July 2020].
- [234] National Aeronautics and Space Administration, "Robotic Refuelling Mission 3 Completes Crucial Series of Tests," National Aeronautics and Space Administration, 20 June 2018. [Online]. Available: <https://www.nasa.gov/feature/goddard/2018/robotic-refueling-mission-3-completes-crucial-series-of-tests>. [Accessed 5 August 2020].
- [235] National Aeronautics and Space Administration, "NASA to Launch New Refueling Mission, Helping Spacecraft Live Longer and Journey Farther," National Aeronautics and Space Administration, 20 November 2018. [Online]. Available: <https://www.nasa.gov/feature/goddard/2018/nasa-to-launch-new-refueling-mission-helping-spacecraft-live-longer-and-journey-farther>. [Accessed 5 August 2020].
- [236] National Aeronautics and Space Administration, "Robotic Tool Operations Bring In-Space Refueling Closer to Reality," National Aeronautics and Space Administration, 16 August 2019. [Online]. Available: <https://www.nasa.gov/feature/robotic-tool-operations-bring-in-space-refueling-closer-to-reality>. [Accessed 5 August 2020].

- [237] D. Messier, "Robotic Refuelling Mission 3 Can't Perform Cryogenic Fuel Transfer," *Parabolic Arc*, 22 April 2019. [Online]. Available: <http://www.parabolicarc.com/2019/04/22/robotic-refueling-mission-3-perform-cryogenic-fuel-transfer/>. [Accessed 5 August 2020].
- [238] David A. Vallado, "Low-Thrust, Noncoplanar Transfers," in *Fundamentals of Astronautics and Applications*, Hawthorne, Microcosm Press, 2013, pp. 381-388.
- [239] Belgian Institute for Space Aeronomy, "SPENVIS," Belgian Institute for Space Aeronomy, [Online]. Available: <https://www.spennis.oma.be/>. [Accessed 19 August 2020].
- [240] European Space Agency, "Mitigating space debris generation," European Space Agency, [Online]. Available: [https://www.esa.int/Safety\\_Security/Space\\_Debris/Mitigating\\_space\\_debris\\_generation](https://www.esa.int/Safety_Security/Space_Debris/Mitigating_space_debris_generation). [Accessed 11 May 2020].
- [241] NASA Office of Safety and Mission Assurance, NASA TECHNICAL STANDARD NASA-STD-8719.14B Process for Limiting Orbital Debris, National Aeronautics and Space Administration, 2019.
- [242] Altius Space Machines, "MagTag™ Modular Interfaces for Palletized Subsystems and Satellites," Altius Space Machines.
- [243] W. Easdown, "Mission ORCA: Orbit Refinement for Collision Avoidance," William Easdown, Cranfield, 2020.
- [244] Satellite Servicing Projects Division, "On-Orbit Satellite Servicing Study," National Aeronautics and Space Administration Goddard Space Flight Center, Greenbelt, 2010.
- [245] European Space Research and Technology Centre, Concurrent Design Facility Studies Standard Margin Philosophy Description, Noordwijk: European Space Agency, 2017.

- [246] European Space Agency, "Technology Readiness Levels (TRL)," European Space Agency, [Online]. Available: [https://www.esa.int/Enabling\\_Support/Space\\_Engineering\\_Technology/Shaping\\_the\\_Future/Technology\\_Readiness\\_Levels\\_TRL](https://www.esa.int/Enabling_Support/Space_Engineering_Technology/Shaping_the_Future/Technology_Readiness_Levels_TRL). [Accessed 5 August 2020].
- [247] HQ Office of the Chief Engineer/Steven Hirshorn and HQ Office of the Chief Technologist/Sharon Jefferies, "Final Report of the NASA Technology Readiness Assessment (TRA) Study Team," NASA Technology Readiness Assessment (TRA) Study Team, 2016.
- [248] Khan Academy, "Equation for center of mass," Khan Academy, [Online]. Available: <https://www.khanacademy.org/science/physics/linear-momentum/center-of-mass/v/center-of-mass-equation>. [Accessed 6 August 2020].
- [249] J. Branson, "Example: The Inertia Tensor for a Cube," UC San Diego, 21 October 2012. [Online]. Available: [https://hepweb.ucsd.edu/ph110b/110b\\_notes/node26.html](https://hepweb.ucsd.edu/ph110b/110b_notes/node26.html). [Accessed 6 August 2020].
- [250] "Parallel Axis Theorem," Georgia State University, [Online]. Available: <http://hyperphysics.phy-astr.gsu.edu/hbase/parax.html>. [Accessed 6 August 2020].

## **APPENDICES**

The following appendices are the full versions of documents that were created and used by the author during the project.

### **Appendix A Satellite Distribution Research and Orbit Selection**

# Satellite Distribution Research and Orbit Selection

## **A.1 Introduction**

This document outlines research undertaken for the author's individual research project (IRP) into the design of the guidance, navigation and control (GNC) system of an on-orbit servicing tug. It will outline the research carried out to select the orbit in which a servicing station will be placed, from which the servicing tug will operate.

## **A.2 Research Background and Question**

The IRP is focussing on the design of an on-orbit servicing tug, which will be based at a servicing station before being deployed to target customer spacecraft. The tug will use its thrusters to rendezvous and dock with the target, before towing the target to the station if required. Analysis of the orbits expected to be occupied by targets is required to determine the orbital location of the servicing station and the tug's  $\Delta v$  requirement.

The following research questions were investigated:

- 1) In what orbit should the servicing station be placed?

This includes orbital altitude, eccentricity and inclination.

- 2) What range of orbital altitudes and inclinations should the servicing station and tug be capable of serving?

This will determine the amount of  $\Delta v$  needed on the tug to servicing the full required orbit band.

### **A.3 Methodology**

The data analysed during this research [1] were compiled by the Union of Concerned Scientists (UCS), a US-based non-profit organisation [2]. The data are compiled in the UCS Satellite Database, which was first published on December 8<sup>th</sup>, 2005, last updated on April 1<sup>st</sup>, 2020 and contains details of 2,666 satellites. The database contains only satellites considered active – those which are currently manoeuvring and/or communicating [3]. The database was viewed as a Microsoft Excel to allow easy sorting and filtering of the data.

#### **A.3.1 Orbital altitude**

Regarding research question 1, it was decided that the station should be placed in the orbit with the largest population of spacecraft. Orbital altitude was analysed first, with spacecraft apogee used as the analysed parameter. Perigee was also considered but could have caused confusion as spacecraft in a geostationary transfer orbit (GTO) would have been shown as being in a low orbit, despite this not being their final destination.

To give an overview of the spacecraft apogees across the full range of popular orbits from LEO to GEO, a frequency chart was made from all satellite data in the UCS database. This is shown in Figure A-1. From this, it can be seen that the vast majority of spacecraft are in LEO below 1,800 km or around GEO at 35,786 km. The 300-1,800 km includes 1830 satellites, with 543 between 34,800 km and 36,300 km. Although the data show 98 satellites with apogees less than or equal to 300 km, these were discounted from further analysis as they would not be appropriate servicing targets due to their very low orbit lifetimes.

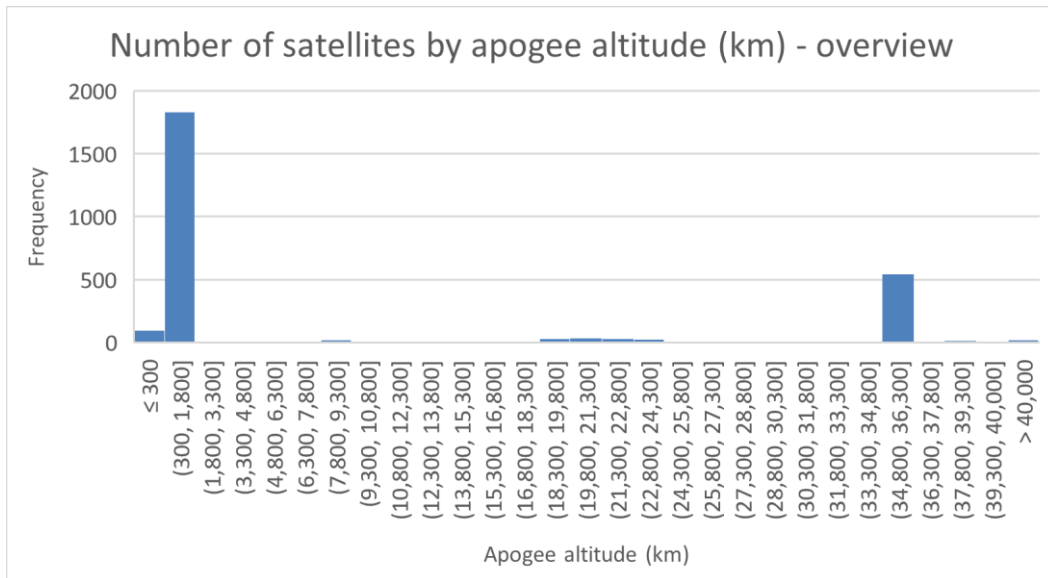


**Figure A-1 - Overview of satellite frequency by apogee**

The analysis was then refined to focus on the LEO regions due to its significantly higher population than other regions. This is shown in Figure A-2. It can be seen that the majority of satellites have apogees between 400 km and 700 km, with the peak between 500 km and 600 km. Therefore, the 400 km to 700 km region will be used for further analysis. This result corresponds to data gathered by the National Aeronautics and Space Administration (NASA) up to July 2018, shown as the intentionally deployed objects curve in Figure A-4. However, it is worth noting that the peak in objects at approximately 780 km in the NASA data is not seen in the UCS data. This may be because the NASA data include the original Iridium constellation, which has now mostly been deorbited [4].

Zooming in further, Figure A-3 shows that the main peak is between 503 and 523 km, with a secondary peak between 543 and 563 km.

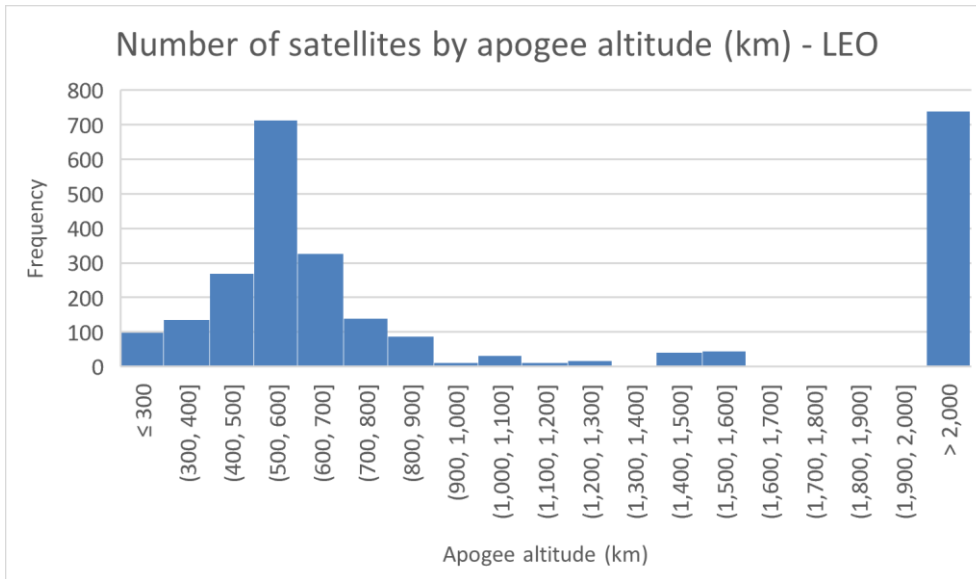


**Figure A-2 - LEO satellite frequency by apogee**

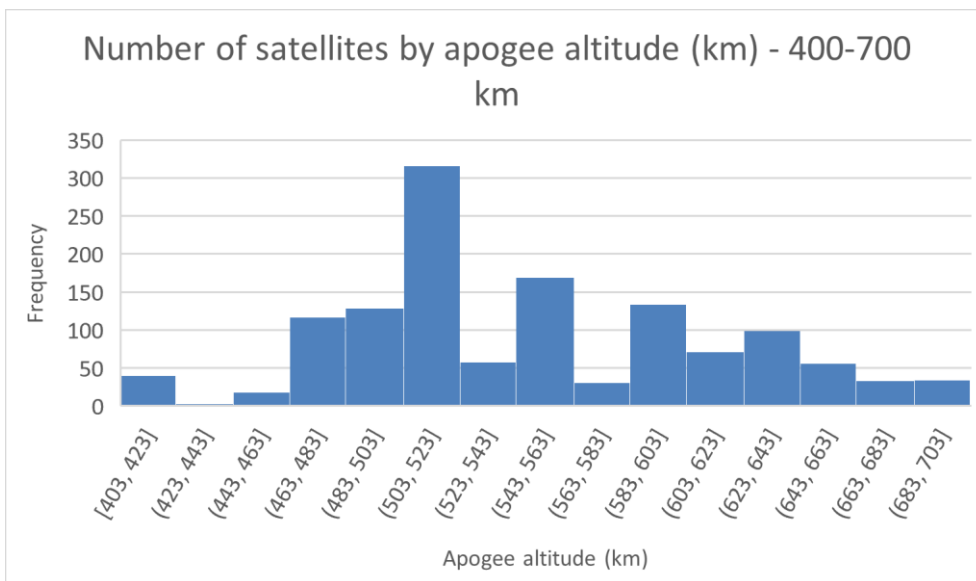


**Figure A-3 - Satellite frequency by apogee between 400 and 700 km**

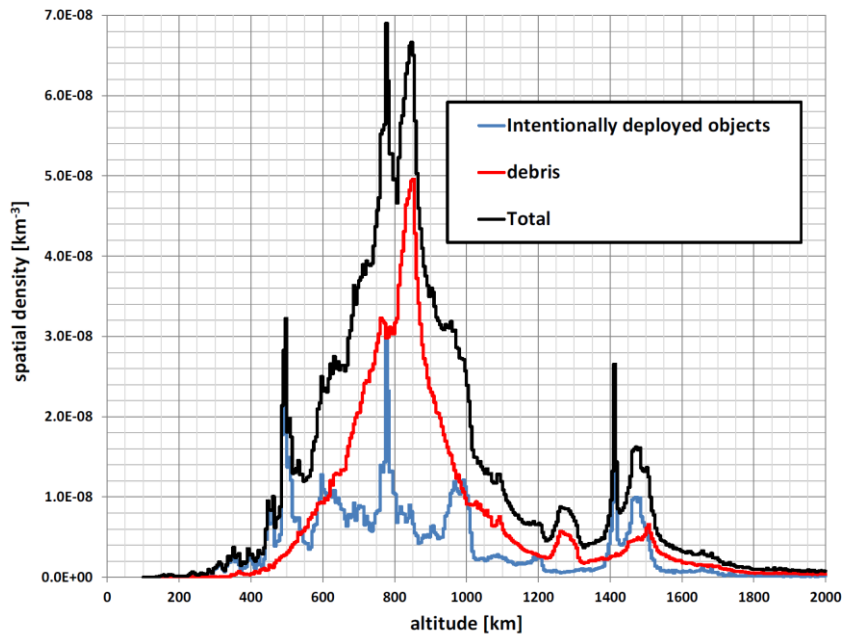
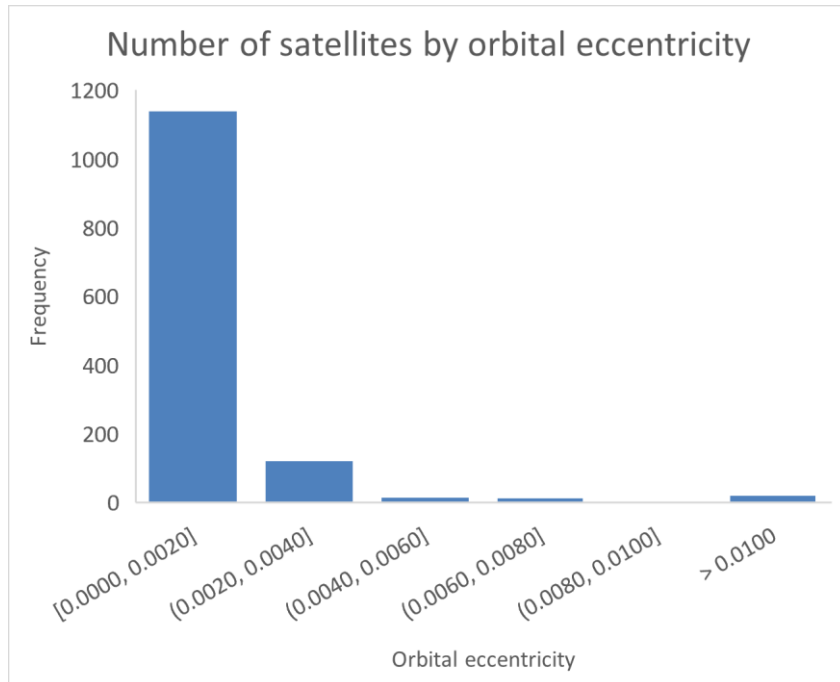


Figure A-4 - The near Earth (up to 2000 km) altitude population [5, p. 6]

### A.3.2 Orbital eccentricity

Considering satellites with apogees between 400 km and 700 km and plotting the frequency of the satellites' various eccentricities resulted in the chart shown in Figure A-5. This shows that the satellites in this altitude band are in orbits that can be considered circular or near-circular, simplifying analysis of the tug's orbital manoeuvres to rendezvous and dock with the target spacecraft.



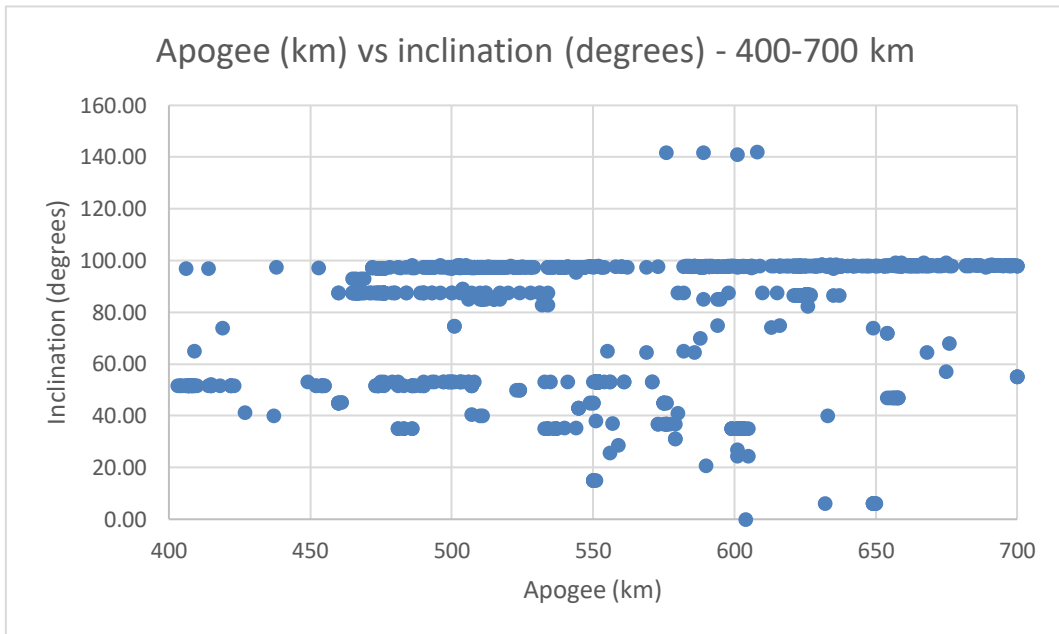
**Figure A-5 - Satellite frequency by orbital eccentricity for apogees between 400 km and 700 km**

### A.3.3 Orbital inclination

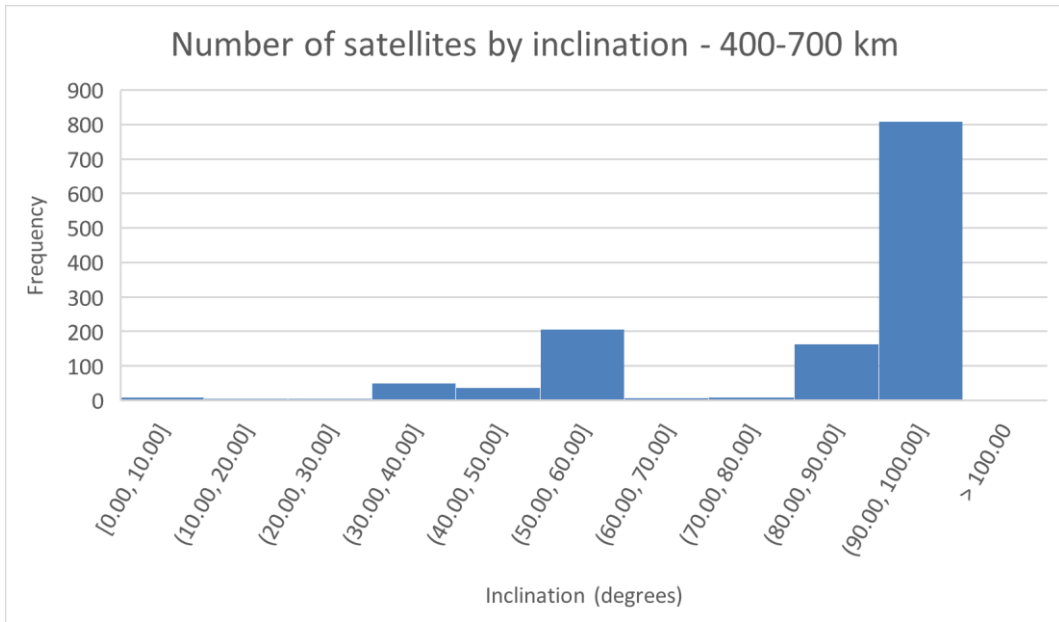
Further analysing the 400 km to 700 km apogee range, apogee was plotted against inclination, giving the chart shown in Figure A-6. Three distinct bands can be seen, with the top band at around 97.5° corresponding to Sun synchronous orbits (SSOs) at this altitude. The middle band, at 87.4° and between 460 and 582 km apogee, is the OneWeb satellite constellation. The lowest of the three bands, at an inclination of 53.0° and between 449 and 571 km apogee, corresponds to the SpaceX Starlink constellation.

Figure A-7 shows a frequency plot of number of spacecraft by inclination. This also highlights the high inclination SSO band, making this orbit a compelling target if launch from high latitude launch sites can be used. The narrow inclination range for SSO is also beneficial, as it means a servicing tug could target a large number of satellites without requiring a  $\Delta v$  intensive inclination change. For example, as shown in Figure A-6, the SSO inclination at 472 km altitude is 97.2°, versus 97.8° at 700 km altitude.

Figure A-8 zooms in further compared to Figure A-6 and showing apogees ranging from 500 to 700 km and inclinations from 97.2 to 97.8°. The plot shows that the satellites are clustered towards the lower apogee end of this apogee and inclination region and tend to favour inclinations between 97.3 and 97.5°. The plot therefore shows a high-density region within which the servicing station should be placed.



**Figure A-6 - Apogee vs inclination for 400 to 700 km apogees and 0° to 160° inclinations**



**Figure A-7 - Satellite frequency by inclination for apogees between 400 km and 700 km**

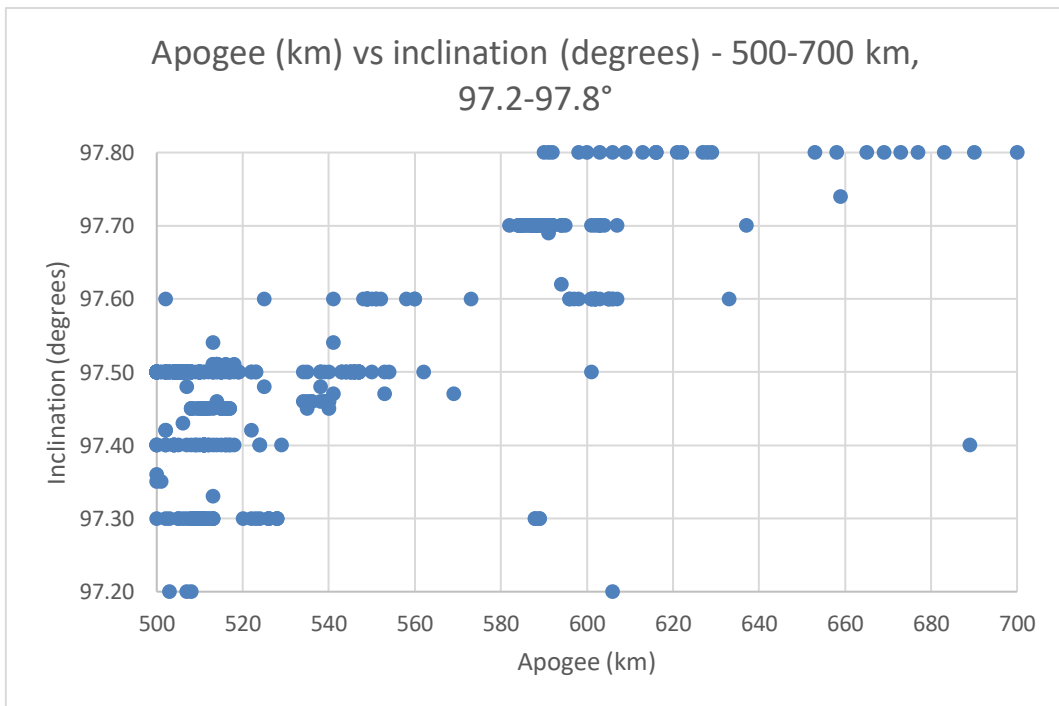


**Figure A-8 - Apogee vs inclination for 500 to 700 km apogees and 97.2° to 97.8° inclinations**

## A.4 Conclusions

Orbital altitudes were analysed first, with the LEO and particularly the 400 to 700 km altitude range being the most commonly used and the highest peak between 503 and 523 km apogee. Orbit eccentricity was analysed next, revealing that orbits in this altitude region can all be considered circular or near-circular. Orbit inclination was considered, with SSO at approximately 97.4° having the highest population for the selected altitude range. The orbit was then refined further, resulting in the selection for the servicing station and tug centre of operations being a circular orbit with an altitude of approximately 510 km and an inclination of approximately 97.4°.

## References

- [1] Union of Concerned Scientists, "UCS Satellite Database," Union of Concerned Scientists, 1 April 2020. [Online]. Available: <https://www.ucsusa.org/resources/satellite-database>. [Accessed 15 May 2020].
- [2] Union of Concerned Scientists, "About," <https://www.ucsusa.org/about>, [Online]. Available: <https://www.ucsusa.org/about>. [Accessed 15 May 2020].
- [3] Union of Concerned Scientists, "UCS Satellite Database User's Manual 1-1-17," Union of Concerned Scientists, 2017.
- [4] C. Henry, "Iridium to finish deorbiting legacy constellation early next year," SpaceNews, 12 September 2018. [Online]. Available: <https://spacenews.com/iridium-to-finish-deorbiting-legacy-constellation-early-next-year/>. [Accessed 15 May 2020].

[5] Phillip D. Anz-Meador; John N. Opiela; Debra Shoots; J.-C. Liou, History of On-Orbit Satellite Fragmentations, 15th ed., Houston: Orbital Debris Program Office, National Aeronautics and Space Administration, 2018.

## Appendix B CONOPS

Space Servicer Concept of Operations

July 2020

## **B.1 Executive Summary**

## B.2 Introduction

- *Heading titles in this document are inspired by those in the JWST Mission Operations Concept Document [1] and the ATHENA Concept of Operations [2]*

### B.2.1 Mission Summary

The selected mission is built around a set of ideas grouped under ESA's [On-orbit Manufacturing Assembly and Recycling \(OMAR\) programme](#). Key points from OMAR:

- Large structures such as parabolic reflectors or booms would particularly benefit from on-orbit recycling/refurbishment
- Satellite lifetimes could potentially be doubled with refurbishment

### B.2.2 Mission Justification

#### B.2.3 Business Case

Generally, the space tug's services will be paid for by satellite operators. For example, an operator will directly pay the servicing company for their satellite to be refuelled or have hardware replaced.

However, the business case for disposal services is less clear due to there being no strict mandate for spacecraft to be disposed of at the end of life (EOL). While there are guidelines from ESA [3] and NASA [4] that satellites with a deployment altitude below 2000 km should re-enter the atmosphere no more than 25 years after EOL, this is not currently enforced. This means that operators have no financial incentive to de-orbit their spacecraft, making selling a service to do this challenging. It is therefore anticipated that for large scale uptake of disposal services, legal changes will need to be made on a national and international level to enforce the current guidelines.

Prices for the space tug's services remain to be determined but should take into account the value given to satellite operators by additional spacecraft lifetime and the potential initial reduction in cost while manufacturing spacecraft due to be able to use smaller propellant tanks and lower lifetime components, for example.

#### **B.2.4 Purpose and Scope**

#### **B.2.5 Document Overview**

#### **B.2.6 Reference Documents**



## B.3 Mission Concept

### B.3.1 Space Tug

#### 1.1.1 Tug Body Axes Definitions

The tug's body axes are defined in Figure B-1. The origin of the body frame is at the tug's centre of mass (CoM).

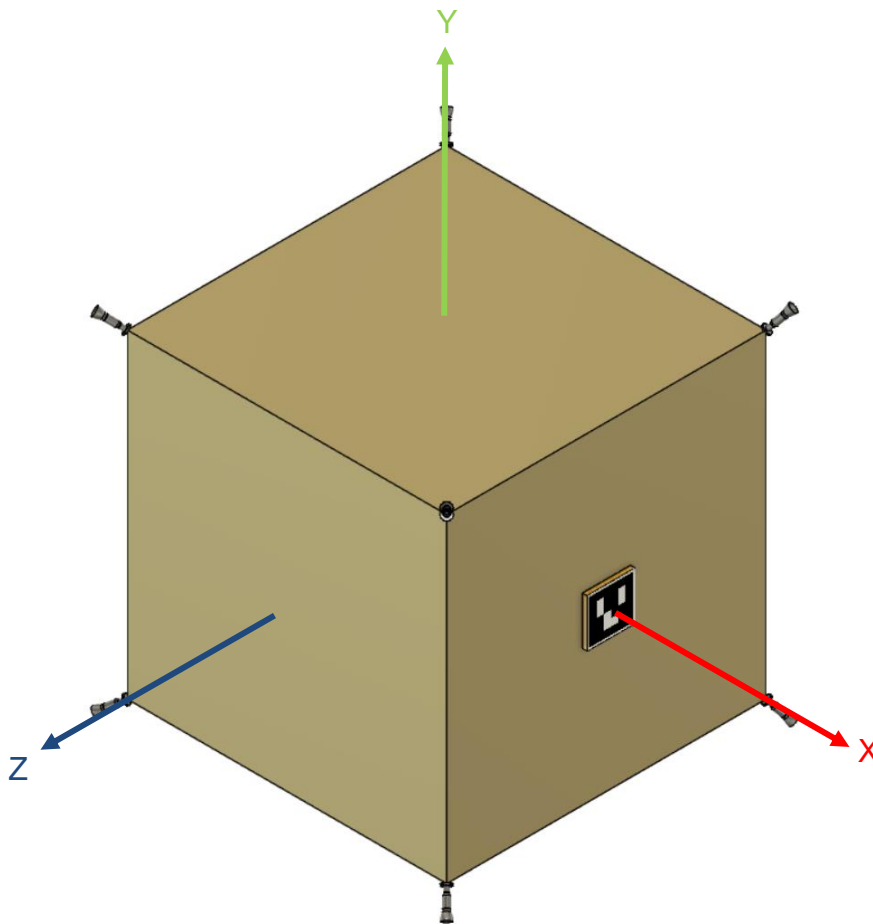


Figure B-1 - Tug body axes definitions

### 1.1.2 Levels of Autonomy

- Describe the three possible levels of autonomy:
  - Tele-operations from the ground (via direct link or other satellites – discuss potential latency)
  - Automatic, where the tug follows a list of detailed commands from the ground
  - Autonomous, where the tug is issued overall instructions from the ground (e.g. replace this component on the target) but must use its own decision-making software to decide how and when to carry out the instructions

### 1.1.3 GNC

#### 1.1.3.1 Control Loop

#### 1.1.3.2 Sensors

- Long range:
- Medium range:
- Short range: camera detects Aruco code on Altius DogTag fiducial marker

#### 1.1.3.3 Plant

#### 1.1.3.4 Actuators

- Four large thrusters on -ve X face for orbit control and as backups for attitude control
- ~~A block of three small thrusters on each of the eight corners of the tug's body cube (24 in total)~~

- Define thrusters including thruster model, thrust, positions, directions and torques (see page 8 of [SADC P6 notes](#) for a good definition example)

## **1.1.4 Servicing Hardware**

### **1.1.4.1 Docking connection**

- Altius Space Machines DogTag™
- Uses Aruco-like optical fiducial marker

### **1.1.4.2 Servicing arm**

- Similar to Next Generation Small Canadarm
- If possible, tools attach by Altius Space Machines MagTag™ to allow easy swapping out of hardware which will also be attached via MagTag™ [5] (expected to reach TRL 7 in Q4 2021)

## **B.3.2 Target Spacecraft**

While the status of the OneWeb constellation is unknown, they can be used as a case study. Their significant payload capability and docking facility suggest that future spacecraft may tend towards their 150 kg size. This will therefore be used as a first approximation of the size of the target spacecraft.

## **B.3.3 Servicing Station**

While the scope of this IRP is only design of the space tug, its interaction with the servicing station should also be considered.

The following assumptions have been made about the servicing station that the mission will support:

- The station will orbit in a low inclination orbit at an altitude of approximately 800 km. This will place it at the bottom end of the high density RSO region [6].

### B.3.4 Orbit

- Refer to and summarise [orbit research document](#)

### B.3.5 Mission Timeline

A description of the mission timeline by phase is shown in Figure B-1, with an overview of the operations to be carried out for OOS shown in Figure B-2.

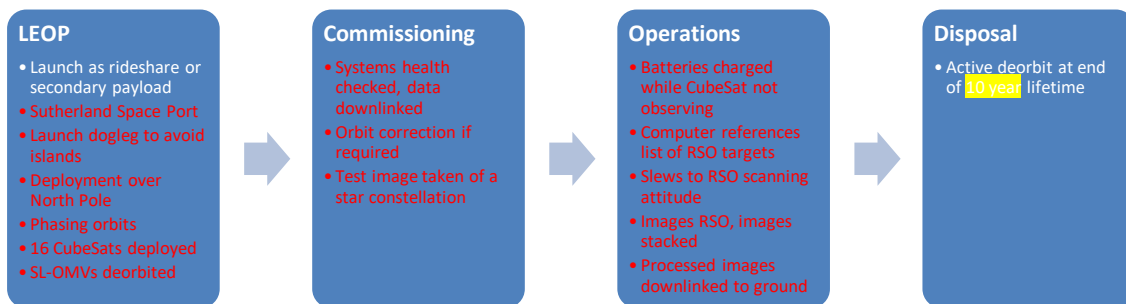


Figure B-1 - Mission timeline

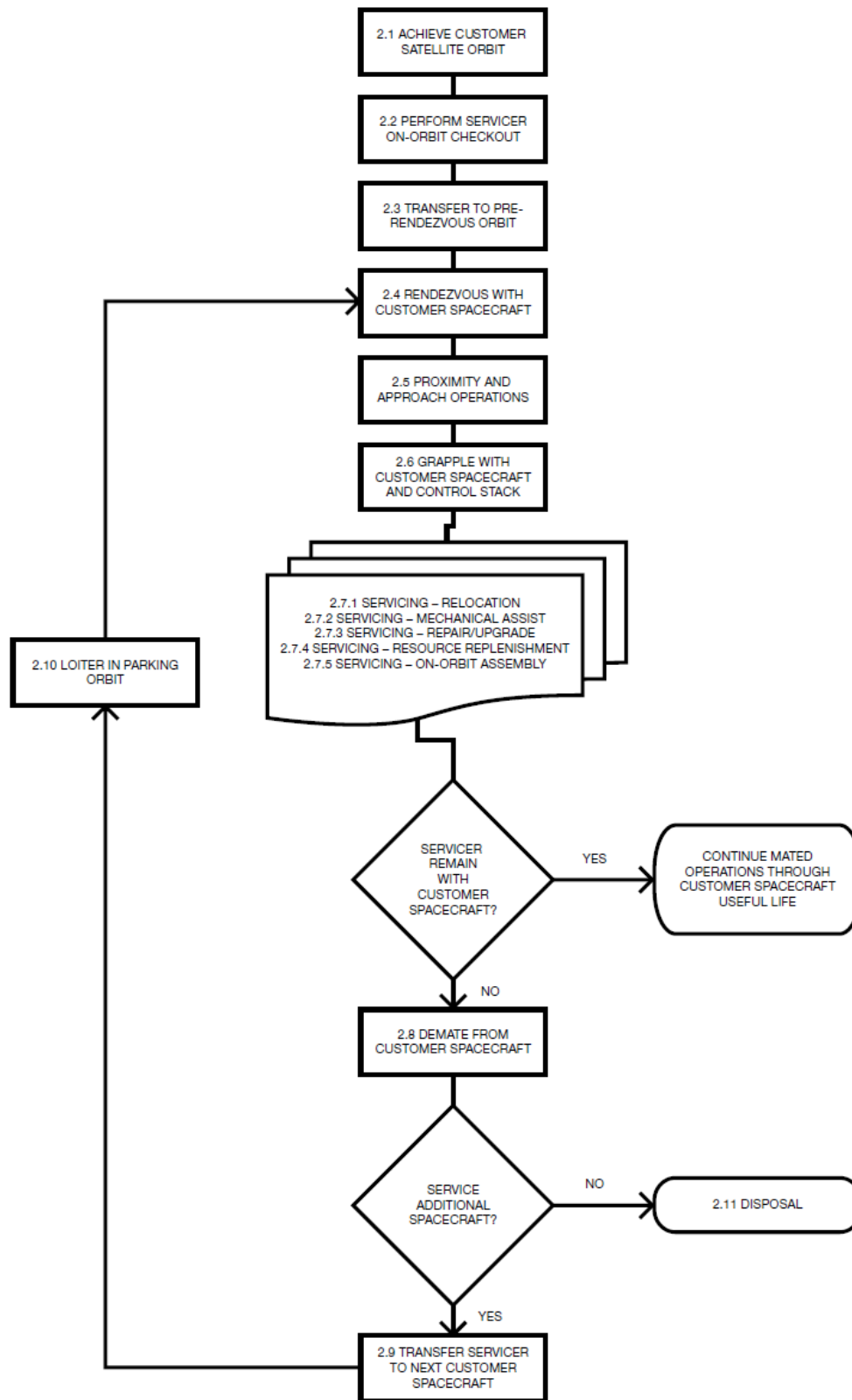


Figure B-2 - Overview of on-orbit servicing operations [246]

### **1.1.5 LEOP**

The LEOP phase shall begin immediately upon lift-off from the launchpad.

LEOP shall contain the following operations...

- Initial orbit insertion
- Order of component switch on (e.g. solar panel deploy (if deployable), radios on etc.)
- Thruster testing
- GNC and other system tests
- Instrument calibration

LEOP shall end when all tests and manoeuvres have been completed.

The start and end points are used to measure the length of the LEOP phase for the purpose of checking it does not exceed its maximum as defined in requirement OPS-0020.

### **1.1.6 Transfer to Station**

In a scenario without a dedicated servicing station, this phase can be skipped.

Summary of manoeuvres to be carried out:

- Initial orbit
- Altitude and plane change
- Arrive in final orbit

### **1.1.7 Operations**

During normal operations, the Space Tug is anticipated to be use for five main use cases. These are detailed in the following subsections. From these use

cases, it can be seen that six main operations are carried out as part of the overall mission:

- Operation 1) Undock from station/target
- Operation 2) Rendezvous with station/target
- Operation 3) Dock with station/target (while towing or alone)
- Operation 4) Perform an orbital manoeuvre (for servicing orbit change, rendezvous or disposal)
- Operation 5) Tow target to new orbit
- Operation 6) Use robot arm to replace hardware on target or refuel it

#### **1.1.7.1 Towing of target to station for servicing**

- 1) Tug starts docked to station or in a parking orbit
- 2) Tug undocks from station if required and rendezvouses with target
- 3) Tug docks with target
- 4) Tug tows target back to station
- 5) Either:
  - a. Tug pushes the target into a controlled docking with the station
  - b. Or the tug performs a controlled, stabilised release of the target in close proximity to the station, with the station then berthing the target using the station's robotic arm

Note that this operation has now been deprecated due to a shift in mission architecture away from one using a space station. This removes the requirement for the target to be towed to the station. The towing operation has therefore been removed from the requirements specification.

#### **1.1.7.2 Redeploying of target into operational orbit**

Same operations as Section 1.1.7.1 but in reverse order. Used to position the target back into its operational orbit once operations such as hardware refurbishment or replacement (if process described in Section 1.1.7.5 is not possible) have been performed at the servicing station.

### **1.1.7.3 Change of target's orbit**

Used to reposition the target into a new orbit for continued operations, standby or disposal.

- 1) Tug starts docked to station or in a parking orbit
- 2) Tug undocks from station if required and rendezvouses with target
- 3) Tug docks with target
- 4) Target repositioned into new orbit
- 5) Tug undocks
- 6) Tug returns to station or parking orbit

### **1.1.7.4 Refuelling of target**

1) to 3) as in Section 1.1.7.1, but specifically using a docking port that supports propellant transfer. Then:

- 4) Propellant transferred to target
- 5) Tug undocks from the target and returns to the station or its parking orbit

### **1.1.7.5 In-situ replacement of hardware on target**

1) to 3) as in Section 1.1.7.1, then:

- 4) Tug uses robot arm to remove hardware from target and stows it in a storage compartment in the tug
- 5) Tug's arm then pulls a replacement part out of the storage compartment and fits it to the target
- 6) Tug undocks from the target and returns to the station or its parking orbit

### **1.1.7.6 Repositioning of servicing station orbit**

All tugs dock to the station and use their thrusters to change the station's orbit, for example to target a satellite constellation in a different orbit. To avoid this mode driving the tug's designed fuel tank capacity, the tug refuelling port will be chosen to be capable of supplying the fuel mass rate needed for the thrusters. In this way, the tug will be able to use the station's fuel supply during the orbit change burn.

#### **1.1.7.7 On-orbit assembly**

The final mission type to be considered for this project is on-orbit assembly (OOA). This will use the tug for assembly of modules or pieces of larger structures, such as observatories or space stations. This could include the assembly of the servicing station discussed in this document. The operations to be carried out for this use case will involve the tug rendezvousing with the parts to be assembled, docking with the first item then using robot arms or other mechanisms to assemble it with other components. This docking and assembly process would repeat until the structure was completed.

#### **1.1.8 Decommissioning**



## B.4 Operational Modes

In the tables in the following subsections, **BOLD BLOCK CAPITALS** refer to operational mode names, **BLOCK CAPITALS** refer to flag names, *ITALIC BLOCK CAPITALS* refer to software flag states.

### B.4.1 Spacecraft Operational Modes

Table B-1 describes the Space Tug's operational modes. For all modes, State of Health (SOH) data are continuously transmitted for reception by ground controllers.

**Table B-1 - Spacecraft operational modes**

Mode name	Description
<b>NORMAL</b>	<ul style="list-style-type: none"> <li>• A general mode used when no other specific operations are required</li> <li>• Unnecessary sensors and other devices kept in standby mode</li> <li>• Attitude set for best battery charging</li> </ul>
<b>RENDEZVOUS</b>	<ul style="list-style-type: none"> <li>• Establish rendezvous with target via long range relative navigation sensors and thruster system</li> </ul>
<b>APPROACH</b>	<ul style="list-style-type: none"> <li>• Used with ~20km of target, when medium-range sensors can take over for more accurate approach vectors</li> </ul>
<b>HOLD WAYP<sub>n</sub></b>	<ul style="list-style-type: none"> <li>• Hold relative position at a given waypoint</li> <li>• Use thrusters to reach the target waypoint if not already there</li> <li>• Stationkeep upon arrival, to a tolerance defined in the CONOPS</li> <li>• Several waypoints can be stored in memory</li> <li>• Mode is called with specified waypoint ID e.g. <b>HOLD WAYP2</b></li> </ul>
<b>FINAL APPROACH</b>	<ul style="list-style-type: none"> <li>• Use close range sensors to acquire target docking point</li> <li>• Detailed range/range rate information feeds into algorithms for slow, controlled approach</li> <li>• <b>ROBO STANDBY</b> mode triggered to prepare arm for use during <b>BERTH</b> mode if required</li> </ul>

<b>DOCK</b>	<ul style="list-style-type: none"> <li>• Spacecraft engages docking mechanism when sensors detect contact with target</li> </ul>
<b>BERTH</b>	<ul style="list-style-type: none"> <li>• Alternative to <b>DOCK</b></li> <li>• Used when spacecraft has arrived at defined berthing location relative to target</li> <li>• Low thrust thrusters used to maintain fine stationkeeping</li> <li>• Arm/other berthing mechanism used to capture target</li> </ul>
<b>ABORT</b>	<ul style="list-style-type: none"> <li>• Cancel the approach</li> <li>• Back track to last holding point</li> <li>• When called, the mode to initiate when pulling away is specified e.g. <b>ABORT HOLD WP3</b> or <b>ABORT FINAL APPROACH</b></li> </ul>
<b>SAFE</b>	<ul style="list-style-type: none"> <li>• Calls <b>HOLD</b> for the most recent waypoint</li> <li>• Solar panels remain Sun-facing</li> <li>• Uses antennas to send health data to ground</li> <li>• Awaits commands from ground controllers</li> </ul>
<b>DESATURATE</b>	<ul style="list-style-type: none"> <li>• Used to desaturate the reaction wheels</li> <li>• Thrusters fire to allow reaction wheels to de-spin without changing the spacecraft attitude</li> <li>• Momentum build up will need to be managed to avoid this mode being necessary during a docked or other critical phase</li> <li>• <b>NORMAL</b> mode called upon completion</li> </ul>

### B.4.2 Software Flags

- *Need to include a flag to highlight a suspected instrumentation error, if possible*

Table B-2 describes the various flags to be used in the spacecraft's onboard computer (OBC) software.

**Table B-2 - Software flags**

Flag name	Description	Effects
MASTER_CAUTION	<ul style="list-style-type: none"> <li>• Set <i>TRUE</i> when a failure has occurred that does not immediately affect vehicle safety</li> <li>• Failed system is logged in telemetry</li> </ul>	<ul style="list-style-type: none"> <li>• Continues with currently active operational mode if component failure modes allow. If other existing failures mean the spacecraft is compromised as per the risk table, <b>SAFE</b> triggered</li> </ul>
MASTER_WARN	<ul style="list-style-type: none"> <li>• Set <i>TRUE</i> when a critical failure has occurred</li> <li>• Failed system is logged in telemetry</li> </ul>	<ul style="list-style-type: none"> <li>• <b>SAFE</b> immediately triggered</li> </ul>
TARGET_LOCK	<ul style="list-style-type: none"> <li>• Set <i>TRUE</i> when the sensors have acquired the target satellite</li> </ul>	<ul style="list-style-type: none"> <li>• Enables <b>APPROACH</b>, <b>FINAL APPROACH</b> and <b>DOCK</b> modes</li> <li>• If spacecraft tries to switch into one of these modes and TARGET_LOCK is not <i>TRUE</i>, <b>HOLD WP1</b> is triggered</li> </ul>
CONTACT	<ul style="list-style-type: none"> <li>• Set <i>TRUE</i> when sensors detect contact</li> </ul>	<ul style="list-style-type: none"> <li>• If in <b>FINAL APPROACH</b> mode, <b>DOCK</b> triggered</li> <li>• If not in <b>FINAL APPROACH</b> mode, <b>ABORT WAYP1</b> triggered</li> </ul>

OUT_OF_MODE	<ul style="list-style-type: none"> <li>• Set <i>TRUE</i> when spacecraft is not in any of the defined operational modes</li> </ul>	<ul style="list-style-type: none"> <li>• <b>SAFE</b> mode triggered</li> </ul>
SENSOR_MISMATCH_[SENSOR_ID]	<ul style="list-style-type: none"> <li>• Set <i>TRUE</i> when a sensor value does not agree with the values from the redundant sensors</li> <li>• The [SENSOR_ID] part of the flag specifies which exact sensor is outputting the suspicious value</li> </ul>	<ul style="list-style-type: none"> <li>• MASTER_CAUTION set</li> </ul>
ROBO_COLLISION_AVOID_SENSE_LOSS	<ul style="list-style-type: none"> <li>• Set <i>TRUE</i> when data is not being received from the servicing arm's end effector collision avoidance sensor</li> </ul>	<ul style="list-style-type: none"> <li>• <b>ROBO HOLD</b> mode triggered</li> <li>• MASTER_CAUTION set</li> </ul>
ROBO_COLLISION_AVOID_ERROR	<ul style="list-style-type: none"> <li>• Set <i>TRUE</i> when data received from the servicing arm's end effector collision avoidance sensor is erroneous</li> </ul>	<ul style="list-style-type: none"> <li>• <b>ROBO HOLD</b> mode triggered</li> <li>• MASTER_CAUTION set</li> </ul>

### B.4.3 Guidance, Navigation and Control (GNC) Operational Modes

Table B-3 - GNC operational modes

Mode name	Description
<b>GNC OFF</b>	<ul style="list-style-type: none"> <li>• All elements of the GNC system are turned off</li> <li>• Used during launch</li> </ul>
<b>THRUST OFF</b>	<ul style="list-style-type: none"> <li>• The GNC thrusters are turned off to disable accidental firings</li> <li>• Used during hardware replacement or other fine operations while docked to the target</li> </ul>

### B.4.4 Robot arm operational modes

Table B-4 - Robot arm operational modes

Mode name	Description
<b>ROBO OFF</b>	<ul style="list-style-type: none"> <li>• All robotics are powered off, with the arm joints locked</li> <li>• Used during launch and any other modes where robotics are not needed</li> </ul>
<b>ROBO STANDBY</b>	<ul style="list-style-type: none"> <li>• Robotic arm is powered,</li> </ul>
<b>ROBO HOLD</b>	<ul style="list-style-type: none"> <li>• Triggered when communication is lost with the servicing arm end effector collision avoidance sensor, or its data is erroneous</li> <li>• The servicing arm maintains its position to avoid colliding with any surrounding objects</li> <li>• Computer awaits instructions from ground operators</li> </ul>
<b>ROBO SHUTDOWN</b>	<ul style="list-style-type: none"> <li>• Triggered when the servicing arm has become uncontrollable, either while moving or stationary</li> <li>• Power is cut to the servicing arm to stop/prevent its motion</li> </ul>

	<ul style="list-style-type: none"><li>• Computer awaits instructions from ground operators</li></ul>
--	--

### 1.1.9 Stowed position

The stowed position for the servicing arm is defined as follows. This is used in requirement ROB-0030.

### B.4.5 GNC range modes

- Long range
- Medium range
- Short range
- For each, describe:
  - Sensors used
  - Actuators used
  - Range accuracy (defined in GNC-0090 and GNC-0130), range rate accuracy (defined in GNC-0100 and GNC-0140)
- Can refer to [Astroscale ELSA-d CONOPS](#) for guidance, but will need detailed study with the hardware being defined in the [Design Definition File](#)

## **B.5 Contingency Operations**

### **B.5.1 Spacecraft Fault Detection and Recovery**

#### **1.1.10 Spacecraft Safing**

- *Triggered when a critical situation is detected*
- *Refer to operational modes*

#### **1.1.11 Loss of Target Lock**

- *Triggered when the tug loses lock on the target spacecraft during proximity operations (e.g. because the Sun blinds an optical sensor)*
- *Related to Section 1.1.12*

#### **1.1.12 Loss of Data Integrity**

- *Triggered when data from multiple sources (e.g. LiDAR and optical sensors) don't match up*

#### **1.1.13 AOCS Failure**

- *Triggered when one or more thrusters fail, but effects of this and resulting actions depend on which thruster(s) fail and what mode the spacecraft is in at the time*
- *Should include thrusters failing to fire and being stuck on*

**1.1.14 Unplanned Detachment of Target**

- *Triggered when a spacecraft under tow becomes detached from the tug*

**1.1.15 Unplanned Detachment from Servicing Station**

- *Triggered when the spacecraft detects that it is no longer docked with the servicing station, when an undocking was not planned*
- *Remedial action:*
  1. *Alert ground control*
  2. *Confirm undocked status*
  3. *Use sensors to calculate position and velocity relative to station*
  4. *Confirm station is ready to accept redocking*
  5. *Attempt autonomous redocking*
  6. *If docking succeeds, resume normal operations. If docking fails, retreat to a safe distance and await further instructions from the ground*

## REFERENCES

- [1 Space Telescope Science Institute (STScI), "JWST Mission Operations  
] Concept Document," Goddard Space Flight Center, Greenbelt, Maryland,  
2006.
- [2 ATHENA Study Team, "ATHENA - Concept of Operations," European  
] Space Agency, Noordwijk, 2015.
- [3 European Space Agency, "Mitigating space debris generation," European  
] Space Agency, [Online]. Available:  
[https://www.esa.int/Safety\\_Security/Space\\_Debris/Mitigating\\_space\\_debris  
\\_generation](https://www.esa.int/Safety_Security/Space_Debris/Mitigating_space_debris_generation). [Accessed 11 May 2020].
- [4 NASA Office of Safety and Mission Assurance, NASA TECHNICAL  
] STANDARD NASA-STD-8719.14B Process for Limiting Orbital Debris,  
National Aeronautics and Space Administration, 2019.
- [5 Altius Space Machines, "MagTag™ Modular Interfaces for Palletized  
] Subsystems and Satellites," Altius Space Machines.
- [6 W. Easdown, "Mission ORCA: Orbit Refinement for Collision Avoidance,"  
] William Easdown, Cranfield, 2020.
- [7 Satellite Servicing Projects Division, "On-Orbit Satellite Servicing Study,"  
] National Aeronautics and Space Administration Goddard Space Flight  
Center, Greenbelt, 2010.

## **Appendix C Space Servicer Requirements Specification**

### **C.1 Introduction**

#### **C.1.1 Overview**

The Space servicer is being designed as part of the author's Individual Research Project in on-orbit servicing. This is in part fulfilment of an MSc in Astronautics and Space Engineering at Cranfield University.

#### **C.1.2 Interpretation of Requirements**

The wording of statements in this document determines their applicability:

- "SHALL" or "MUST" are used to indicate a mandatory requirement.
- "MAY" indicates an option.
- "WILL" indicates a statement of fact or intention.

The phrases "the system" or "the spacecraft", when used without further clarification, refer to the overall Space Tug.

## **C.2 Design Brief**

The Space servicer shall be used for on-orbit servicing of targeted spacecraft that have a design similar to that of OneWeb's spacecraft.

## **C.3 Mission Phases**

The mission phases are defined in the project Concept of Operation (CONOPS) document.



## **C.4 Requirements Specification**

### **C.4.1 General Requirements**

Unless otherwise stated, the general requirements listed in this section apply to all mission phases.

#### **1. Top-Level Requirements**

##### **TLR-0010   Spacecraft wet mass**

The spacecraft shall have a total wet mass of no more than 400 kg.

##### **TLR-0020   Dimensions**

The spacecraft shall have a length of no more than 1.5 m, a height of no more than 1.5 m and a width of no more than 1.5 m.

##### **TLR-0030   Autonomy**

The spacecraft shall perform all servicing operations defined in the CONOPS fully autonomously.

#### **2. Operations Requirements**

##### **OPS-0010   Lifetime**

The spacecraft shall have an operational lifetime of no less than 10 years.

##### **OPS-0020   LEOP maximum duration**

The maximum duration of the launch and early orbit phase (LEOP) shall be three months, using the start and end points defined in the CONOPS.

### **3. GNC Requirements**

#### **GNC-0010 Minimum $\Delta v$**

The GNC thrusters shall provide a minimum  $\Delta v$  of 500 m/s when the servicer is docked to a target and shall provide a minimum  $\Delta v$  of 800 m/s when the servicer is not docked to a target.

#### **GNC-0020 Angular acceleration**

The GNC thrusters shall provide a minimum angular acceleration of 0.5 °/s<sup>2</sup>.

#### **GNC-0030 GNC and RNS volume**

The guidance, navigation and control (GNC) system and relative navigation system (RNS) shall together take up no more than 15 % of the overall spacecraft volume budget.

#### **GNC-0040 GNS and RNS power**

The guidance, navigation and control (GNC) system and relative navigation system (RNS) shall together take up no more than 75 % of the overall spacecraft power budget.

#### **GNC-0050 GNC degrees of freedom (DoF)**

The GNC system shall provide six degrees of freedom control throughout all mission phases.

#### **GNC-0060 Redundancy**

All GNC sensors, buses, computers and actuators shall have at least one backup to be used in the event of a failure of the nominal system.

#### **GNC-0070 Orbit determination accuracy**

The GNC shall achieve orbit determination accuracies for each mission mode as defined in Table C-1. For those modes marked N/A, this requirement does not

apply as the servicer will use its relative navigation system rather than the GNC system.

**Table C-1 - Orbit determination accuracy per mission mode**

<b>Mission Mode</b>	<b>Orbit determination accuracy (m)</b>
General	100
Undocking	N/A
Rendezvous	50
Final Approach & Docking	N/A
Orbital Manoeuvring	N/A
Hardware replacement	N/A

**GNC-0080 Attitude determination accuracy**

The GNC system shall achieve attitude determination accuracies for each mission mode as defined in Table C-2.

**Table C-2 - Attitude determination accuracy per mission mode**

<b>Mission Mode</b>	<b>Attitude determination accuracy (°)</b>
General	0.25
Undocking	0.05
Rendezvous	0.05
Final Approach & Docking	0.05
Orbital Manoeuvring	0.05

Hardware replacement	0.05
----------------------	------

### **GNC-0090 Pointing accuracy**

The GNC shall achieve pointing accuracies for each mission mode as defined in Table C-3.

**Table C-3 - Pointing accuracy per mission mode**

<b>Mission Mode</b>	<b>Pointing accuracy (°)</b>
General	0.25
Undocking	0.05
Rendezvous	0.05
Final Approach & Docking	0.05
Orbital Manoeuvring	0.05
Towing	0.025
Hardware replacement	0.05

### **GNC-0100 Stability margins**

The GNC stability margins shall be as follows and are taken from requirement MAR-AOC-060 in the ESA CDF guidance [245]:

- The gain margin shall be  $\geq 6$  dB
- The phase margin shall be  $\geq 30^\circ$
- The peak sensitivity and complementary sensitivity function shall be  $\leq 6$  dB
- The modulus margin shall be  $\geq 0.5$ .

**GNC-0110 Selection of stability margins**

If SISO loops are used, the gain margin, phase margin and modulus margin from GNC-0100 shall be used as the default stability margin indicators. If MIMO loops are used, the sensitivity and complementary sensitivity functions from GNC-0100 shall be used as the default stability margin indicators. This is derived from requirement MAR-AOC-030 in the ESA CDF guidance [245].

**GNC-0120 Slew rate**

The GNC shall achieve a maximum slew rate of 0.5 °/s while docked with the target and 1 °/s while undocked.

**4. Robotics Requirements****ROB-0010 Autonomy**

The servicing arm shall support tele-operation from the ground or automatic or fully autonomous operations using commands issue from the ground and the tug's on-board computer (OBC). These levels of autonomy are further defined in the CONOPS.

**ROB-0020 COTS**

The servicing arm shall be a commercial off the shelf (COTS) unit.

**ROB-0030 Servicing arm reach**

The servicing arm shall have a minimum reach of 2 m.

**ROB-0040 Servicing arm stowed volume**

The servicing arm shall have a maximum stowed volume of 2 m<sup>3</sup>.

**ROB-0050 Servicing arm stowage**

The servicing arm shall remain stowed at all times other than when being actively used for servicing in Operation 5 – Hardware Replacement. This stowed position is defined in the CONOPS.

**ROB-0060 Servicing arm maximum load**

The servicing arm shall support a maximum load of 25 kg.

**ROB-0070 Servicing arm maximum mass**

The servicing arm shall support a maximum load of 55 kg.

**ROB-0080 Servicing arm hold**

If communication is lost with the servicing arm end effector collision avoidance sensor, or its data is erroneous, the servicing arm shall enter the **ROBO HOLD** mode, as defined in the CONOPS.

## **C.4.2 Operation 1 - Undocking**

### **5. Operations Requirements**

#### **OPS-0030 Servicing arm stowage before undocking**

The servicer shall not undock before the servicing arm has completed its operations and has completed its stowing process in accordance with ROB-0050.

### **6. GNC Requirements**

#### **GNC-0130 Target lock**

The GNC shall maintain tracking of the tug's range and range rate relative to the target while within a range of 500 m.

### **C.4.3 Operation 2 – Rendezvous**

#### **7. GNC Requirements**

##### **GNC-0140 Absolute navigation**

The servicer shall perform absolute navigation to place the servicer within 10 km of the target.

##### **GNC-0150 First target lock**

The GNC shall achieve first lock on the target's position while at a range of at least 5 km and first lock on the target's range and range rate while at a range of at least 5 km.

##### **GNC-0160 Rendezvous range accuracy**

The GNC system shall have a range accuracy of 5 km while in long range mode and 500 m in medium range mode, where the range modes are defined in the CONOPS.

##### **GNC-0170 Rendezvous range rate accuracy**

The GNC system shall have a range accuracy of 5 km while in long range mode and 500 m in medium range mode, where the range modes are defined in the CONOPS.

### **C.4.4 Operation 3 – Final Approach & Docking**

#### **8. Operations Requirements**

##### **OPS-0040 Sun angle**

The angle between the docking camera boresight and the tug-Sun vector shall be at least 30 ° throughout final approach & docking.

##### **OPS-0050 Ground link**

The servicer shall have a continuous communications link with ground controllers during the final approach & docking phase, which shall allow controllers to abort the phase if required.

##### **OPS-0060 Thruster plume**

No thruster plumes shall impinge upon the target. The plume geometry is defined in CONOPS.

#### **9. GNC Requirements**

##### **GNC-0180 Final approach target lock**

The GNC system shall maintain a lock on the target's docking point throughout the full final approach process.

##### **GNC-0190 ABORT mode trigger**

The on-board computer shall trigger the **ABORT** mode if the GNC system loses target lock during final approach. This mode is defined in the CONOPS.

##### **GNC-0200 Docking range accuracy**

The RNS shall have a range accuracy of 1 cm in short range mode, where the mode is defined in the CONOPS.

##### **GNC-0210 Docking range rate accuracy**

The RNS shall have a range accuracy of 1 cm/s in short range mode, where the mode is defined in the CONOPS.

**GNC-0220 Docking pose accuracy**

The RNS shall have a pose accuracy of 1 ° in short range mode, where the mode is defined in the CONOPS.

**GNC-0230 Docking pose rate accuracy**

The RNS shall have a pose accuracy of 1 °/s in short range mode, where the mode is defined in the CONOPS.

**GNC-0240 Maximum position and velocity errors at contact**

The GNC system shall reduce the range, range rate, attitude and attitude rate amounts to below the values shown in Table C-4 before contact with the target's docking fixture.

**Table C-4 - Maximum errors at moment of docking fixture contact**

Axis	Range (m)	Range rate (m/s)	Attitude (°)	Attitude rate (°/s)
X	0.0	0.02	5	0.5
Y	0.03	0.02	5	0.5
Z	0.03	0.02	5	0.5

## **C.4.5 Operation 4 – Orbital Manoeuvring**

### **10.GNC Requirements**

#### **GNC-0250 Linear acceleration**

The maximum acceleration provided by the orbital manoeuvring thrusters shall be at least  $0.36 \text{ m/s}^2$  (when not docked to the target).

## **C.4.6 Operation 5 – Hardware Replacement/Refuelling**

### **11. Operations Requirements**

#### **OPS-0070 Docking maintenance**

The tug's docking fixture shall remain attached to the target's docking fixture throughout the hardware replacement operation.

### **12. GNC Requirements**

#### **GNC-0260 Thruster disable**

The tug's thrusters shall be kept in the **THRUST OFF** mode during the hardware replacement operation.

### **13. Robotics Requirements**

#### **ROB-0090 Arm contact**

The robot arm shall only come into contact with contact points on the target spacecraft that are pre-defined in the CONOPS, unless explicitly commanded by ground controllers.

## References

- [1] European Space Research and Technology Centre, Concurrent Design Facility Studies Standard Margin Philosophy Description, Noordwijk: European Space Agency, 2017.
- [2] T. Burger, "How Fast is Realtime? Human Perception and Technology," PubNub Inc., 9 February 2015. [Online]. Available: <https://www.pubnub.com/blog/how-fast-is-realtime-human-perception-and-technology/>. [Accessed 30 July 2018].
- [3] A. Witze, "Software error doomed Japanese Hitomi spacecraft," Macmillan Publishers Limited, 28 April 2016. [Online]. Available: <https://www.nature.com/news/software-error-doomed-japanese-hitomi-spacecraft-1.19835>. [Accessed 30 July 2018].
- [4] Concrete Construction Staff, "Recommended Floor Slope and Tolerance," Hanley Wood Media, Inc, 1 February 1998. [Online]. Available: [https://www.concreteconstruction.net/how-to/recommended-floor-slope-and-tolerance\\_o](https://www.concreteconstruction.net/how-to/recommended-floor-slope-and-tolerance_o). [Accessed 29 July 2018].
- [5] California Polytechnic State University, CubeSat Design Specification, San Luis Obispo: Cal Poly SLO, 2014.
- [6] ISS Multilateral Control Board, International Docking System Standard (IDSS) Interface Definition Document (IDD) Revision E, 2016.

## Appendix D Technology Readiness Levels

When assessing the suitability of hardware and software for use in space, it is critical that their level of maturity be judged in an objective way. To achieve this, the European Space Agency (ESA) and National Aeronautics and Space Administration (NASA) both have defined scales for Technology Readiness Level (TRL), which are shown in Figure D-1 and Figure D-2. These scales will be referred to throughout this report when judging the suitability of components for the final design. The report will aim to select components that are at least TRL 6.

Both scales will be used as components are judged based on the local scale, so parts designed in the US and Canada are normally judged by the NASA scale, with European parts judged by the ESA scale.

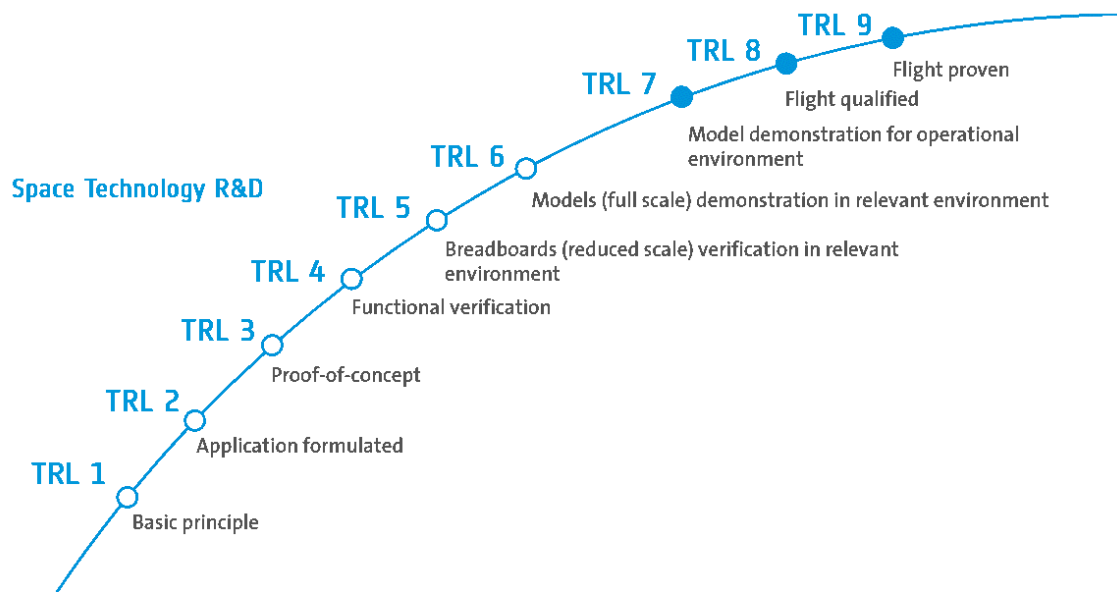


Figure D-1 - ESA TRL definitions [240]

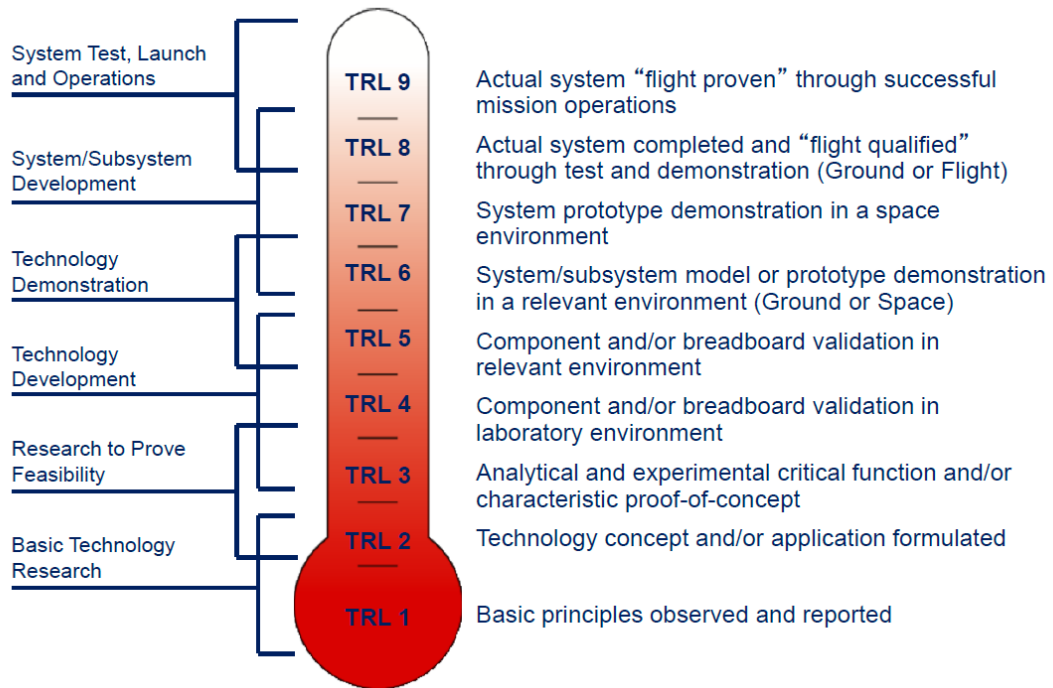
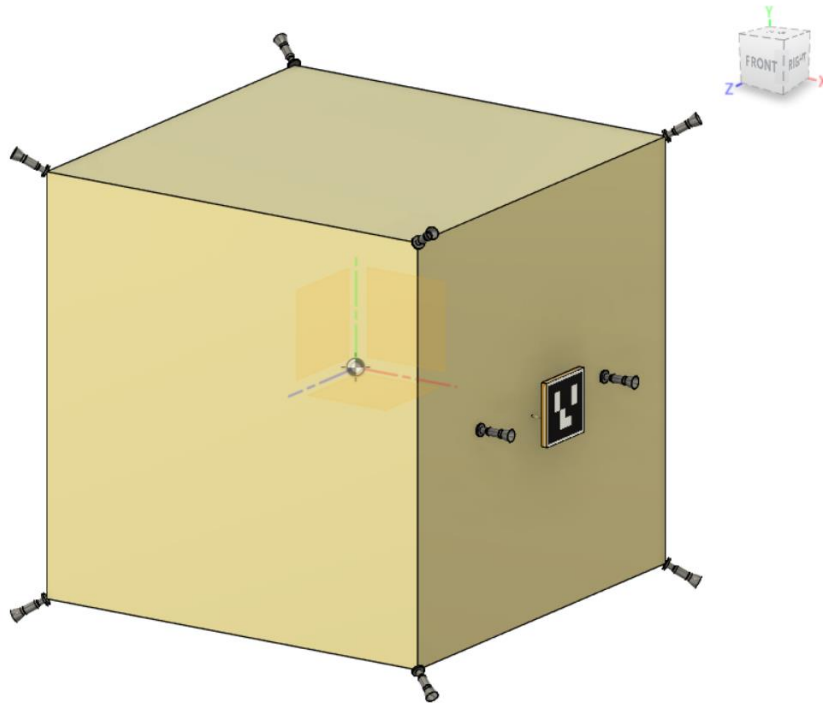


Figure D-2 - NASA TRL definitions [241, p. 23]

## Appendix E Centres of Mass and Moment of Inertia Matrices Calculations

### E.1 Centres of Mass

The servicer body frame has its origin at the centre of mass of the servicer by definition. The X, Y and Z axes of this frame are then defined as shown in the computer-aided design (CAD) model shown in Figure E-1. Therefore, the servicer centre of mass is at  $[0 \ 0 \ 0]^T$  m in the servicer body frame. The DogTag grappling fixture (see Section 9.1 Grappling Fixture) is located on the +X face.



**Figure E-1 – CAD model showing the servicer body frame definition**

The target's body frame is defined similarly and is shown in Figure E-2. Note that the target's DogTag is located on the -X face. Therefore, the target centre of mass is at  $[0 \ 0 \ 0]^T$  m in the target body frame.

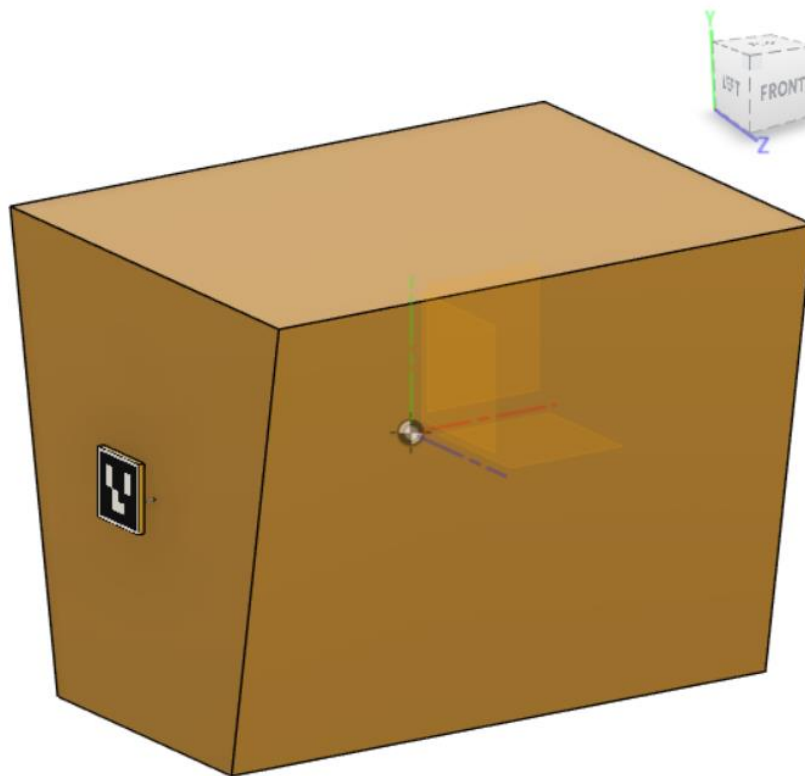


**Figure E-2 – CAD model showing the target body frame definition**

When the two spacecraft are docked together, the servicer body frame is used to describe the combined vehicle but is referred to as the docked body frame to avoid confusion. The servicer is a cube with length 1 m (see Section 5.3 Servicer sizing) with the length of the DogTag being 64.60 mm [139]. The target is roughly 1.3 m long [157]. The DogTags are fitted to the two vehicles such that when the spacecraft are docked, the centres of mass of the two spacecraft and the two DogTags all lie on the X axis, as shown in Figure E-3. Therefore, the target centre of mass is at  $[1.2792 \ 0 \ 0]^T$  m in the docked body frame.

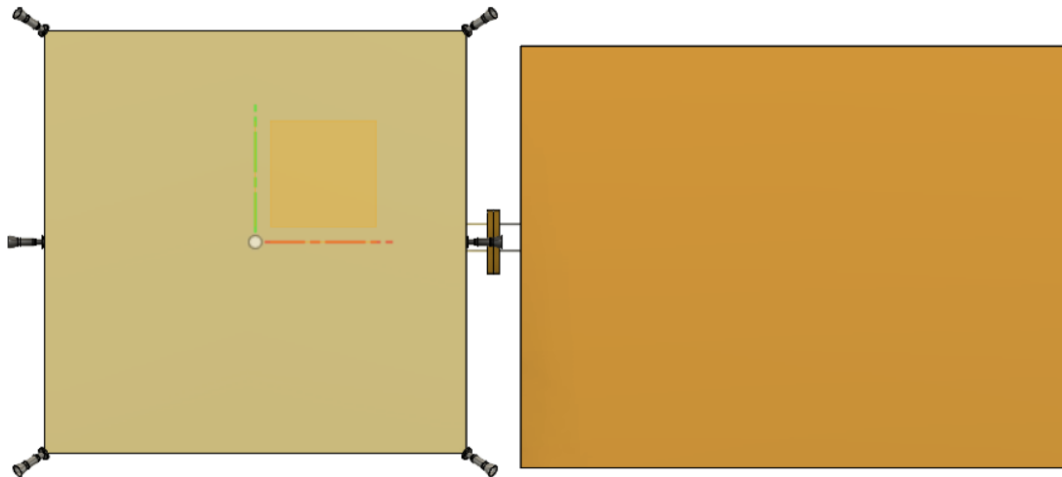


**Figure E-3 – CAD model showing the docked configuration**

Any misalignment of the centres of mass away from the x-axis will make finding the combined inertia matrix more complex and have an effect on the combined vehicle dynamics. The combined centre of mass could also change while docked due to fuel sloshing or if appendages like the servicer’s robot arm or solar panels or antennas move. However, the analysis of these factors and their effects on the dynamics is beyond the scope of this project and is therefore discussed in Section 10 Areas for Future Development. The assumption of aligned centres of mass also drives the location of the DogTag grappling fixture (see Section 9.1 Grappling Fixture) on the target to a location such that it is aligned with the target’s centre of mass when looking towards the grappling fixture and centre of mass.

To find the combined centre of mass, Equation (E-1) was used [242]. Quantities with a 1 subscript denote the servicer and 2 the target. The maximum wet mass of the servicer is 323.97 kg as described in Section 5.3.2 Fuel requirement estimation, with the target being in the “200 kg class” [157].

$$X_{cm} = \frac{m_1 x_1 + m_2 x_2}{m_1 + m_2} \quad (\text{E-1})$$

$$\therefore X_{cm} = \frac{323.97 \times 0 + 200 \times 1.2792}{323.97 + 200}$$

$$\therefore X_{cm} = 0.4883 \text{ m}$$

This combined with the assumption of alignment means the combined centre of mass is at  $[0.4883 \ 0 \ 0]^T$ . As the servicer burns its propellant, the combined centre of mass will move closer to the target.

## E.2 Moments of Inertia

To model the servicer's dynamics in the Main Central Control spreadsheet (see Section 3.3.2 Main Central Control spreadsheet), the author needed an estimate of the servicer's moment of inertia matrix. As the spacecraft was being estimated as a cube with length 1 m and mass 291.47 kg (see Section 5.3 Servicer sizing), the formula for the moment of inertia of a cube could be used. This is shown in Equation (E-2) [243], where  $M$  is the cube's mass in kilograms and  $s$  is the length of its side in metres.

$$I = M \frac{s^2}{6} \begin{bmatrix} 1 & 0 & 0 \\ 0 & 1 & 0 \\ 0 & 0 & 1 \end{bmatrix} \quad (\text{E-2})$$

$$\therefore I_{servicer} = \frac{323.97}{6} \begin{bmatrix} 1 & 0 & 0 \\ 0 & 1 & 0 \\ 0 & 0 & 1 \end{bmatrix}$$

$$\therefore I_{servicer} = \begin{bmatrix} 53.99 & 0 & 0 \\ 0 & 53.99 & 0 \\ 0 & 0 & 53.99 \end{bmatrix} \text{ kg m}^2$$

The servicer's moment of inertia could only be used in the plant when the servicer was not docked to the target. When docked, the moments of inertia of the servicer and target needed to be combined to give a moment of inertia matrix for the single docked spacecraft. The moment of inertia matrix of the target in the target body frame was found using the moment of inertia tool in the CAD model of the target.

$$I_{target} = \begin{bmatrix} 28.23754 & 0 & 0 \\ 0 & 39.99213 & 0 \\ 0 & 0 & 44.57873 \end{bmatrix} \text{ kg m}^2$$

The rotation axis while docked passes through the combined centre of mass found previously, so this is used when calculating the combined inertia matrix. To

find the combined inertia matrix, the parallel axis theorem shown in Equation (E-3) was used [244]. This gives the moment of inertia of an object when it is spinning around an axis that is parallel to an axis that passes through its centre of mass. The equation needs to be used to convert both the Y and Z axes terms of the inertia matrices, as only the X axis is aligned.

$$I_{\text{parallel axis}} = I_{cm} + Md^2 \quad (\text{E-3})$$

In the equation,  $I_{cm}$  is the term of the initial inertia matrix for the relevant axis. For example, if the servicer is now rotating round an axis parallel to the Y-axis,  $I_{cm}$  is the  $I_{YY}$  term of the servicer inertia matrix.  $M$  is the mass of the spacecraft in kilogrammes and  $d$  is the distance in metres between the original axis and the parallel axis. In this case,  $d$  represents the distance between the spacecraft's individual centre of mass and the combined centre of mass when docked.

The equation was used to convert the inertia matrices of both the servicer and the target so that the vehicles were now both rotating around the combined centre of mass. For the servicer,

$$I_{Y', \text{ servicer}} = I_{Z' \text{ servicer}} = 53.99 + 323.97 \times 0.4883^2$$

$$\therefore I_{Y', \text{ servicer}} = I_{Z' \text{ servicer}} = 131.23 \text{ kg m}^2$$

$$\therefore I'_{\text{servicer}} = \begin{bmatrix} 53.99 & 0 & 0 \\ 0 & 131.23 & 0 \\ 0 & 0 & 131.23 \end{bmatrix} \text{ kg m}^2$$

For the target,

$$I_{Y', \text{ target}} = 39.99213 + 200 \times (1.2792 - 0.4883)^2$$

$$\therefore I_{Y', \text{ target}} = 165.11 \text{ kg m}^2$$

$$I_{Z', \text{ target}} = 44.57873 + 200 \times (1.2792 - 0.4883)^2$$

$$\therefore I_{Z', \text{ target}} = 169.69 \text{ kg m}^2$$

$$\therefore I'_{target} = \begin{bmatrix} 28.23754 & 0 & 0 \\ 0 & 165.11 & 0 \\ 0 & 0 & 169.69 \end{bmatrix} \text{ kg m}^2$$

To find the combined inertia matrix, the two converted inertia matrices were simply added, giving:

$$I_{docked} = \begin{bmatrix} 82.23 & 0 & 0 \\ 0 & 296.34 & 0 \\ 0 & 0 & 300.92 \end{bmatrix} \text{ kg m}^2$$